ornl

OAK RIDGE NATIONAL LABORATORY

MARTIN MARIETTA

Review and Evaluation of Design Analysis Methods for Calculating Flexibility of Nozzles and Branch Connections

S. E. Moore
E. C. Rodabaugh
K. Mokhtarian
R. C. Gwaltney

Engineering Technology Division

REVIEW AND EVALUATION OF DESIGN ANALYSIS METHODS FOR CALCULATING FLEXIBILITY OF NOZZLES AND BRANCH CONNECTIONS

S. E. Moore   K. Mokhtarian
E. C. Rodabaugh   R. C. Gwaltney

iii

CONTENTS

PREFACE

This report began as one of several scoping studies on various aspects of nuclear power plant piping system design. The objectives of those studies, which were informally identified as status reports, were to identify and collect the pertinent literature on the subject and to identify needed improvements in the design methods and criteria. This particular study of flexibility factors, however, quickly outgrew its original purpose and has become a comprehensive discourse on the state of the art with specific recommendations for developing needed improvements.

Even though this report does not recommend formalistic changes in the flexibility analysis methods available to the designer, we feel that publication at this stage of our study is timely because of the errors and misconceptions that we have been able to identify and document. Hopefully, this information will help designers to avoid potentially costly mistakes. A follow-on report, which is currently being written, will include specific recommendations for the design of piping systems. Until that report is available, we recommend that designers exercise due caution in the use of the currently available flexibility analysis methods.

This report was prepared for the Office of Nuclear Regulatory Research, U.S. Nuclear Regulatory Commission (NRC) under the ASME Code Sect. III — Technical Assistance Project. D. J. Guzy was the NRC project manager. We extend our gratitude to him for his enthusiastic support. We also thank the reviewers of the report, especially those who offered suggestions and/or constructive criticisms.

LIST OF FIGURES

ix

LIST OF TABLES

REVIEW AND EVALUATION OF DESIGN ANALYSIS METHODS FOR CALCULATING FLEXIBILITY OF NOZZLES AND BRANCH CONNECTIONS

S. E. Moore   K. Mokhtarian

E. C. Rodabaugh   R. C. Gwaltney

ABSTRACT

Modern piping system design generally includes an ana-
lytical determination of displacements, rotations, moments,
and reaction forces at various positions along the piping
system by means of a flexibility analysis. The analytical
model is normally based on a strength-of-materials descrip-
tion of the piping system as an interconnected set of
straight and curved beams, along with "flexibility factors"
that are used to compensate for inaccuracies in the model
behavior. This report gives an in-depth evaluation of the
various analytical descriptions of the flexibility factors
associated with piping system branch connections and nozzles.
Recommendations are given for developing needed improvements.

---

1. INTRODUCTION

Flexibility factors have been used in piping system design for many
years in the analytical determination of displacements, moments, and
forces at various positions along the piping system, as well as the
determination of reaction forces at the supports and anchors. The ana-
lytical model used in the design calculations is normally based on a
strength-of-materials description of the piping system as an intercon-
nected set of straight and curved beams with uniformally round cross
sections. Flexibility factors are introduced into the analytical model
to correct, in a gross sense, for the differences in structural behavior
between the strength-of-materials model and the piping system components
that make up a real piping system. The current interest in flexibility
factors for nozzles and branch connections comes most directly from
recent efforts to develop design criteria that will permit the construc-
tion of more-flexible nuclear piping systems and, thereby, reverse a
design practice that is seen by many as being less safe and considerably
more costly.

Flexibility factors under consideration in this report are for noz-
zles and branch connections within the piping system itself and for noz-
zles in cylindrical vessels that interact with connected piping systems.
An adequate characterization of the flexibility factors for both types
of nozzles is important to the development of improved design criteria
for flexible piping systems. The latter, however, may have the greater

impact on improving overall design practice. The traditional practice has been to ignore nozzle flexibility at the piping-vessel interface and to model the piping system termination as rigid. The resulting calculation produces higher reaction loads that must then be supported by additional pipe supports and restraints or by stiffening the vessel shell.

The primary objectives of this report are to (1) summarize available data on flexibility factors for nozzles in cylindrical shell structures (pressure vessels and tanks) and branch connections and tees in piping systems and (2) compare those data with analytical methods for calculating flexibility factors for use in piping system design analyses. A later report based on the observations, conclusions, and recommendations of this report will present design practice guidance that will provide a more accurate basis for the evaluation of piping systems under both static and dynamic loadings.

2. BACKGROUND

2.1 DEFINITION OF NOZZLE FLEXIBILITY FACTORS

The most commonly accepted definition of a flexibility factor was expressed by Markl in his discussion of piping flexibility analysis[1] as

the ratio of the rotation per unit length of the part in question produced by a moment, to the rotation per unit length of a straight pipe of the same nominal size and schedule or weight produced by the same moment.

Figure 1(a) shows a simple one-dimensional model of a piping system that can be used to illustrate the concepts and use of flexibility factors in a piping system analysis. This piping system consists of three straight pipes (SP); an elbow (CP); a branch connection (BC); and three anchors at points A, B, and C. The analytical model consists of three round beams to represent the straight pipe segments; a curved bar to represent the elbow; a rigid tee-joint at I to represent the branch connection; and fixed end conditions at A, B, and C to represent the anchors.

Flexibility factors for each component in the piping system can be developed by considering the rotations (and displacements) of one end of the component relative to the other end. For example, Fig. 1(b) shows the analytical strength-of-materials model for a segment of straight pipe of length L fixed in space at end A (x = 0) and loaded with orthogonal moments $M_1(L)$, $M_2(L)$, and $M_3(L)$ at end B. The rotation of end B with respect to end A in the direction of M_1 that would be caused by the moment $M_1(L)$ is given by the strength-of-materials formula

$$(\theta_1)_{nom} = \frac{1}{EI_x} \int_0^L M_1(x) \, dx , \tag{1}$$

where E and I_x are the elastic modulus and the moment of inertia about the x axis, respectively. A flexibility factor k for a given piping component is then defined, according to Markl, as

$$k_1 = \theta_1 / (\theta_1)_{nom} , \tag{2}$$

where $(\theta_1)_{nom}$ is given by the normalized form of Eq. (1), that is, L = 1 or y = x/L evaluated at y = 1, and θ_1 is the actual rotation of the component per unit length caused by the moment $M_1(L)$.

In general, the actual rotation θ_1 must be determined by experiment or by a rigorous theoretical analysis. Numerous experimental and theoretical studies of beam bending, however, confirm that the actual rotation of the end of a cantilevered beam is adequately described by Eq. (1) if the length is greater than several times the depth (or diameter) of the beam. Thus, the flexibility factor k_1 associated with M_1 and θ_1 for

ORNL–DWG 87–4618 ETD
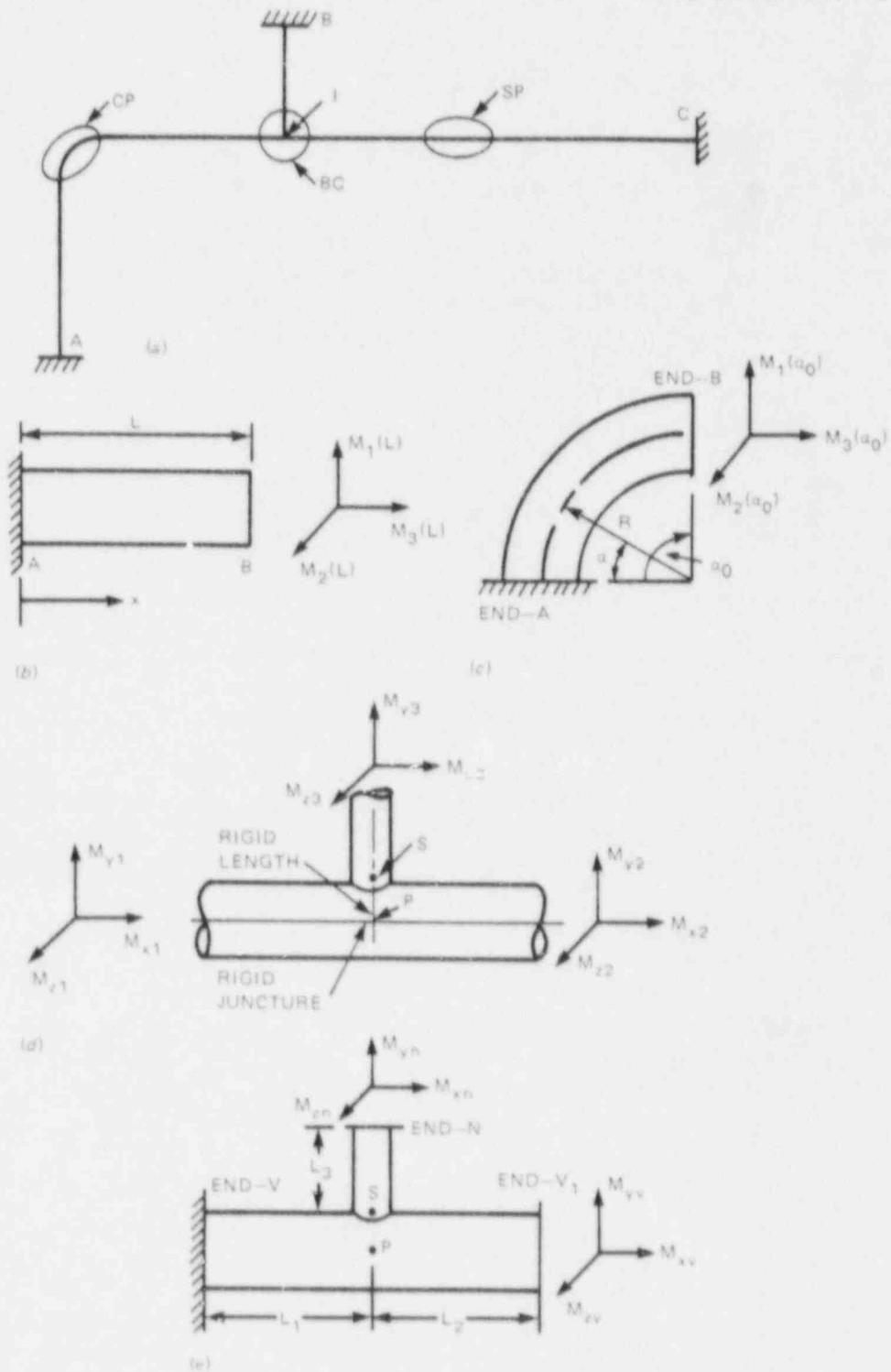
Fig. 1. Strength-of-materials models for piping system components.
(a) One-dimensional beam model of piping system, (b) straight pipe,
(c) curved pipe, (d) branch connection, (e) test or analysis arrangement.

a straight pipe segment is

$$k_1 = \theta_1/(\theta_1)_{nom} = 1.0 . \tag{3}$$

The other two flexibility factors k_2 and k_3, associated with M_2, θ_2 and M_3, θ_3, respectively, are given by

$$k_2 = \theta_2/(\theta_2)_{nom} = 1.0 ,$$

and

$$k_3 = (\theta_3/(\theta_3)_{nom} = 1.0 , \tag{4}$$

where $(\theta_2)_{nom}$ is given by Eq. (1) with M_1, I_x replaced by M_2, I_y and $(\theta_3)_{nom}$ for the torsional moment M_3 is given by

$$(\theta_3)_{nom} = \frac{1}{GJ} \int_0^L M_3(x) \, dx = \frac{1.3}{EI} \int_0^L M_3(x) \, dx . \tag{5}$$

Figure 1(c) shows the strength-of-materials beam model of an elbow or curved pipe anchored at end A and loaded with a set of orthogonal moments $M_1(\alpha_o)$, $M_2(\alpha_o)$, and $M_3(\alpha_o)$ at end B. Both experimental and theoretical studies of curved pipe or elbows snow that the in-plane rotation θ_2 at end B with respect to end A associated with an in-plane bending moment $M_2(\alpha_o)$ at end B is given by the rather simple expression

$$\theta_2 = \frac{k_2}{EI} \int_0^{\alpha_o} M_2 R \, d\alpha , \tag{6}$$

where R is the bend radius of the elbow centerline, k_2 is the in-plane bending flexibility factor defined by $k_2 = \theta_2/(\theta_2)_{nom}$, and $(\theta_2)_{nom}$ is the end rotation of a strength-of-matrials model of a curved bar. For an elbow or curved pipe with zero internal pressure, subparagraph NB-3686.2 of the ASME Code* (Ref. 2) gives $k_2 = 1.65/h$, where $h = t R/r^2$.

Complete expressions for out-of-plane and torsional rotations for elbows in terms of flexibility factors k_1 and k_3 are somewhat more complicated because an out-of-plane moment M_1 at the loaded end of a 90° elbow must be balanced by a torsional moment at the reference end, and vice versa. For a more in-depth discussion of flexibility factors for elbows and curved pipe, see Ref. 3.

For branch connections and tees, flexibility factors have been prescribed in industrial piping codes since 1955; for Classes 2 and 3

---

*The terms "Code" or "ASME Code," as used herein, refer to Sect. III of the ASME Boiler and Pressure Vessel Code, Nuclear Power Plant Components.[2]

nuclear power plant piping, flexibility factors have been included in the ASME Code since 1971. In those documents, the flexibility factor is given as $k = 1$. However, they do not define a strength-of-materials component model for which a nominal rotation θ_{nom} can be determined for use with the flexibility factor definition, Eq. (2). As a consequence the intent of those codes has never been clear. Apparently, most piping system analysts have interpreted the codes to mean simply that the junction between the branch and run centerlines is to be modeled as a rigid joint, as indicated at Point 1 in Fig. 1(a). This interpretation, however, is completely inadequate to describe the actual behavior of branch connections and tees in a real piping system.

Figure 1(d) shows a schematic diagram of a branch connection as modeled in present day nuclear Class 1 piping system analyses. This model has a rigid junction between the branch and run centerlines at point P and a rigid linkage between points P and S equal in length to the run pipe radius. Additional nozzle flexibility can be introduced into the model by including a point spring at S.

Markl's definition of a flexibility factor is not entirely adequate for a branch connection modeled like Fig. 1(d) because there is no well-defined "length of straight pipe" for which θ_{nom} can be determined. To accommodate this model, as well as the other piping system component models, Markl's definition of a flexibility factor needs to be broadened to something like the following:

A flexibility factor for piping system analysis is the ratio of the angular rotation or linear displacement of the point in question produced by a moment or thrust load to the angular rotation or linear displacement of the strength-of-materials model of the part produced by the same moment or thrust load.

With this definition, θ_{nom} can be determined precisely by analyzing the one-dimensional strength-of-materials beam model of a branch connection that is actually used in the piping system flexibility analysis; also, the flexibility factor k as defined by Eq. (2) can be determined from a knowledge of the real behavior of the structure.

Theoretically, there would be a 6 × 6 matrix of moment-rotation flexibility factors associated with the branch connection model shown in Fig. 1(d). Because the matrix is symmetric, there would be 21 independent flexibility factors, 4 identically 0 from symmetry arguments, leaving 17 non-zero flexibility factors to be determined from experimental or theoretical studies. The limited available data, however, indicate that only two of these, k_i for in-plane and k_o for out-of-plane moment loads on the branch, are significant.

For Class 1 nuclear piping, the ASME Code now contains a precise definition of the component model, as well as the two flexibility factors k_i and k_o to be used for the analysis of branch connections. The strength-of-materials model shown in Fig. NB-3686.5-1 of the Code and included here as Fig. 2 includes a "point spring" at S of negligible length with a rotational characteristic equal to $k \theta_{nom}$, where θ_{nom}, given by

$$\theta_{nom} = M(d/EI_b) ,$$ (7)

ELEMENT OF NEGLIGIBLE LENGTH
WITH LOCAL FLEXIBILITY FOR
M_{x3} AND M_{y3} SUCH THAT ϕ
ACROSS THE ELEMENT IS EQUAL
TO kMd/EI_b

BRANCH

RUN

RIGID LENGTH

RIGID JUNCTURE
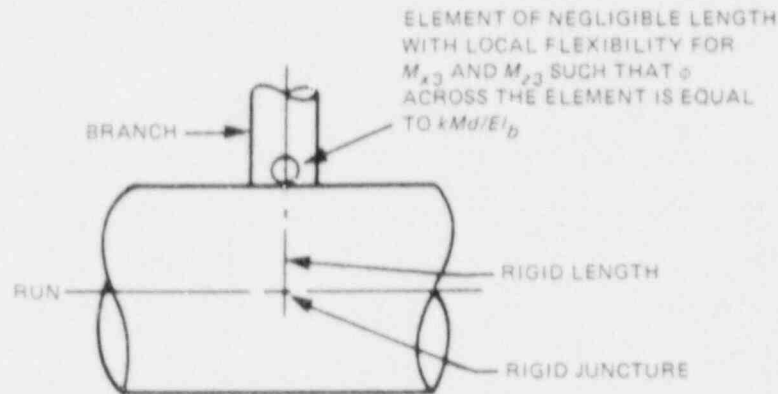
Fig. 2. Definition of flexibility factors for branch connections, from Fig. NB-3686.5-1, Sect. III, ASME Code (Ref. 2).

is the simple beam equivalent rotation for a one-diameter length of branch pipe. The two flexibility factors k_o and k_i are given in subparagraph NB-3686.5 of the Code as

$$k_o = 0.1 \ (D/T)^{3/2} \ [(T/t_n) \ (d/D)]^{1/2} \ (t/T) \ , \tag{8}$$

$$k_i = 0.2 \ (D/T) \ [(T/t_n) \ (d/D)]^{1/2} \ (t/T) \ , \tag{9}$$

where d,D and t,T are the outside diameters and wall thicknesses of the branch and run pipes, respectively; t_n is the nozzle reinforcement thickness (shown in Fig. 3) for four commonly used nozzle designs.

The preceding discussion has been framed in terms of flexibility factors because since 1955 the piping codes have given design guidance for flexibility factors. Many current computer programs for piping system analysis, however, use a stiffness formulation rather than the flexibility formulation used in the earlier analysis methods. A stiffness formulation involves the inverse of the flexibility (e.g., moment per unit rotation rather than rotation per unit moment). When the design guidance is given in terms of flexibility factors, as for elbows, for example, these computer programs first evaluate the flexibility matrix and then form its inverse to obtain the stiffness matrix. The stiffness matrix for branch connections is formed in the same manner as for elbows.

2.2 SIGNIFICANCE OF NOZZLE FLEXIBILITY

The definition of flexibility factors for branch connections based on the analytical model of Fig. 2,

$$\theta = k \ (Md/EI_b) \ , \tag{10}$$
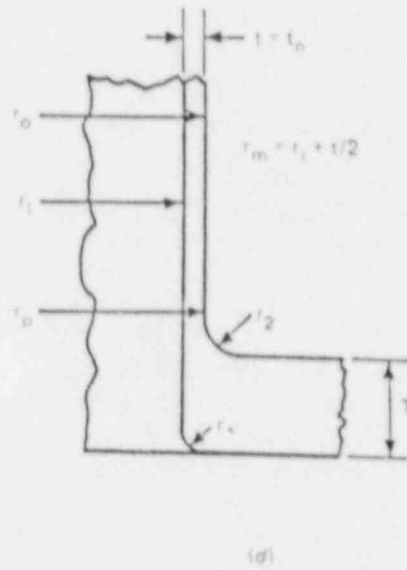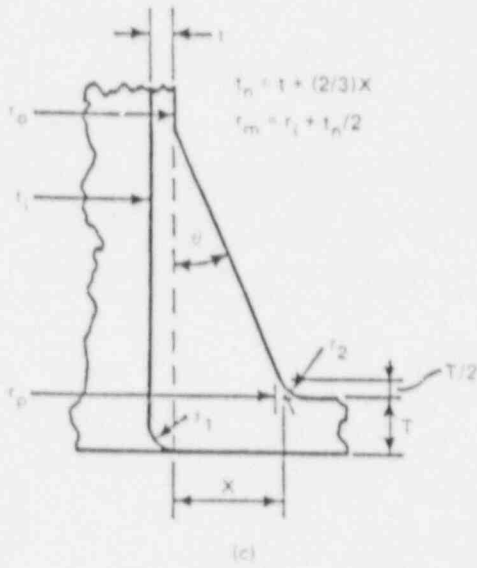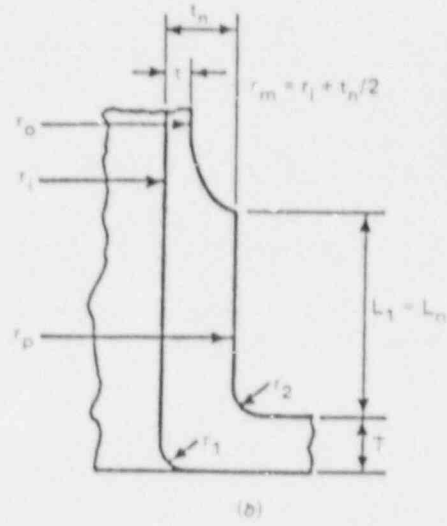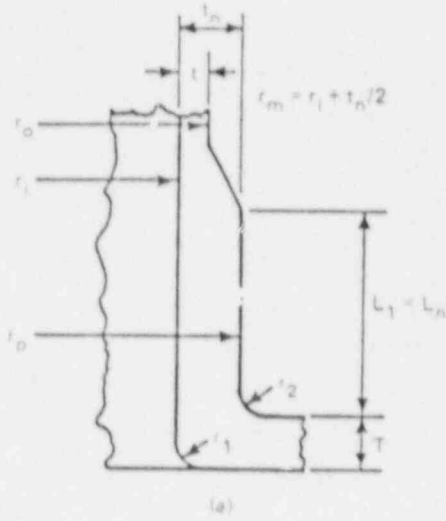
Fig. 3. Nozzle configurations associated with Code definition of t_n.

gives the angular rotation of the branch caused by local distortion of
the intersecting shells in terms of the k factor and the nominal rotation
of a one-diameter length of branch pipe.

The influence of including branch connection flexibility factors in
a piping system analysis will be different for different piping systems.
If k is small (e.g., 2 or 3) relative to the overall flexibility of the
branch pipe or if k is small relative to the flexibility provided by
other nearby piping components, such as elbows, then including k for the
branch connections in the piping system analysis will have only a minor
influence on the calculated forces, moments, and displacements. Con-
versely, of course, if k for the branch connection is large relative to
the other piping system flexibilities, then it would have a major influ-
ence. The largest influence would be to reduce the magnitude of the
calculated forces, moments, and resulting stresses at the branch connec-
tion. If pipe supports were located nearby or if the terminal end of the
piping system were actually a nozzle in a vessel instead of a rigid
anchor, then including a large value for k would significantly reduce the
calculated forces and moments acting on those supports. This, in turn,
might permit the elimination of some dynamic snubbers, massive pipe sup-
ports, or special shell reinforcements. The influence would be smaller
at more-distant locations and would depend, as well, on how other flex-
ibilities (e.g., from elbows) were distributed in the piping system.

A recent sensitivity study on the influence of various factors that
might affect the accuracy of piping system analyses[4] showed that (1) the
influence of including appropriate flexibility factors for nozzles in
tanks and branch connections in run pipes with large D/T ratios can be to
reduce the calculated moments and stresses by several orders of magnitude
and (2) it is not possible to define a flexibility factor that is *conser-
vative* for either static or dynamic loadings.

The reason that a conservative flexibility factor cannot be defined
is that a change in the flexibility of some portion of a piping system
leads to a change in loads on other portions of the piping system, in-
cluding the possibility that loads and resulting stresses in other por-
tions of the piping will actually *increase* with an increase in a given
flexibility factor rather than decrease as one might expect. Accord-
ingly, even for a static loading, one cannot define a conservative flex-
ibility factor. For dynamic loadings, a change in flexibility will also
change the response frequencies of the piping system. If the forcing
functions (e.g., from an earthquake) vary with frequency, then an in-
accurate flexibility factor may indicate that the piping response is off-
the-peak of the forcing functions; with an accurate flexibility factor,
however, the calculated piping response may be on-the-peak. Accordingly,
the best that can be hoped for is reasonable accuracy with a small amount
of uncertainty.

2.3 DIMENSIONAL PARAMETERS OF INTEREST

Various studies of nozzle flexibility indicate that reasonably
accurate design equations can be developed in terms of dimensionless
ratios of the characteristic dimensions of the nozzle and vessel or run

pipe. These include the diameter and wall thickness of the vessel or run pipe (D,T); the diameter and wall thickness of the branch pipe (d,t); the diameter, thickness, and length of the nozzle reinforcement (d_n, t_n, L_n); and a characteristic axial length L for the vessel or run pipe.

To get a better understanding of the types and sizes of branch connections and vessel nozzles that are actually used in nuclear power plant construction, we asked a number of utilities, architect engineers, and nuclear steam system supply (NSSS) vendors to provide actual design data from one or two typical nuclear plants of their own choosing. Seven organizations responded with a substantial amount of dimensional and design practice data.[5-11] In alphabetical order, they were Duke Power Company; FRAMATOME of Paris, France; General Electric Company; Sargent and Lundy Engineers; Stone and Webster Engineering Corporation; Tennessee Valley Authority; and Westinghouse Electric Corporation. Duke Power Company also provided a complete listing of the nozzles in the auxiliary tanks and vessels for one of their modern nuclear power plants.

Analysis of the survey data indicates that branch connections are used in straight pipe that ranges in diameter from 1 to 42 in. nominal pipe size (NPS) and wall thicknesses that range from sched. 40 to sched. 160. The range of diameter-to-thickness ratios for the run pipes is $\sim 5 < D/T < 115$. Branch sizes cover the complete parameter range $0.02 < d/D < 1.0$ with most of the smaller-size branch connections $d < 2$ in. made from welded-on American National Standards Institute (ANSI) standard half-couplings or welding bosses. The wall thickness for half-coupling or welding bosses is considerably greater than for the corresponding nominal pipe size.

Branch connections larger than 2 in. in diameter are usually made with ANSI standard or Manufacturers Standardization Society (MSS) standard butt welding tees; specialty product contoured fittings, such as WFI International Vesselets or Bonney Forge Sweepolets; or specialty product reinforced fittings, such as WFI Pipettes or Bonney Forge Weldolets. The ANSI and MSS standard butt welding tees range in size up to the maximum run pipe sizes but are restricted to branch-to-run diameter ratios in the range of $\sim 1/3 < d/D < 1.0$. The specialty product fittings are normally used with run pipe sizes larger than 4 in. (NPS) for branch connections with d/D less than ~ 0.8.

Diameter-to-thickness ratios for the branch d/t, including nozzle reinforcement, cover about the same range as for the run pipe with, however, more usage in the smaller values $d/t < 5$ because of the greater wall thickness of half-couplings and welding bosses $(2 < d/t < 100)$. Branch thickness-to-run thickness ratios t/T seem to be fairly evenly distributed over the range $0.2 < t/T < 2.0$.

For nozzles in reactor pressure vessels and steam generators, the utility data indicate that the dimensional ratios fall within the same parameter ranges as for branch connections. For nozzles in the nuclear plant auxiliary tanks, however, the parameter ranges are somewhat different. The one nuclear plant for which we have data has ten ASME Code Class 2 or 3 auxiliary tanks ranging in diameter from 2 to 40 ft (24- to 480-in. OD) with wall thicknesses ranging from 7/32 to 5/8 in. The diameter-to-thickness ratios D/T are fairly evenly distributed between ~ 75 and 2000. The minimum and maximum nozzle diameters range between 1/2 and 30 in., essentially independent of the tank diameter, so that the

ratios $(d/D)_{max}$ and $(d/D)_{min}$ decrease with increasing D/T (Fig. 4). The range of nozzle diameter-to-thickness ratios d/t is fairly evenly distributed between ~5 and 100 over the full range of D/T (Fig. 5). The range of nozzle thickness-to-vessel thickness t/T is shown in Figs. 6 and 7 as a function of D/T and d/D, respectively. In both figures, t/T is somewhat randomly distributed between 0.2 and 1.5, about the same range as noted for branch connections in pipe. Figure 7 also shows that most of the nozzles in the auxiliary tanks are thinner walled than the vessels (i.e., t/T < 1.0), reflecting the need for structural stability in the tank wall rather than internal pressure resistance as a major design criterion.

Another dimensional parameter is of primary interest to both branch connections in piping and nozzles in vessels; that is, the axial distance along the run or vessel from the branch/nozzle to the first major discontinuity. In piping, this distance L/2 might be the distance from the branch centerline to the nearest support or the next branch connection or
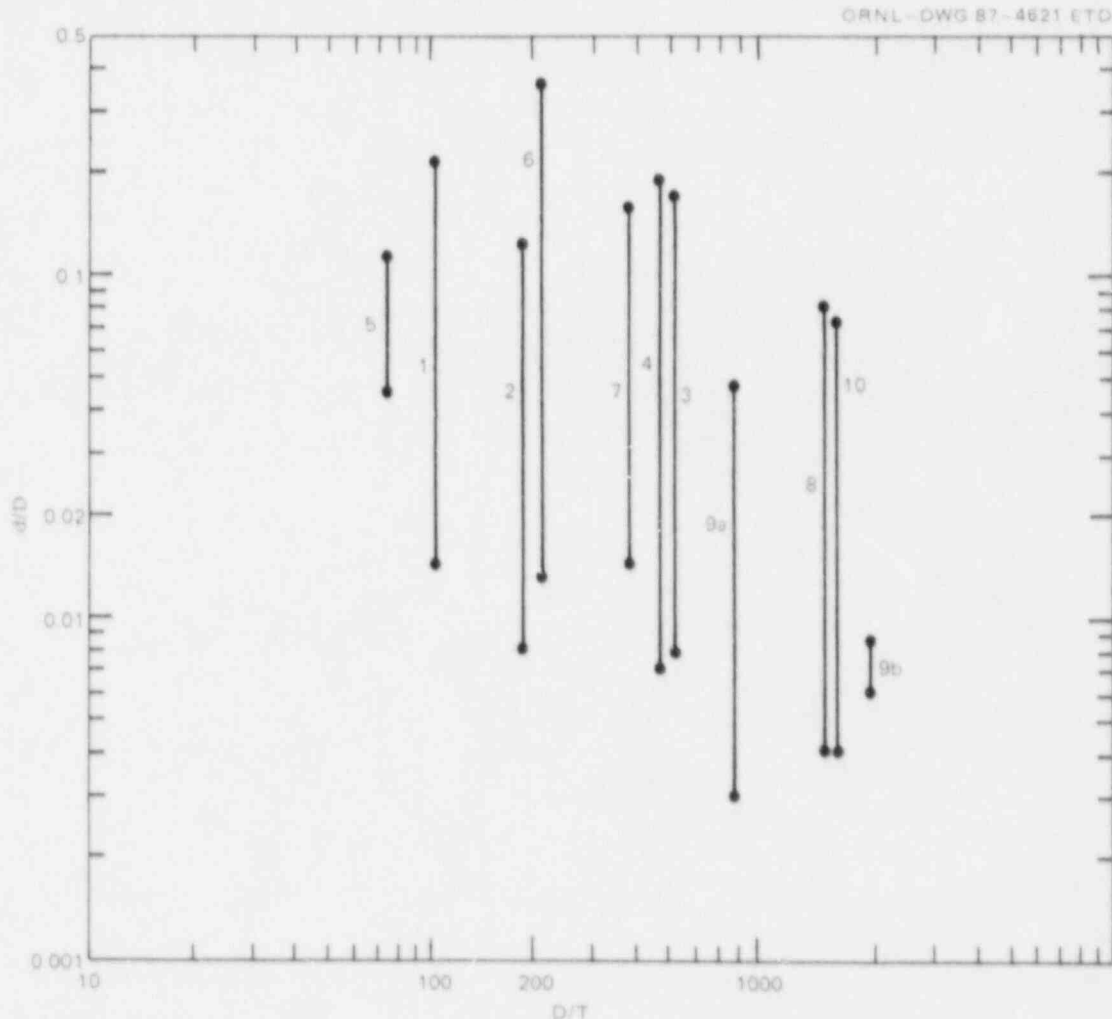
Fig. 4. Diameter ratios (d/D) for auxiliary tank nozzles in nuclear power plant as function of tank diameter-to-thickness ratio (D/T).
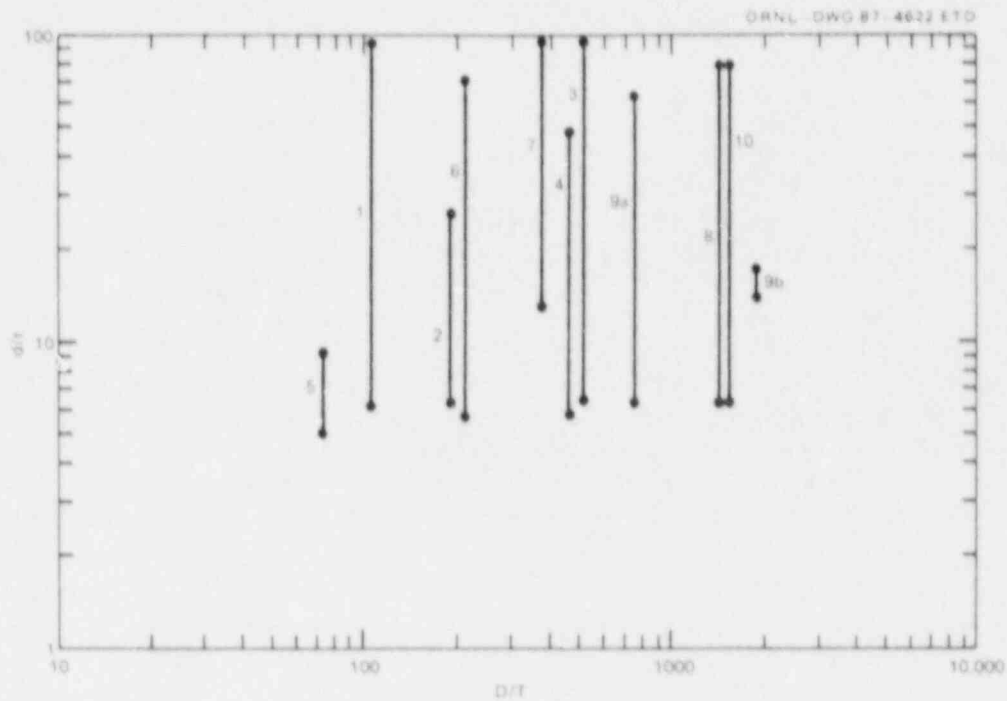
Fig. 5. Nozzle diameter-to-thickness ratios (d/t) for auxiliary tank nozzles in a nuclear power plant as function of tank diameter-to-thickness ratio (D/T).
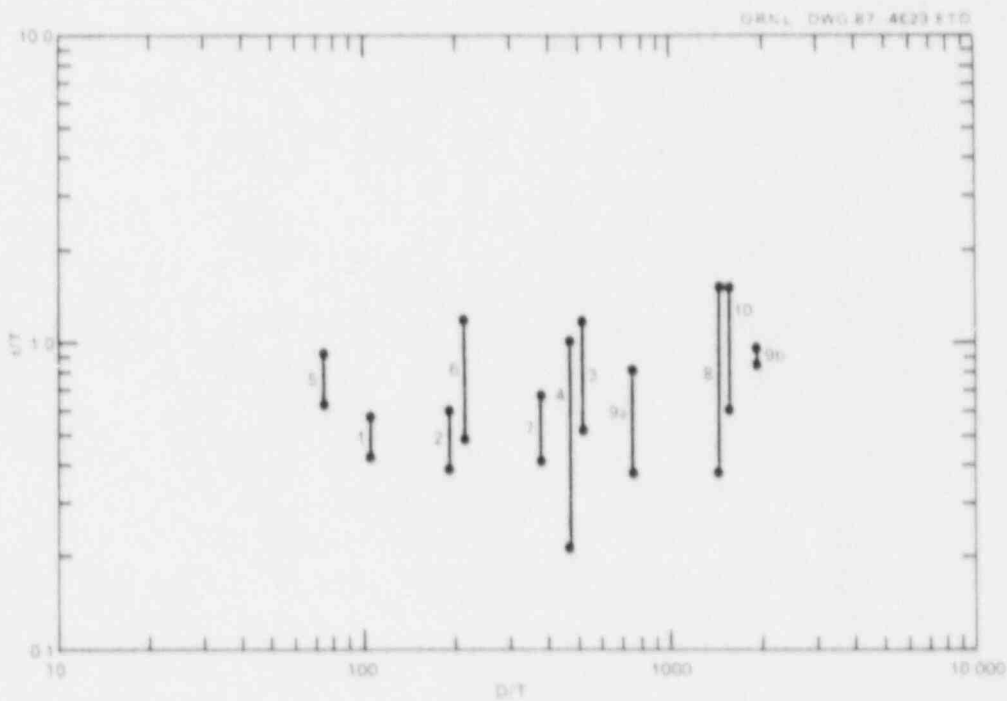
Fig. 6. Nozzle-to-tank wall thickness ratios (t/T) for auxiliary tank nozzles in nuclear power plant as function of tank diameter-to-thickness ratio (D/T).

ORNL—DWG 87—4624 ETD
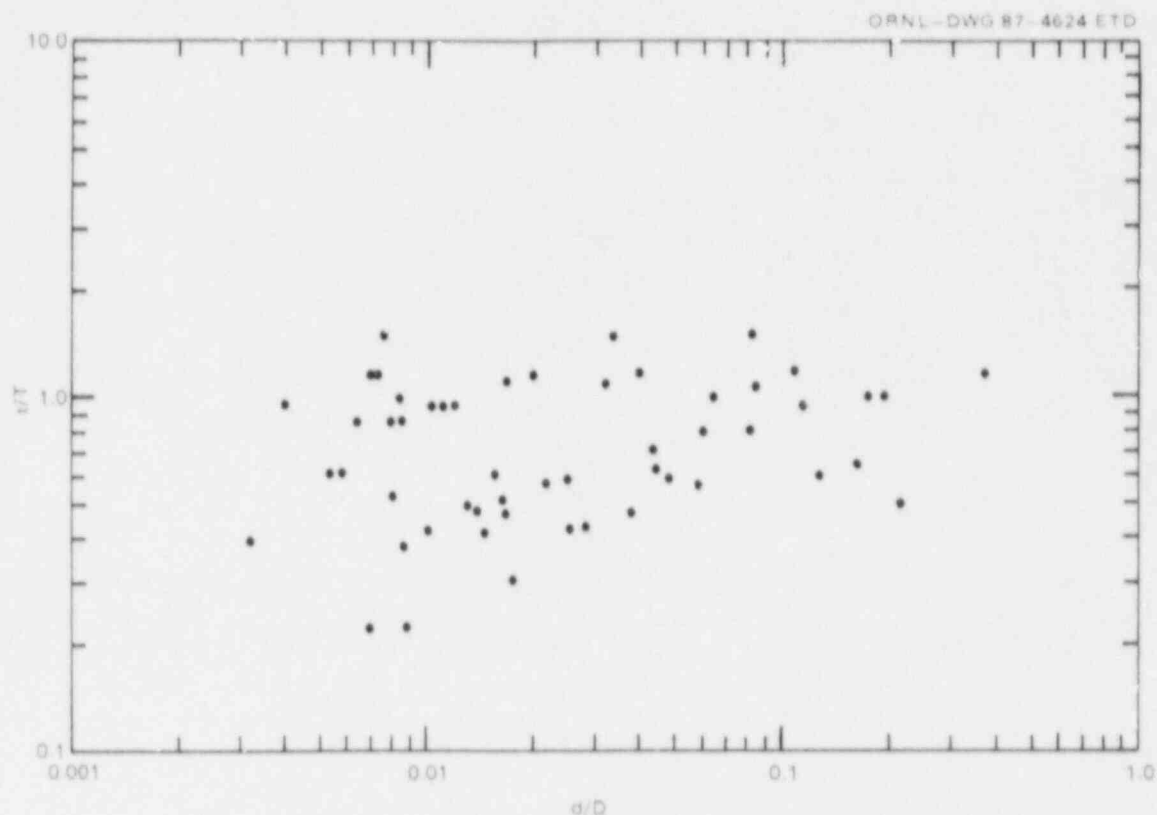
Fig. 7. Nozzle-to-tank wall-thickness ratios (t/T) for auxiliary tank nozzles in nuclear power plant as function of nozzle-to-tank diameter ratios (d/D).

other piping component. In vessels, L/2 might be the axial distance from the nozzle centerline to the vessel head(s), shell stiffner, or major discontinuity. This distance is important because the amount of constraint provided at the pipe/vessel "ends" will have some influence on the local flexibility at the branch/nozzle-pipe/vessel intersection. If L is long enough, it should be possible to separate the local and global bending effects and, thus, treat the nozzle as "isolated." If L is not long enough, then some consideration must be given to the pipe/vessel "end" boundary conditions. For example, Bijlaard's theory (discussed later) puts a practicable limit on L/R of 4.

For branch connections in pipe, the axial distance to the first major discontinuity will often be 4R or greater. For nozzles in vessels, however, L/R > 4 will be the exception rather than the general rule. The larger-diameter auxiliary tanks discussed above, for example, were generally less than twice as tall as their diameter. In many cases, the nozzles are located very close to either the top or bottom heads. Thus, L/R may not be a significant parameter for piping; for vessel nozzles, however, it probably will be.

3. METHODS FOR ESTIMATING NOZZLE FLEXIBILITY FACTORS

Analytical methods for calculating piping design flexibility factors have been developed in the past from three basic sources: thin-shell theory, finite-element analysis, and experimental load-displacement data. The purpose of this section is to introduce those methods that, in the authors' opinion, are most useful for design purposes. Later in this report, we will compare the various methods with available benchmark data as a basis for further development work. The methods discussed here are (1) the ASME Code equations,[2] (2) Bijlaard's theory,[12] and (3) Steeles' theory.[13,14] Two studies on the flexibility of nozzles in spherical shells are also discussed briefly.

3.1 ASME CODE EQUATIONS

As noted earlier, subsubparagraph NB-368   of the ASME Code gives equations for calculating branch connection flexibility factors for in-plane and out-of-plane moment loads. The basis for those equations [Eqs. (8) and (9) in Sect. 2] was given by Rodabaugh and Moore[15] in 1979. Briefly, they are "best-fit" equations based on finite-element analyses of 25 nozzle-reinforced models (see Table 12 of Ref. 15). The types of reinforcement considered were those shown earlier in Fig. 3.

The Code equations are limited to isolated radial nozzles with $D/T < 100$ and $d/D < 0.5$. They were validated by comparison with independent finite-element analyses of five other models and with experimental data from ten test models with dimensional ratios $D/T < 100$ and $d/D < 0.64$ (see Table 15 of Ref. 15). Because the equations were empirically developed from a limited data base, extrapolation to nozzles with $d/D > 0.5$ or $D/T > 100$ is prohibited by the Code (NB-3686.5). [Note: The paragraph reference given in NB-3686.5 should be NB-3683.8(a) rather than NB-3338.]

3.2 BIJLAARD'S THEORY

In the mid-1950s, Prof. Bijlaard of Cornell University published a series of papers on the stresses and displacements in a thin-walled cylindrical shell, simply supported at the ends and loaded with either a radial point load or a distributed load on a small, rectangular region centered midway between the ends. The loading on the rectangular region could be distributed in an arbitrary manner, but he discussed in detail only those three cases that represent a thrust load and in-plane and out-of-plane moment loadings on the rectangle (Fig. 8). His theoretical solution,[12] based on the equations of shallow-shell theory, was given in terms of infinite double Fourier series that are conditionally convergent with the number of terms required for a stable solution dependent mainly on the length-to-radius ratio $a = L/R$ and the diameter-to-thickness ratio D/T of the cylindrical shell. Bijlaard was aware of the limitations of

ORNL-DWG 87-4625 ETD
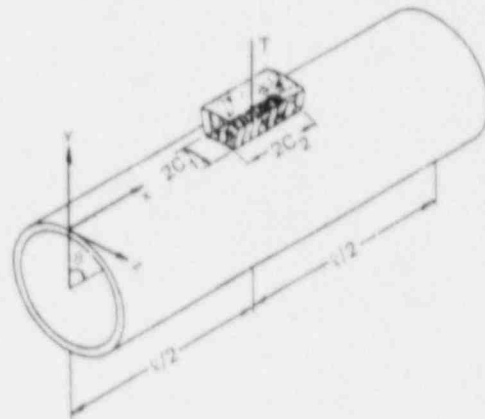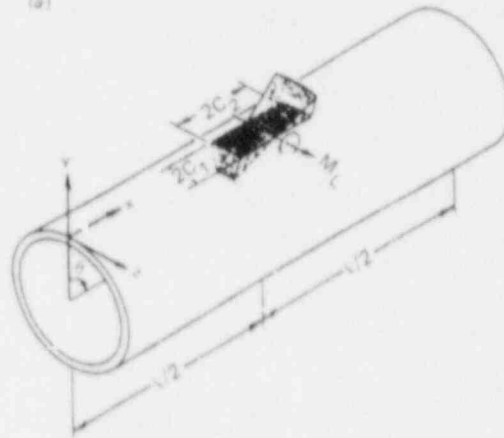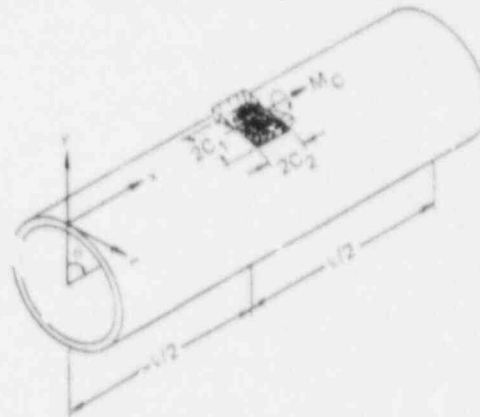
Fig. 8. Bijlaard's loading assumptions for thrust and for in-plane and out-of-plane moments on a nozzle. (a) Uniform radial loading, (b) longitudinal moment loading, (c) circumferential moment loading.

his theory but essentially dismissed the matter by pointing out (correctly) that for engineering structures of common interest, his solution was relatively easy to use and gave results of acceptable accuracy. (See the discussion in Ref. 12.) In later publications[16-19] Bijlaard gave extensive numerical results obtained using $L/R = 4$ and $D/T < 100$.

Although Bijlaard's theoretical model does not include either an opening (hole) in the cylindrical shell or an attachment to the cylindrical shell, his solution has been used extensively during the past 30 years as the theoretical basis for calculating both flexibility factors and maximum stresses in nozzle-cylindrical vessel structures. In 1967 Rodabaugh and Atterbury (R&A)[20] used Bijlaard's theory, along with other thin-shell theory solutions and available experimental data, as reference material for developing flexibility design guidance for the ASME Code. That guidance was extended in 1977 (Ref. 21) and again in 1979 (Ref. 15) to the present Code equations.

In 1965 the Welding Research Council (WRC) published Bulletin No. 107 (Ref. 22), which includes a detailed methodology for calculating stresses caused by out-of-plane moments, in-plane moments, and radial loads on nozzles in cylindrical shells. The design data given in WRC-107 are based in large part on Bijlaard's theory but include large empirical adjustments to account for the shell opening and the discontinuity stresses at the nozzle-shell junction, as indicated by the experimental data available at that time. It is, therefore, not correct to state or to imply that Bijlaard's theory and WRC-107 are equivalent. It is only correct to state that Bijlaard's theory was used as a guide in developing the design method. As additional experimental data have become available, WRC-107 has been revised several times since 1965 with the latest revision published in 1979. It is still limited, however, to parameter values of $d/D < 0.5$ and $D/T < 600$.

3.2.1 Murad and Sun (M&S) Design Charts

Although Bijlaard's theory gives displacements that are readily translated into flexibility factors, WRC-107 does not give any flexibility data or flexibility design guidance. In 1984 M&S[23] evaluated Bijlaard's displacement equations to obtain design curves for radial thrust and for in-plane and out-of-plane moments over the range of diameter-to-thickness ratios $20 < D/T < 300$ and d/D ratios from 0.05 to 0.55. They also included the influence of internal pressure. In all cases, they used an axial length parameter of $L/R = 4$. Their curves for the zero internal pressure case are included here as Figs. 9-11.

The parameters used by M&S in Figs. 9 and 10 for the moment loadings can be converted to flexibility factors consistent with the Code definition by the following:

$$k = (a^3/K) \, \pi E \, (d/D)^2 \, (t/T)/(D/T) , \tag{11}$$

where $a^3/K = R^3/K_c$ or $a^3/K = R^3/K_L$ and $\beta = d/D$.
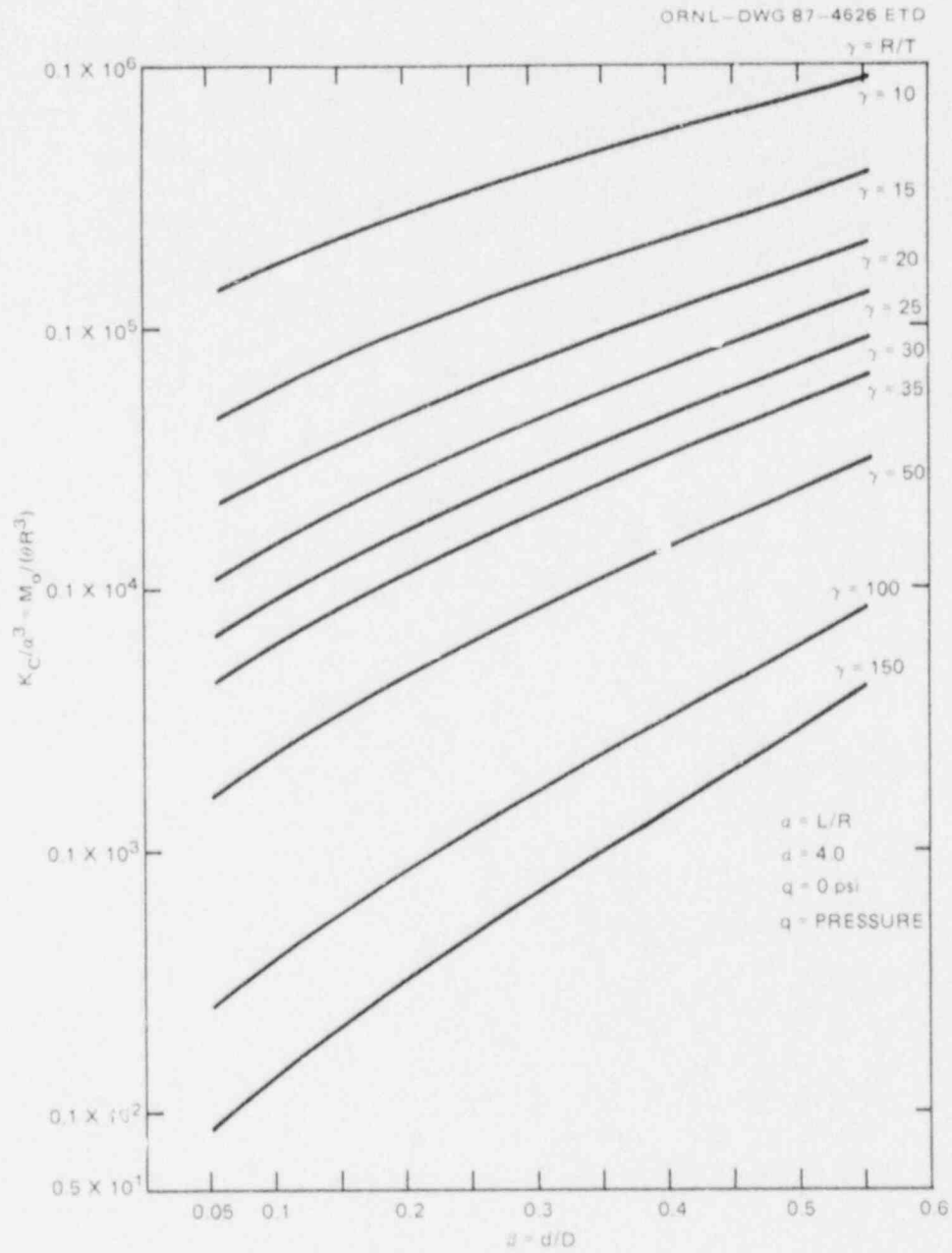
Fig. 9. M&S[23] stiffness factor K_c/a^3 for out-of-plane moment loads M_o.
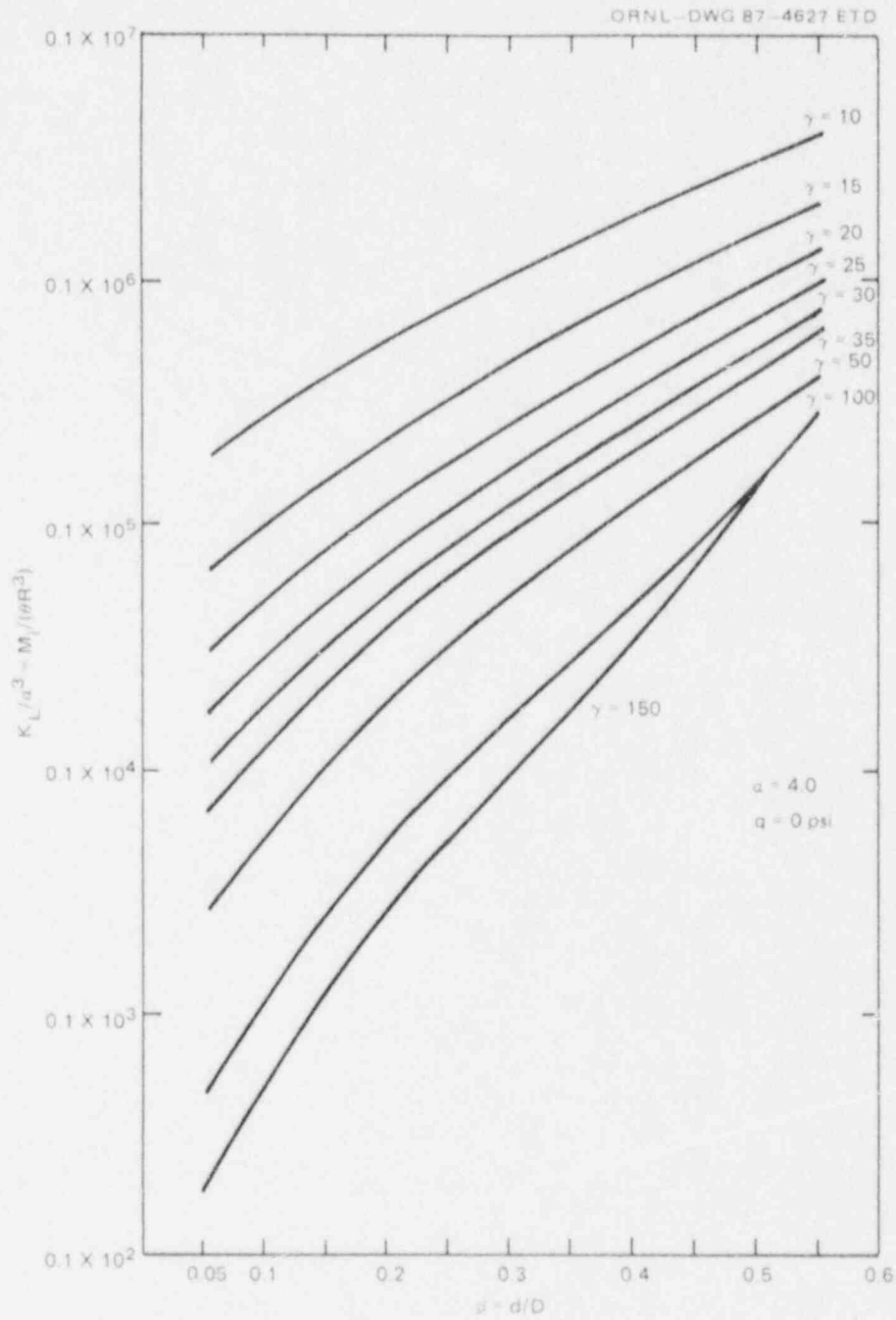
Fig. 10. M&S[23] stiffness factor K_L/a^3 for in-plane moment loads M_i.
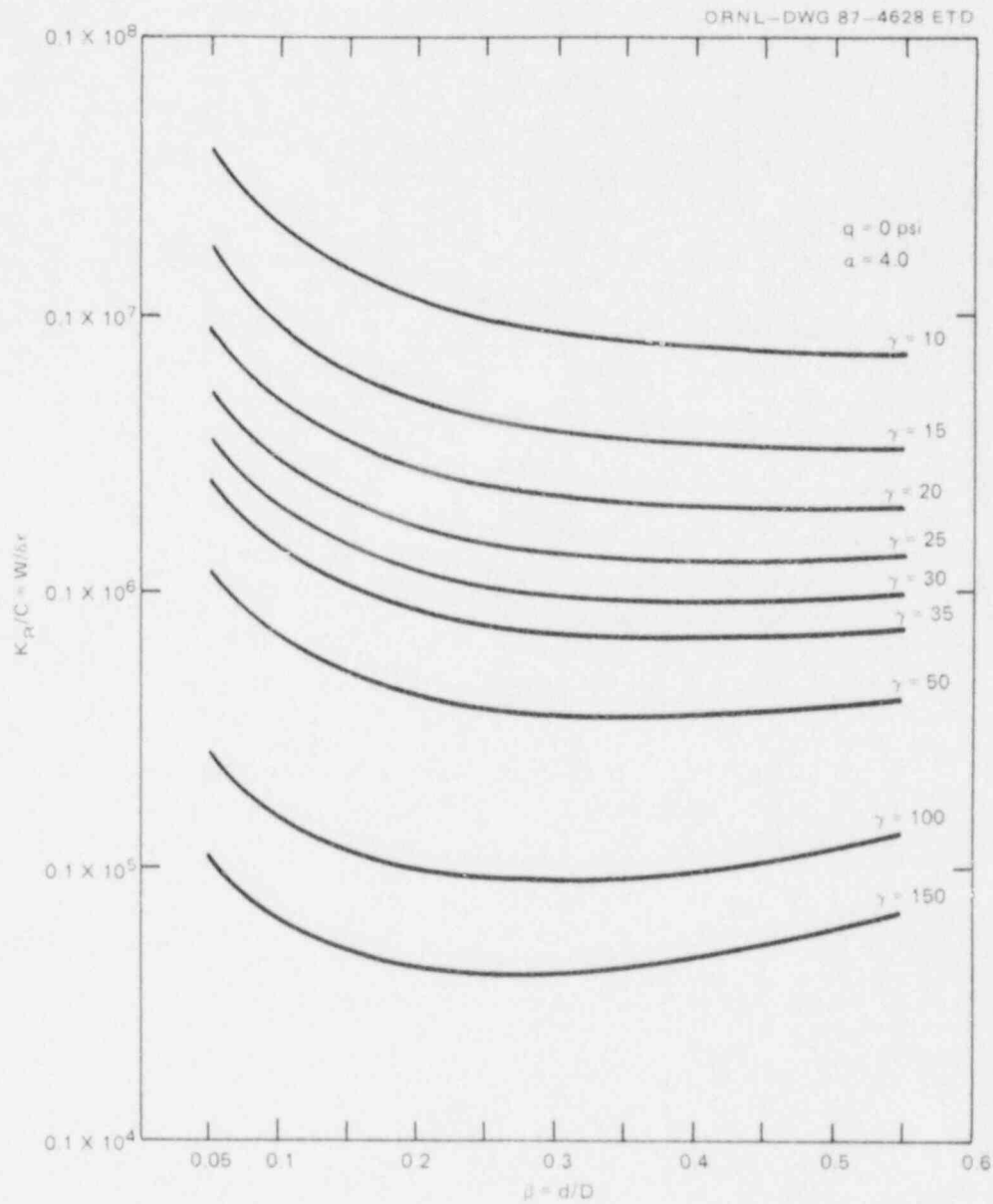
Fig. 11. M&S[23] stiffness factor K_R/C for thrust loads W, revised October 1984.

3.2.2 LUGS Computer Program

Because Bijlaard's theory does not consider the existence of an opening in the cylindrical shell, it is more appropriate for the design of solid attachments than for the design of nozzles. In 1974 Dodge[24] and Rodabaugh, Dodge, and Moore[25] evaluated Bijlaard's equations, including certain modifications suggested by the reviewers of Bijlaard's original paper, and developed guidance for the design of lug attachments

to straight pipe. The computer program LUGS,[26] written by Dodge, calculates the displacements, as well as the stresses, in the cylindrical shell so that flexibility factors, comparable to those obtained from M&S's design charts, can be obtained. The computer program LUGS also considers the length parameter L/R as an independent variable so that its influence on the flexibility can be studied. The flexibility factor $\theta^* = \theta/(M/ER^3)$ given in the program output can be converted to the Code definition by

$$k = \pi \; \theta^* \; (d/D)^2 \; (t/T)/(D/T) . \tag{12}$$

Flexibility factors based on Bijlaard's theory are compared in Table 1 as calculated by each of the three methods — R&A, M&S, and

Table 1. Comparisons of flexibility factors based
on Bijlaard's theory ($t/T = 1$, $L/R = 4$)

D/T	d/D	Out-of-plane moment k_o			In-plane moment k_i		
		R&A[a]	M&S[b]	LUGS[c]	R&A	M&S	LUGS
20	0.05	1.1	0.9	1.0	<1.0	0.62	0.67
	0.10	3.3	2.6	3.0	2.0	1.9	1.8
	0.20	8.5	7.5	8.1	4.0	3.8	3.8
	0.30	14.0	11.8	13.6	5.0	5.0	5.1
	0.50	20.0	17.8	23.4	4.9	5.4	5.7
50	0.05	5.7	4.7	4.9	3.4	2.9	3.2
	0.10	16.0	13.0	14.0	8.4	7.0	7.6
	0.20	36	33	34	13	12	12.7
	0.30	50	45	52	13	13	13.8
	0.50	57	57	74	9	10	11.7
100	0.05	20	16	17	11	9.8	10.2
	0.10	50	43	45	23	20	20.6
	0.20	100	94	99	27	27	27.4
	0.30	135	120	137	22	23	25.3
	0.50	130	130	168		15	17.4

[a]From design charts, R&A[20] with Bijlaard's parameters $\beta = 7/8 \; d/D$, $\alpha = L/R = 4$.

[b]From design charts, M&S[23] with Eq. (11) of text, Bijlaard's parameters $\beta = 7/8 \; d/D$, $\alpha = L/R = 4$.

[c]From LUGS computer program,[26] with Eq. (12) of text, Bijlaard's parameter $\beta = 7/8 \; d/D$, $\alpha = L/R = 4$.

LUGS — for the parameter ranges $20 < D/T < 100$ and $0.05 < d/D < 0.5$ for $t/T = 1$ and $L/R = 4$. Each of the methods gives essentially the same results for $d/D < 0.3$; the differences for $d/D = 0.5$ are attributed to the number of terms evaluated in the solution series.

To study the influence of the length parameter $\alpha = L/R$ on k, we permitted the LUGS program to compute a value α^*, using a convergence algorithm built into the program. The results, over the same range of parameters as Table 1, are given in Table 2. The calculated flexibilities are obviously influenced by L/R, apparently much more for k_o than k_i and for the larger values of D/T and d/D. This suggests that any design method based on Bijlaard's theory should be tempered by comparison with experimental data over the full range of intended application.

Table 2. Influence of L/R on computed flexibility factors
based on Bijlaard's theory and LUGS program

D/T	d/D	Out-of-plane moment				In-plane moment			
		L/R	k_o	L/R	k_o	L/R	k_i	L/R	k_i
20	0.05	4	1.0	7.4	1.1	4	0.67	7.4	0.67
	0.10		3.0		3.3		1.78		1.79
	0.20		8.1		9.4		3.8		3.8
	0.30		13.6		16.6		5.1		5.1
	0.50		23.4		31.2		5.7		5.8
50	0.05	4	4.9	10.4	5.5	4	3.2	10.4	3.2
	0.10		14.0		16.3		7.6		7.6
	0.20		34.2		43.3		12.7		12.9
	0.30		52		72		13.8		14.0
	0.50		74		127		11.7		12.2
100	0.05	4	17	13.4	19	4	10.2	13.4	9.9
	0.10		45		53		20.6		20.7
	0.20		99		131		27.4		27.8
	0.30		137		209		25.3		25.5
	0.50		168		355		17.4		18.6

3.3 STEELES' THEORY

Because of the inherent limitations of Bijlaard's theory and the need for more-accurate design tools for cylinder-cylinder intersections, especially for large-diameter, thin-walled vessels, the WRC Pressure Vessel Research Committee (PVRC) has been sponsoring both theoretical and experimental work on the problem for a number of years. One of those efforts resulted in the development by Steele and Steele[13,14] of

Stanford University and Shelltech Associates of a new and novel solution to the thin-shell theory equations for intersecting right circular cylinders (nozzles in cylindrical vessels). Although their theoretical solution is currently limited to d/D ratios of 0.5 or less, it overcomes many of the shortcomings of Bijlaard's theory. Whereas Bijlaard's theory is for a rectangular surface area loading on the cylinder, Steeles' theory is for two intersecting cylindrical shells, which is more appropriate for the study of nozzles in cylindrical vessels and straight pipe. Steele also used a different and more compact formulation of the thin-shell theory and a better-behaved series representation for the solution.

3.3.1 FAST2 Computer Program

Steele and Steele wrote a computer program for calculating the stresses and deformations in the nozzle and in the vessel for internal pressure and for forces and moments applied to the nozzle. The axial length of the vessel and a number of different boundary conditions at the vessel ends are input parameters. The computer program is marketed through Shelltech Associates under the acronym FAST. The program is extremely fast (2- to 3-CPU s per case on an IBM 4381 Model Z computer) and is well suited for conducting parameter studies, as well as individual analyses. The FAST2 computer program used in this study and owned by C8I Na-Con, Inc., is an improved and proprietary version of Shelltech's program. All of the FAST2 data given in this report were obtained by C8I under subcontract to Oak Ridge National Laboratory (ORNL).

3.3.2 WRC Bulletin No. 297

WRC Bulletin No. 297 (Ref. 27), published in August 1984, is an extension of WRC-107, developed by the PVRC Subcommittee on Reinforced Openings and External Openings (S/C ROEL) to cover large-diameter thin-walled vessels, D/T < 2500, as well as the vessels covered in WRC-107, D/T < 600. This new bulletin (WRC-297) incorporates the design methodology of WRC-107 in a more compact format and includes methods for calculating stresses in the nozzle, as well as in the vessel. The design stress curves given in WRC-297 are applicable to uniform wall-thickness nozzles like those shown earlier in Fig. 3(d) or Fig. 3(b) if L_n is sufficiently long. WRC-297 is based on Steeles' theory and numerical values calculated with the FAST computer program, as well as on a meager amount of experimental data for large D/T vessels.

Although the bulk of WRC-297 is concerned with calculating stresses for nozzle intersections (55 design charts), a limited amount of flexibility design guidance is given in Figs. 59 and 60, included here as Figs. 12 and 13. Both figures give stiffness values as a function of three dimensionless parameters: $\lambda = (d_o/D) \sqrt{D/T}$, $\Lambda = (L/D) \sqrt{D/T}$, and T/t. The stiffness parameters given in these figures, "α" for radial thrust load (Fig. 12) and $[M/(ET^3\theta)]$ for moment loadings (Fig. 13), can be converted to ASME Code compatible flexibility factors (as discussed in Sect. 2.1) in the following manner. For radial load W, we define the
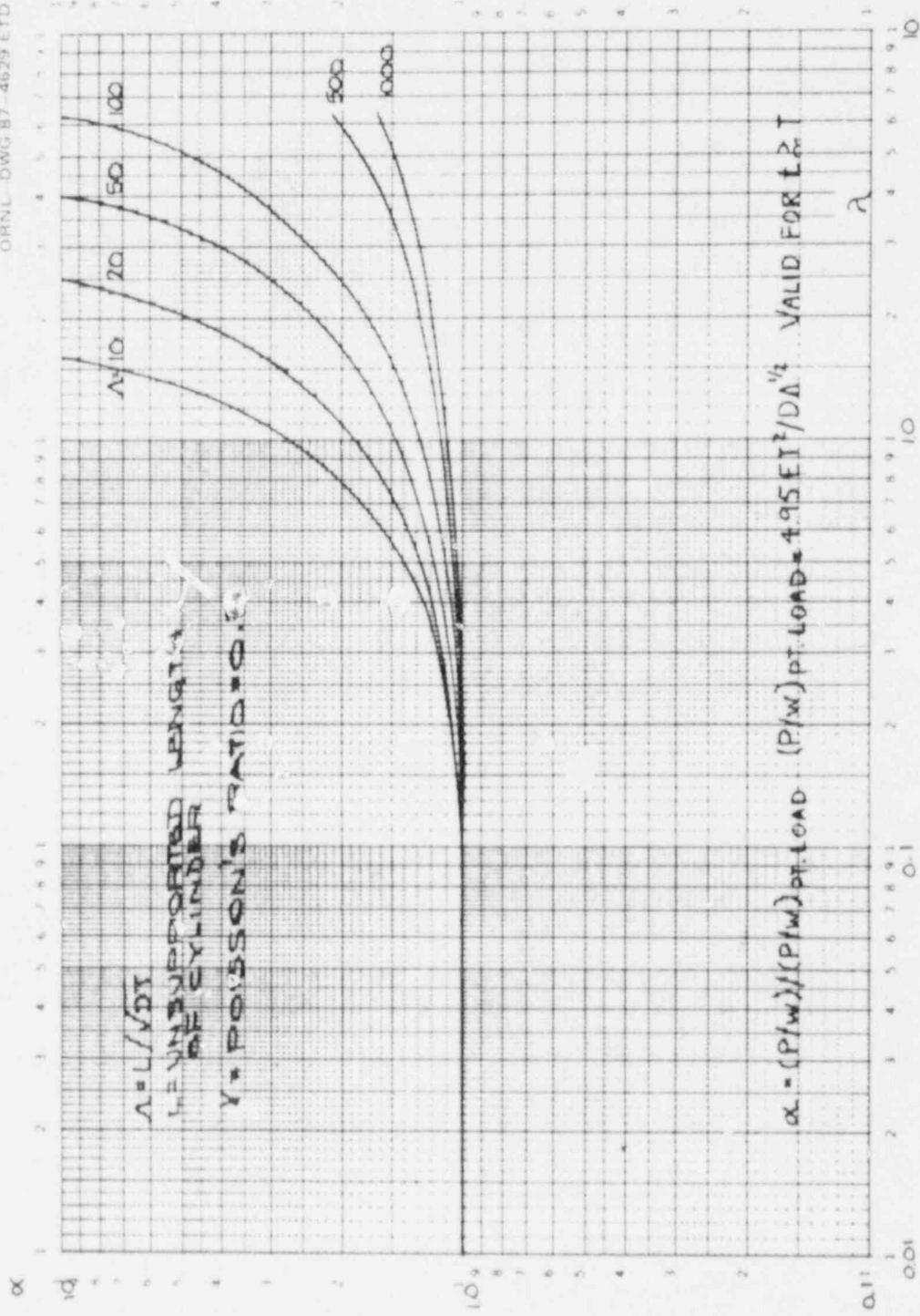
Fig. 12. Steeles' stiffness factor α for radial load, Fig. 59 of
WRC-297 (Ref. 27).
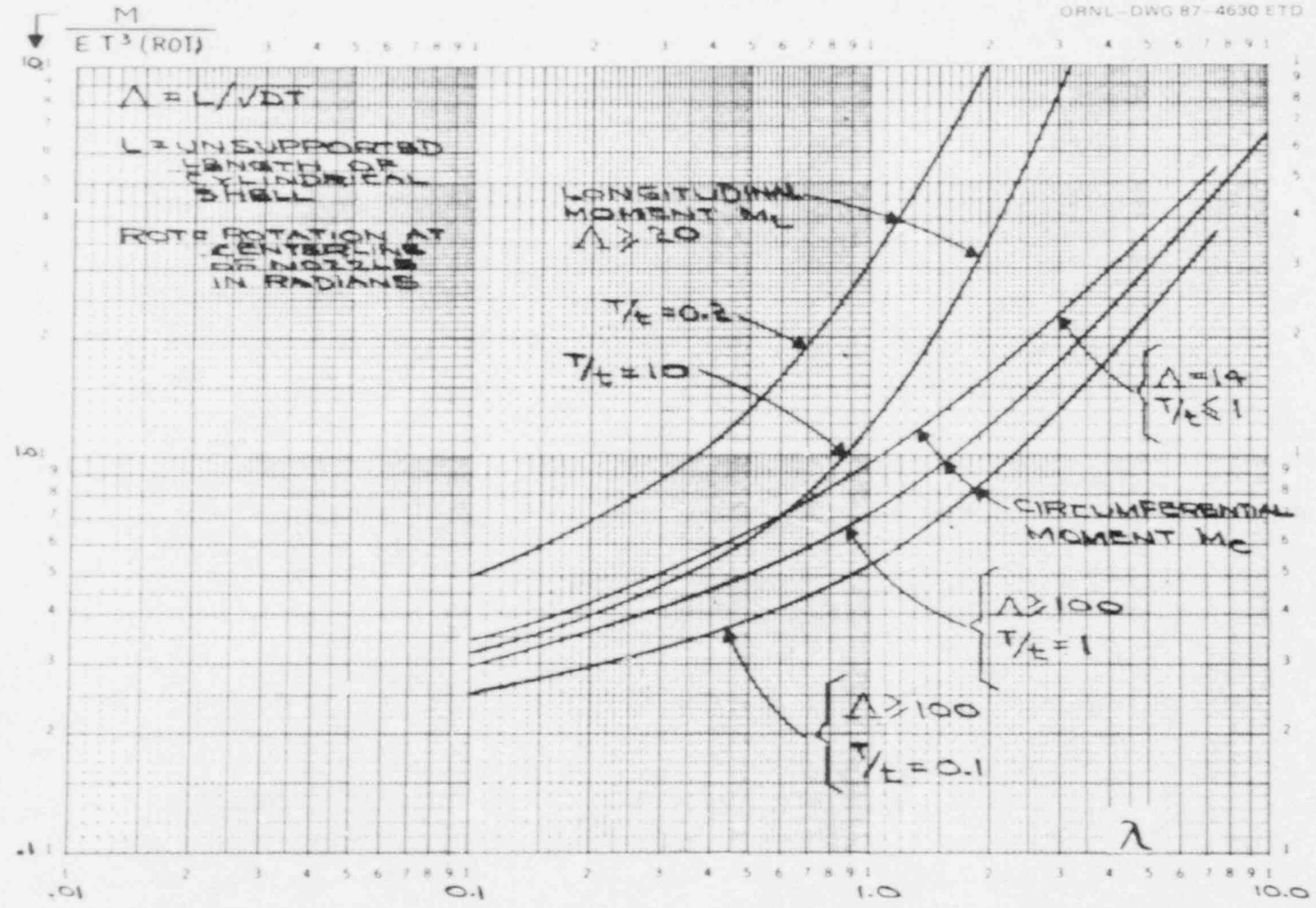
Fig. 13. Steeles' stiffness factor $M/ET^3\theta$ for moment loads M_o and M_i, Fig. 60 of *WRC-297* (Ref. 27).

flexibility factor k_w by

$$\delta = k_w (Wd/EA_n) , \qquad\qquad (13)$$

where δ is the radial shell displacement in the longitudinal plane at the nozzle intersection and A_n is the cross-sectional area of the nozzle, given by $A_n = \pi dt$. Then k_w for radial loads is given by

$$k_W = (1/\alpha) \ (\pi/4.95) \ (D/T) \ (t/T) \ \Lambda^{1/2} , \qquad\qquad (14)$$

where α is obtained from Fig. 12. For in-plane and out-of-plane moment loadings, the flexibility factors, as defined by Eq. (10) (Sect. 2.2) and with $I_b = (\pi/8) \ D^3 T$, are given by

$$k_{i,o} = (ET^3\theta/M) \ (\pi/8) \ (D/T)^2 \ (d/D)^2 \ (t/T) , \qquad\qquad (15)$$

where $(ET^3\theta/M)$ is obtained from Fig. 13 for either in-plane moments $M = M_L$ or out-of-plane moments $M = M_C$.

Figure 12, for radial thrust loading, gives stiffness values as a function of the two dimensionless parameters λ and Λ, said to be valid for "stiff" nozzles with thickness ratios $t/T \geq 1.0$. Accordingly, no design guidance is given for nozzles with $t/T < 1$, which is probably more common in design (see Fig. 7). Indeed, Fig. 12 is based on the results given by Steele for a rigid nozzle (i.e., solid rod) in an early progress report[28] to PVRC S/C ROEL (see Fig. 5 of that report). Unfortunately, WRC-297 does not discuss the significance of the parameter T/t on the radial stiffness. We, therefore, question whether its significance has been adequately investigated.

Figure 13 gives stiffness curves for both in-plane moment (M_L) and out-of-plane moment (M_C) loadings. For in-plane moment, the guidance is fairly broad, provided, of course, that the user is satisfied that $\Lambda \geq 20$ is appropriate for his application. The trend of decreasing flexibility with increasing branch wall thickness t appears reasonable. There is a problem, however, with this figure. Because it gives only two curves, for $T/t = 0.2$ and for $T/t = 10$, it is difficult to interpolate with any assurance of accuracy. For example, if $\lambda = 1.0$ and $T/t = 1.0$, the stiffness value obtained from the figure probably lies in the range of 2 ± 0.5; that, however, is an uncertainty of 50%. In subsequent comparisons with test data, it will be necessary to interpolate between these lines, and it should be understood that such comparisons involve large uncertainties in the WRC-297 data.

For out-of-plane moments, Fig. 13 gives the choice of either using the two $\Lambda \geq 100$ lines with interpolation on T/t between 0.2 and 10 or using the single line for $\Lambda = 14$, provided that $t \geq T$. For $\Lambda \geq 100$,

Fig. 13 indicates that decreasing values of t gives decreasing flexibility for out-of-plane moments (M_c). This trend is opposite to that for in-plane moments and intuitively appears questionable.*

There is another problem that is potentially more serious with both figures: the number of independent parameters appears to be deficient. In these figures, the stiffness values are given as a function of three independent dimensionless parameters: $\lambda = (d_o/D) \sqrt{D/T}$, $\Lambda = (L/D) \sqrt{D/T}$, and T/t, involving the five dimensional variables D, T, d, t, and L. An important theorem in dimensional analysis[29] states that the number of dimensionless parameters in a complete set is equal to the total number of variables minus the rank of their dimensional matrix. Because all five variables involve only the dimension of length (mass and time are not included), the rank of their dimensional matrix equals one. Hence, for every set of vessel end boundary conditions, four independent parameters are needed to compose a complete set.

In their 1983 paper, Steele and Steele[14] stated that four parameters are significant: λ, T/t, d/t, and Λ. Only in the extreme cases when T/t $\gg$ 1 or T/t $\ll$ 1 will the specific value of d/t become insignificant. However, because both Figs. 12 and 13 claim to be valid for T/t = 1, the curves are not unique for different values of d/t. Because WRC-297 does not recognize this problem, it might be unwise to use the stiffness curves for design until the question is resolved.

---

*See discussion in "SUMMARY" Sect. 12.1.

4. BENCHMARK DATA

4.1 EXPERIMENTAL AND ANALYTICAL DATA

Benchmark data, considered appropriate for development of nozzle-to-cylinder flexibility factors, are not very plentiful. In a few cases, displacement or rotation data have been obtained specifically for determining flexibility or stiffness. But in most cases, the experimental and analytical studies of branch connections or vessel nozzles have been directed at determining the stresses. Displacement data either were not obtained or were obtained only as auxiliary information.

Existing experimental data that we consider appropriate for flexibility studies are contained in Refs. 30–47. These 18 reports span the time from 1953 to 1986 and include studies on the behavior of unreinforced branch connections, branch connections with various types of reinforcements, solid attachments, forged piping tees and drawn outlets, and specialty product nozzle or branch connection fittings. The data that were available before 1978 (Refs. 30–39) were used by Rodabaugh and Moore[15] in the development of the present (1986) ASME Code flexibility equations for Class 1 branch connections.

Most recently, Moffat and Kirkwood[47] provided experimental flexibility factors for each of the three branch moment loadings M_{ib}, M_{ob}, and M_{tb} and for each of the three run moment loadings M_{ir}, M_{or}, and M_{tr} for four unreinforced full outlet models ($d/\Delta = 1.0$; $t/T = 1.0$) with $11.4 < D/T < 41.4$.

Three of the models, reported in Refs. 41–44, with five different nozzles had diameter-to-thickness ratios (D/T) large enough to be classed as thin-walled tanks. Steele and Steele[14] used data from Ref. 41 in their experimental validation of the FAST computer program.

Finite-element displacement data that have been adequately benchmarked against experimental data are given in Ref. 15. We have also used the finite-element displacement data given in WRC-297 (Ref. 27), even though they were not properly benchmarked, because they provide the only reference information for vessels with $D/T > 2500$.

4.2 FLEXIBILITY FACTORS FROM TEST DATA

4.2.1 Tests for Models with D/T < 100

Figure 14 shows a schematic arrangement that is representative of all of the test models with $D/T < 100$ considered in this report. Figure 14(a) indicates by scale that the length of the run pipe is about four diameters long with the nozzle at midlength. The branch pipe is ~4d long. These lengths are intended to be long enough that the influences of the end restraints on the local deformations at and near the branch intersection are negligible (i.e., infinite effective length). In some of the tests on small d/D branch connections, both ends of the run pipe were restrained. However, for $d/D < 1/3$, it probably is not significant

28

ORNL-DWG 87-4631 ETD
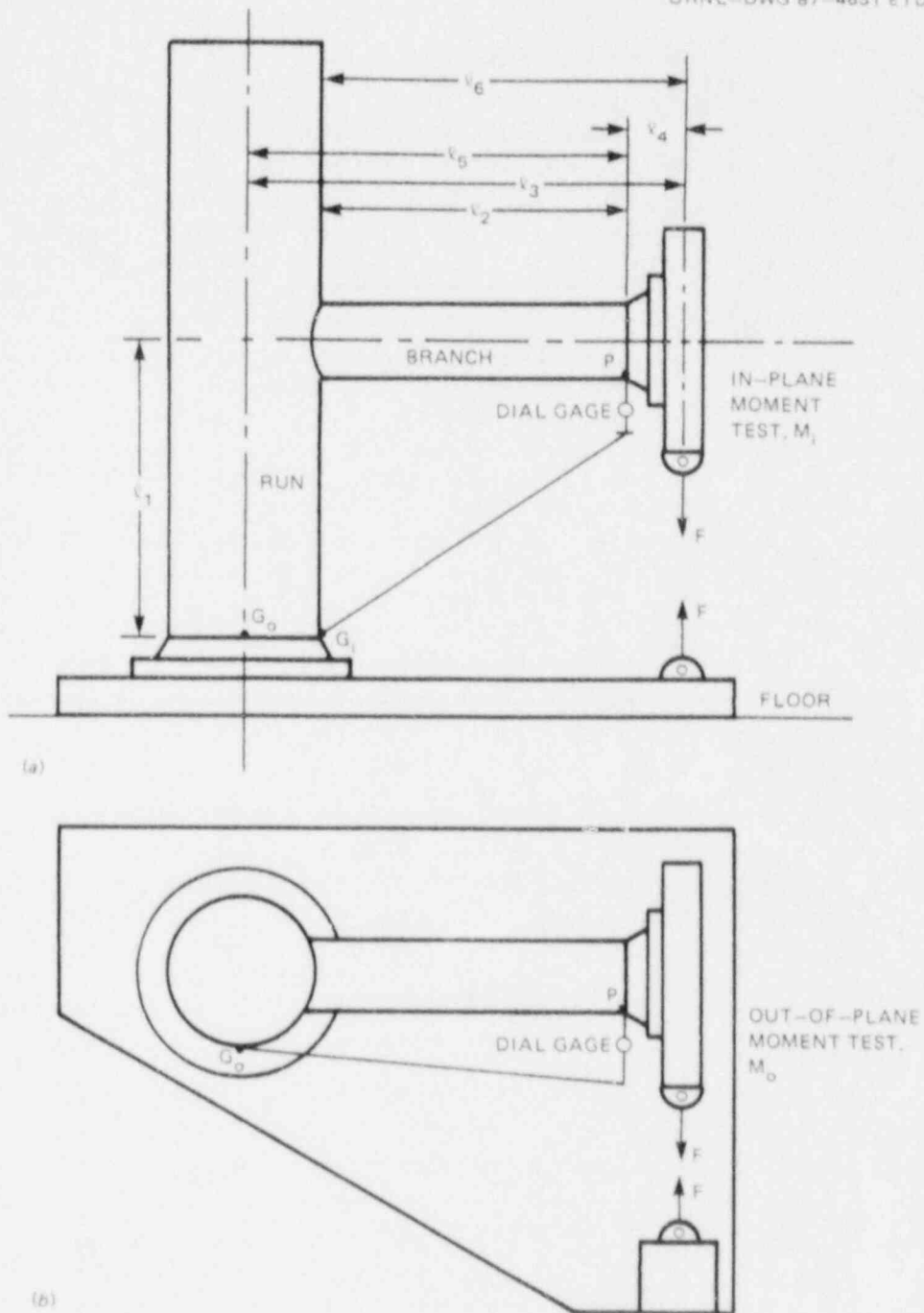
Fig. 14. Typical flexibility test arrangement for moment loadings on models with D/T < 100. (*a*) Elevation, (*b*) plan.

whether one end or both ends were restrained. The loading in Fig. 14(a) is for an in-plane moment; the loading in Fig. 14(b) is for an out-of-plane moment test.

If properly determined, the deflection at point P in the direction of the load will provide the data needed to determine the flexibility factor. One major problem in obtaining flexibility displacement data is to ensure that the measured model displacements are isolated from the displacements of the loading frame because they are very likely to be of the same order of magnitude. If the loading frame is significantly more rigid than the test assembly, the displacement measuring device [dial gage or linear variable differential transformer (LVDT)] can be supported from the loading frame. For the out-of-plane test illustrated in Fig. 14(b), however, where a vertical post is used to support the loading device, the loading frame (post) may be nearly as flexible as the test assembly. In that case, if the dial gage is supported from the loading frame, it will not be possible to obtain an accurate displacement measurement for the test assembly.

A suitable alternative is to support the dial gage from an appropriate reference point on the test piece itself, such as point G_i or G_o in the figure. The reference point should be sufficiently far from the nozzle intersection that the local effects have damped out. The dial gage support frame itself only needs to be sufficiently rigid to resist the small forces, on the order of an ounce, needed to actuate the dial gage.

Having appropriately installed deflection or rotation measuring devices, the next step is to load the model over a range where the loads and displacements are linearly related. Figure 15 shows the load-displacement data obtained by Khan[45] from one of the WFI test models. Those data may then be used in conjunction with the nominal displacement/rotation calculated from the "point spring" strength-of-materials model to determine a numerical value for the test specimen flexibility factor.

For the in-plane bending test illustrated in Fig. 14(a), the nominal deflection of the strength-of-materials model without a point spring is given by

$$\delta_n/F = [\ell_4 \ell_2^2/(2I_b) + \ell_2^3/(3I_b) + \ell_3 \ell_1 \ell_5/I_r]/E , \qquad (16)$$

where I_b, I_r are the moments of inertia of the branch, and run and $\ell_1 - \ell_5$ are the dimensions shown in the figure. The difference between the measured deflection δ_m and the nominal deflection δ_n, which we will call the excess deflection

$$\delta_e/F = (\delta_m - \delta_n)/F , \qquad (17)$$

is the deflection due to the point spring. The point spring rotation is then
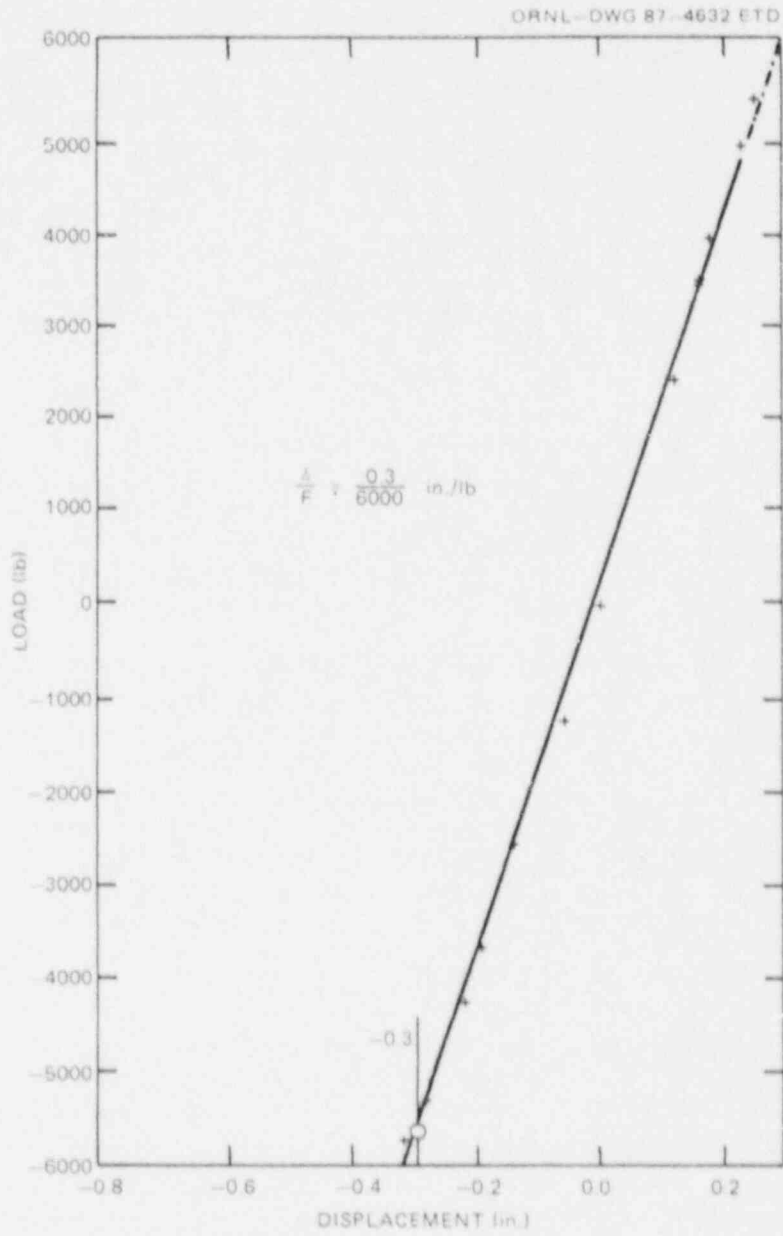
Fig. 15. Khan's[45] WFI test model 1, load-displacement plots for in-plane moment load.

$$\theta/F = (\delta_m - \delta_n)/(F\ell_2) . \tag{18}$$

For bending moment evaluation, the rotation with respect to the moment acting on the point spring θ/M_s is needed to be consistent with the ASME Code (see Fig. 2). In this case, $M_s = F\ell_6$. Accordingly,

$$\theta/M_s = (\delta_m - \delta_n)/(F\ell_2\ell_6) , \tag{19}$$

and M_s is the value of the branch moment at the outside surface of the run pipe. The final step in determining the flexibility factor is to normalize Eq. (19) with respect to a one-diameter length of branch pipe, as defined earlier by Eq. (10) in Sect. 9. Thus,

$$k = [(\delta_m - \delta_n)/(F\ell_2\ell_6)]/(d_o/EI_b) . \tag{20}$$

To go through this process, the test report must either state the modulus of elasticity of the test specimen material or, generically, the material so that E can be estimated (e.g., for carbon steel, $E = 3 \times 10^7$ psi). In addition, of course, the test data report must describe the test specimen in sufficient detail so that the lengths ℓ_1–ℓ_6 can be determined.

If k is a large value, the measured displacement δ_m will be significantly larger than δ_n, and accurate test values of k can be established. Conversely, of course, for small k extremely accurate experimental techniques must be used to establish even an approximate value of k. Roughly, at best, experimental k's should be considered as $k \pm 1$. For example, an experimentally determined k of 1 might lie between 2 and 0, but a carefully determined k of 40 should lie between 41 and 39. For larger k's, perhaps a more realistic estimate of the accuracy would be $\pm 10\%$ (e.g., 40 ± 4).

4.2.2 Tests for Models with D/T > 900

To our knowledge there have only been five nozzle flexibility tests in very large D/T thin-walled cylindrical vessels. Four of these, identified as CBI-1, -2, -3, and -4, were tested by Chicago Bridge and Iron Co.[41-43] The fifth model, identified as LPV2, was tested at the University of Waterloo by Schroeder.[44] The nominal dimensions and dimensionless parameters of these models are given in Table 3.

The test model for CBI-3 (Fig. 16) consists of a 60- by 60-in. curved panel with the edges attached to channels. The test model for CBI-4 used the same curved panel but with a larger nozzle. The panel for models CBI-1 and -2 was 134 by 134 in. The LPV2 test model also used a curved panel, 80 in. in the longitudinal direction and semicircular ($120\pi = 377$ in.) in the circumferential direction.

Table 3. Nominal dimensions for nozzles in very large diameter,
thin-walled, cylindrical tanks

Model	Ref.	D (in.)	T (in.)	d_o (in.)	t (in.)	L (in.)	λ^a	Λ^a	T/t	d/t
CBI-1	41	310.5	0.296	3.5	0.187	134	0.346	13.99	1.583	17.72
CBI-2	41	310.5	0.296	8.63	0.322	134	0.867	13.99	0.919	25.80
CBI-3	42	251	0.0993	2.51	0.0523	60	0.492	12.02	1.899	46.99
CBI-4	43	251	0.0993	12.55	0.0523	60	2.503	12.02	1.899	238.96
LPV2	44	240	0.25	1.00	0.25	80	0.097	10.33	1.000	3.00

$^a\lambda = d_o/D\sqrt{D/T}$, $\Lambda = L/D\sqrt{D/T}$.

32
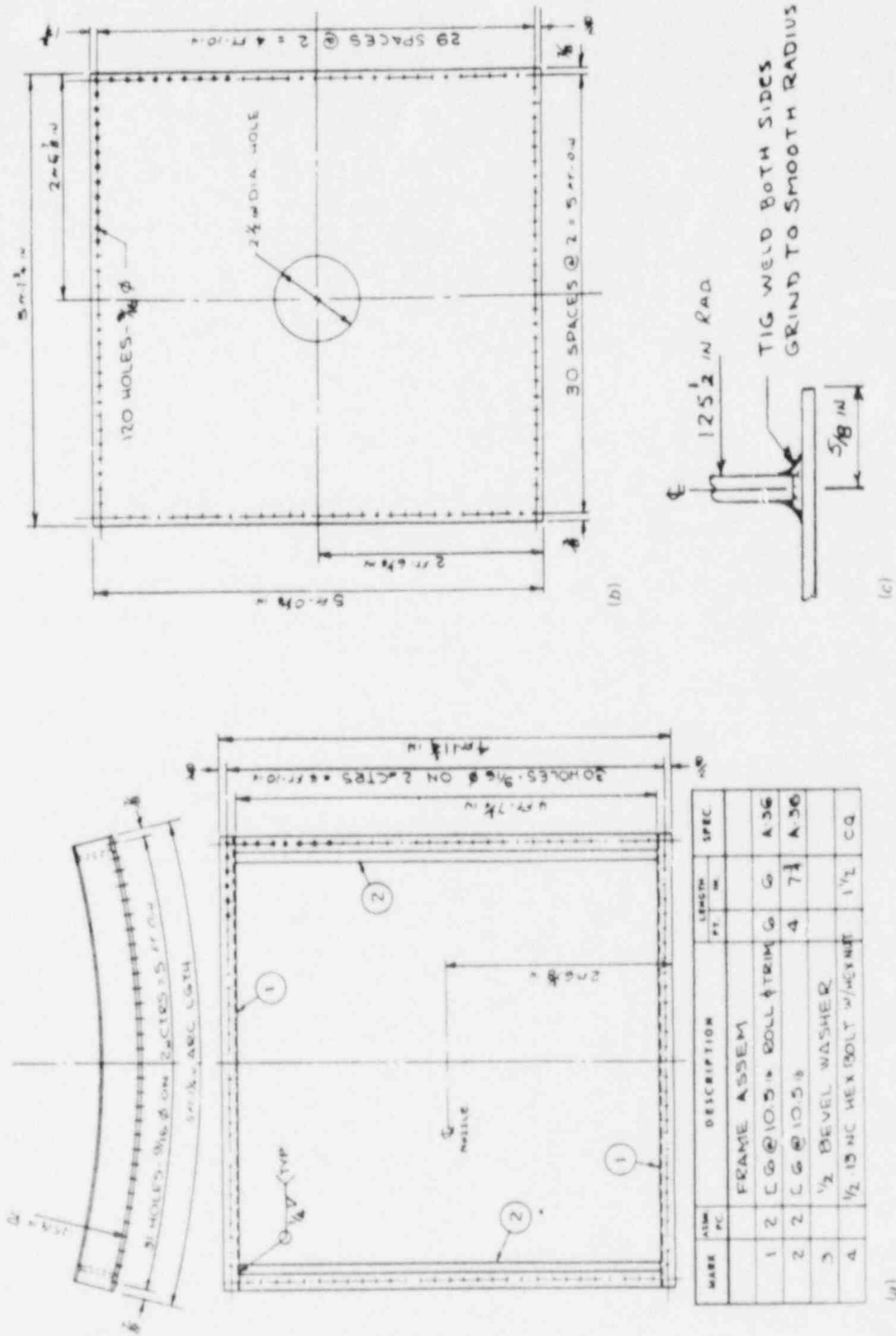
Fig. 16. Test model CBI-3. (a) Frame assembly, (b) shell plate,
(c) weld detail.

Reference 42 states: "The entire (panel) assembly was then anchored securely in a vertical position to a large four-poster jacking frame, roughly 89 in. high by 85 in. wide and 68 in. deep . . . Strain gages and deflection sensors were then placed on the shell." The deflection monitors, as judged by Fig. 9 of Ref. 42, appear to be placed on the *inside* of the shell, adjacent to the inwardly protruding nozzle. The point of support of the deflection monitors (transducers) is not apparent, but considering the seeming rigidity of the frame relative to the center of the panel, deflections of the support points for the deflection transducers are probably not significant. Presumably, similar test apparatus was used for CBI-1 and -2.

Figures 17 and 18 show the test arrangement used for LPV2. The dial gages were supported from the concrete floor (Fig. 18).

Figure 19 shows measured deflections and rotations for CBI-3 from Ref. 42. The displacement/load relationships are reasonably linear for M_o and M_i but not for radial load. Results for CBI-4 from Ref. 43 are similar. Figure 20 shows the radial load plot. Steele[13] includes a tabulation of the displacement-rotation parameters for all four CBI models. We have checked the original references, and approximately agree with Steele's moment parameters. We will discuss the nonlinear aspect of radial loading later in this report.

Figure 21 is representative of the displacement load data provided by Schroeder[44] for LPV2. The data are summarized in Table 4. No mention is made of linearity of displacement/loads, but, as can be seen in Table 4, both positive and negative loads were applied, and they are in reasonable agreement with each other. Because the displacements were measured at the end of an 11.5-in. length of nozzle, the nominal displacements must be subtracted from the measured displacements to obtain the effect of local displacements; this, along with a reduction to Steeles' stiffness parameters and to k-factors, has been done in Table 4.

For radial loads, Schroeder's load-displacement curves for outward loading and inward loading, respectively, both give a displacement of $\delta = 0.106$ in. for a force of 1330 lb. Steeles' parameters are then

$$(W/\delta) (4.95 \ ET^2)/DA^{0.5}) = 1.043 .$$

(21)

Figure 22 shows data for a torsional moment from Ref. 44. However, the significance of these data are not apparent because the author states:

For the application of the twisting couple an attachment was screwed to the threaded end of the nozzle and the twisting couple was applied at a distance of 22 inches from the vessel. Thus, the rotation given in [Fig. 22 herein] has significance only for the rotation of the twisting couple, and is not directly related to the angle of twist at the end of the nozzle, which is only 11.5 inches long.
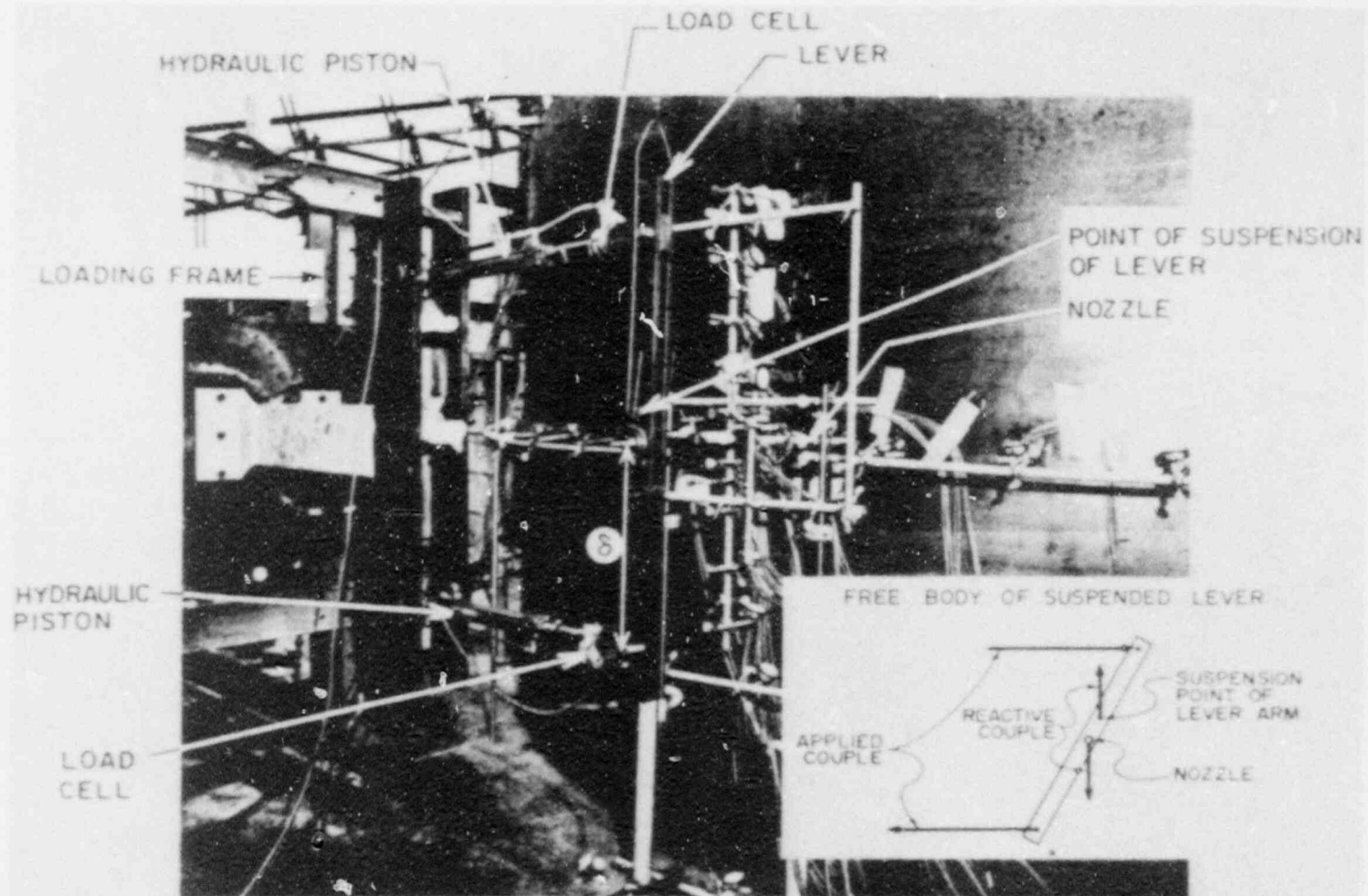
Fig. 17. View of loading fixture for Schroeder's[44] model LPV2 test.
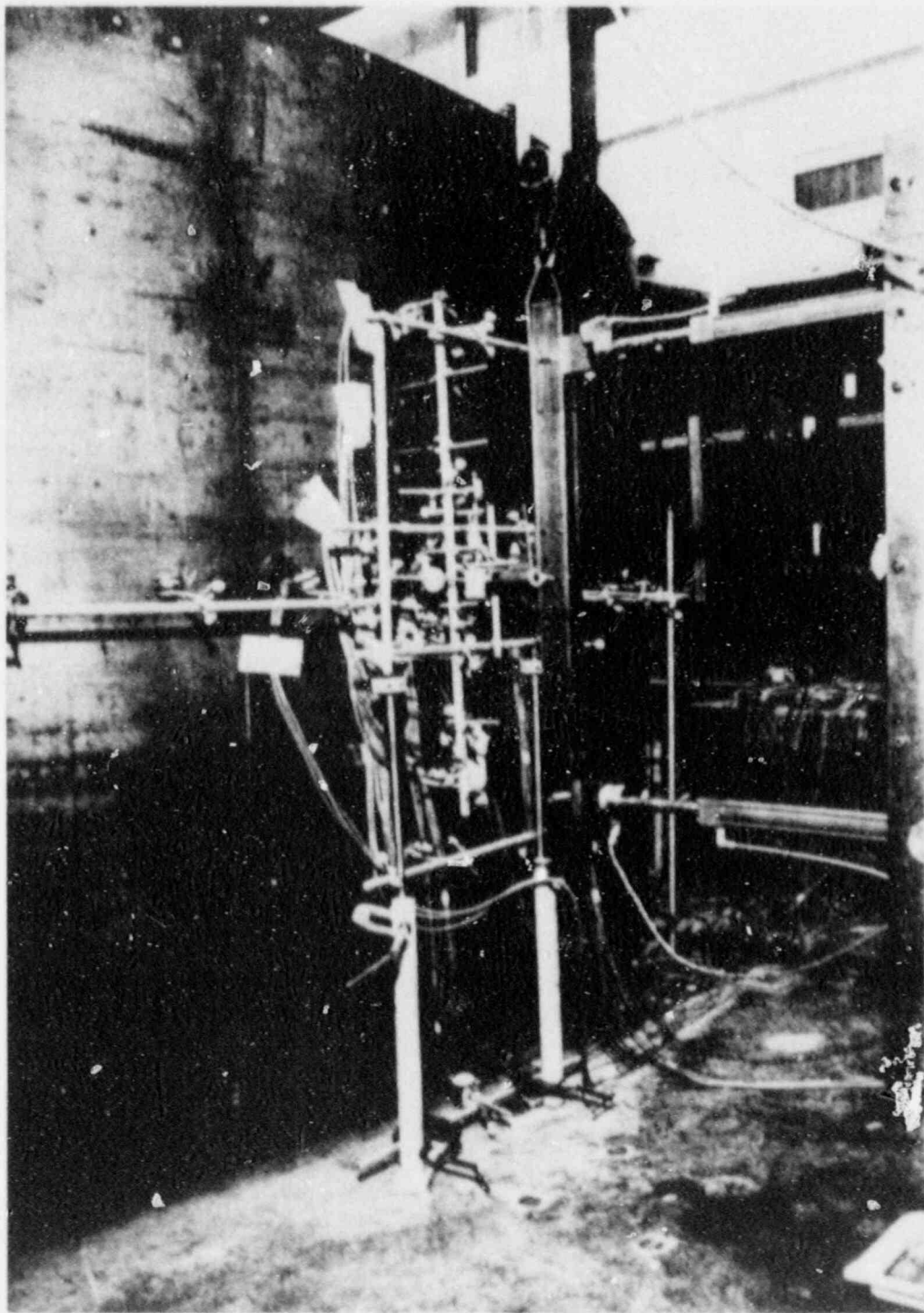
Fig. 18. View of displacement measuring device support frame for Schroeder's[44] model LPV2 test.

ORNL—DWG 87—4634 ETD
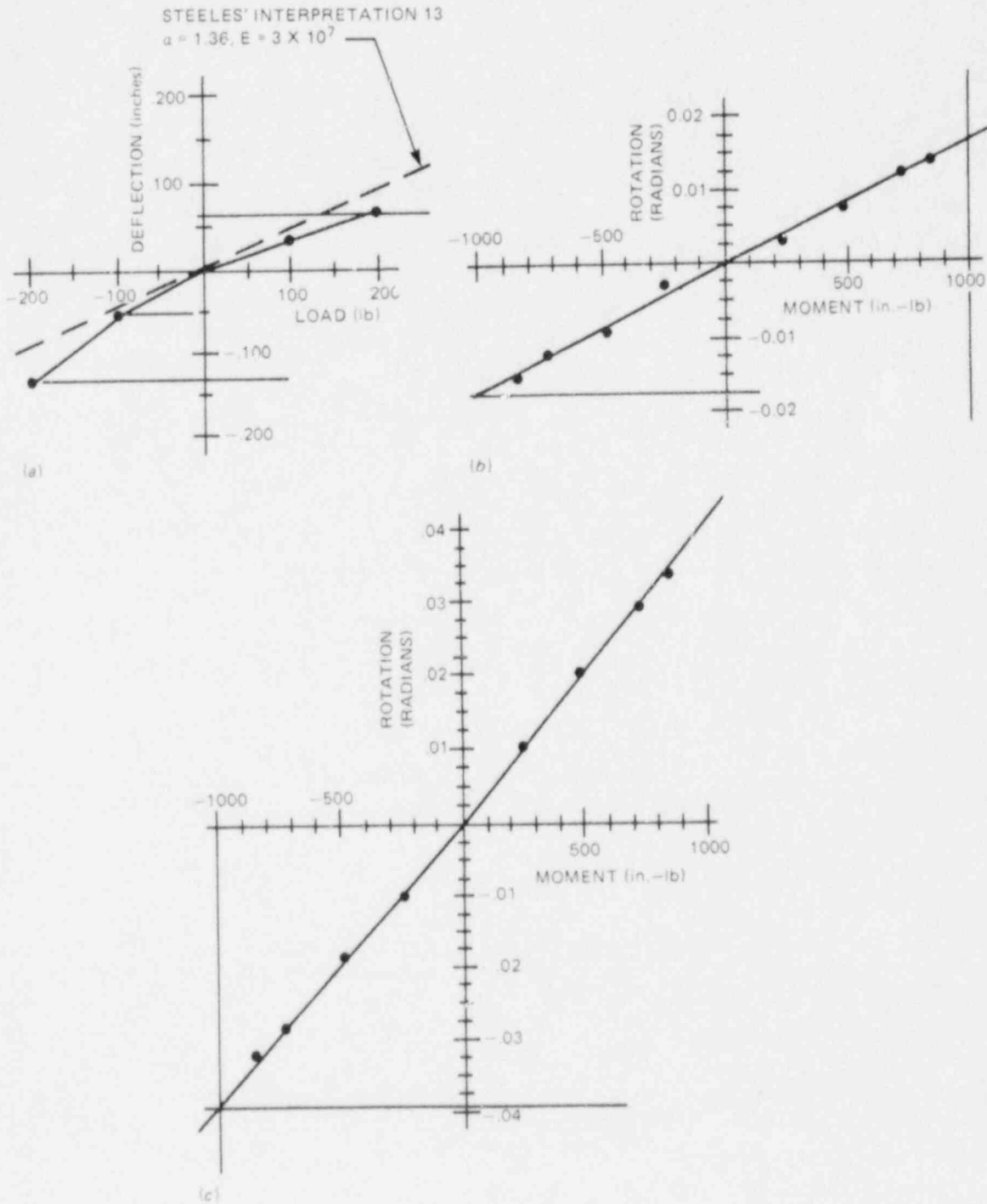
Fig. 19. Load-displacement plots for CBI test model CBI-3.
(a) Radial load, (b) longitudinal moment, (c) circumferential moment.
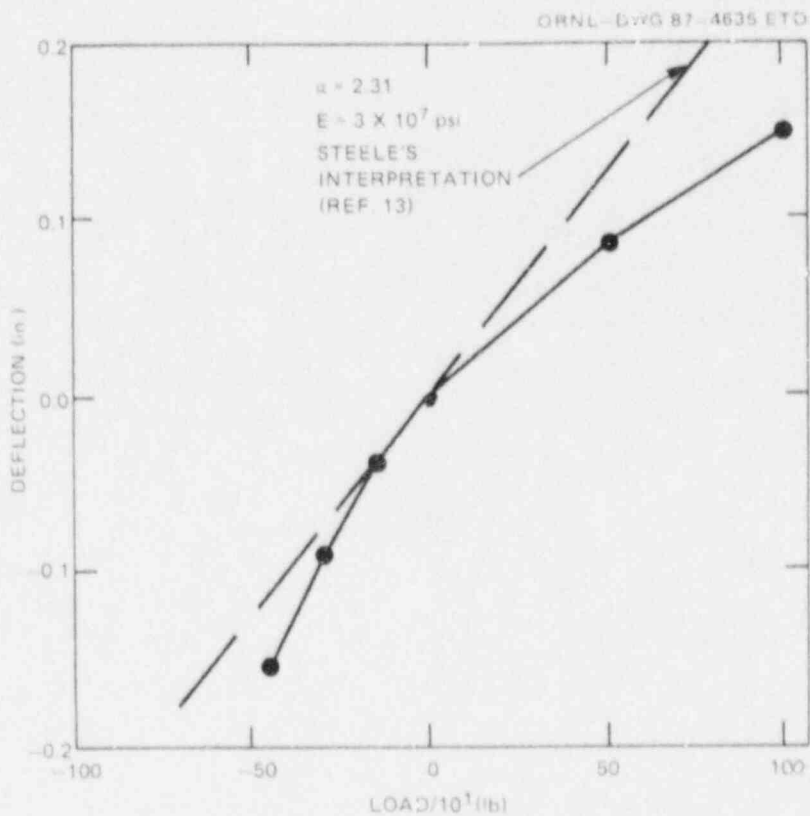
Fig. 20. Load-displacement plots for CBI test model CBI-4 from Whipple.[43]
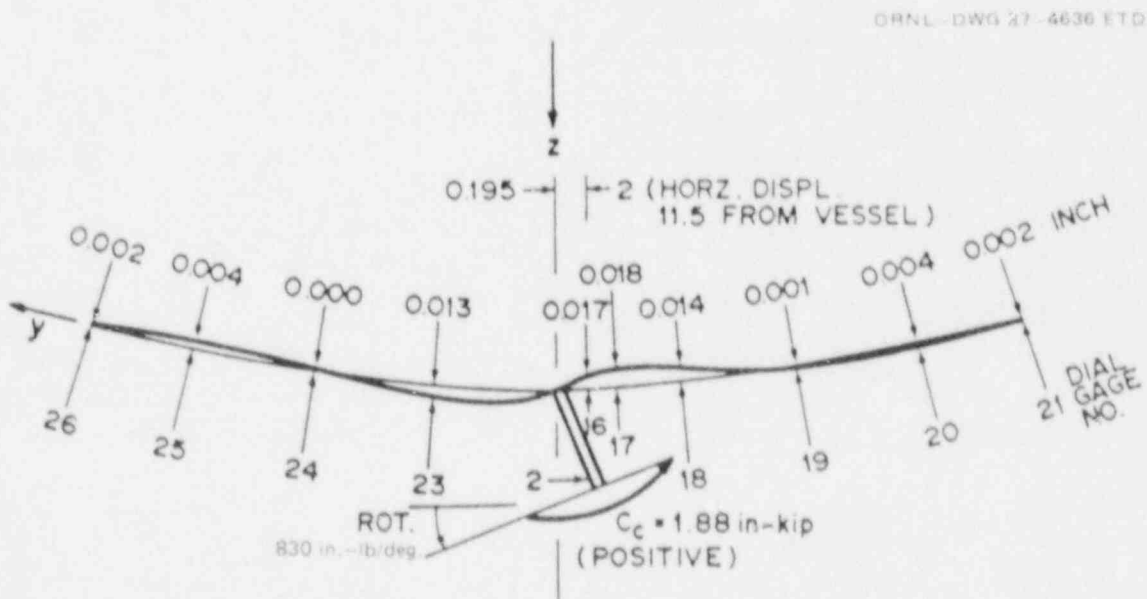
Fig. 21. Typical out-of-plane moment (M_o) displacement data for Schroeder's model LPV2 from Fig. 20, Ref. 44.

Table 4. Test data summary for nozzle moment
loads on Schroeder's model LPV2

Fig. No.[44]	Load	M (in.-lb)	θ_m [a] (rad.)	θ_n [b] (rad.)	θ_e [c] (rad.)	d	k [e]
24	$+M_o$	1880	0.0395	0.0157	0.0238	0.169	17.5
25	$-M_o$	1850	0.0409	0.0154	0.0255	0.157	19.0
32	$+M_i$	2100	0.0359	0.0175	0.0184	0.243	12.1
33	$-M_i$	2060	0.0360	0.0172	0.0188	0.234	12.6

[a] θ_m = measured rotation.

[b] θ_n = nominal rotation ML/EI_n with L = 11.5 in.,
$E = 3 \times 10^7$ psi, $I_n = (\pi/64)(1.0^4 - 0.5^4) = 0.04602$ in.

[c] $\theta_e = \theta_m - \theta_n$.

[d] Steeles' stiffness parameter, $M/(ET^3\theta_e)$, with T = 0.25 in.

[e] $k = \theta_e/(Md_o/EI_n)$.

ORNL-DWG 87-4638 ETD
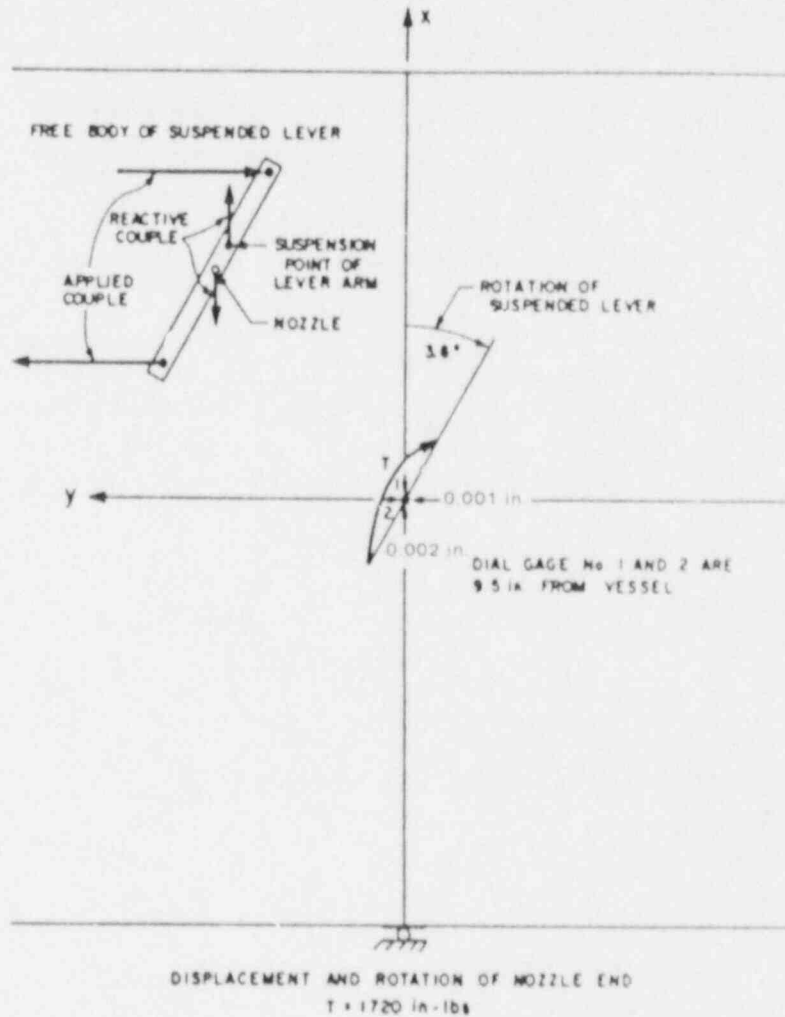
Fig. 22. Torsional moment rotation data for Schroeder's model LPV2 from Fig. 13, Ref. 44.

5. BRANCH MOMENT FLEXIBILITY FACTORS COMPARED WITH TEST DATA

The various methods discussed earlier in Sect. 3 for calculating piping design flexibility factors are compared with the available data base in this section and in the following four sections. The comparisons discussed in this section are for both in-plane and out-of-plane moment loadings on the branch, for unreinforced and reinforced branch connections, for branch connections with $d/D < 0.5$ and those with $d/D > 0.5$, and for branch connections made with ANSI standard tees and those made with specialty fabricated reinforcements. This breakdown of branch connection types corresponds roughly with the design practice discussed in Sect. 2.3, as well as with the available test data.

5.1 UNREINFORCED BRANCH CONNECTIONS WITH $d/D < 0.5$

The available test data, along with dimensional parameters and flexibility factors calculated by the various methods, are summarized in Tables 5—7. We have also included data from three drawn outlet models because the nozzles are essentially unreinforced [see Fig. 23(a)]. Superscripts 1 or 2 on the values given for L/D indicate whether one or both ends of the run were restrained (fixed) during the test. If both ends were restrained, as indicated by a superscript 2, the FAST2 analysis used L/D as given. If, however, only one end was restrained during the test, L/D for the FAST2 analysis was based on assuming that the distance from the nozzle to the free end was four times the distance from the nozzle to the fixed end. Both ends were then restrained in the analysis. The data in Tables 5 and 6 were from model tests with $D/T < 100$ for which the ASME Code equations were developed. The data in Table 7 on models with $D/T > 900$ are outside the intended range of the Code equations. Both Bijlaard's basic theory and Steeles' theory are applicable to all of the test models. The design methods based on these theories (M&S and LUGS) and (WRC-297 and FAST2), however, have certain limitations, as discussed earlier. This fact is reflected by the absence of an entry in the tables; there are no entries for M&S in Table 7 because the design charts are limited to branch connections with $D/T < 300$.

At first glance it is apparent that all five design methods give flexibility factors that differ from the test data by various and seemingly random amounts. Because the amount of data is clearly insufficient to do a meaningful statistical analysis, we have used a "ratio-of-sums" method to calculate a goodness-of-fit value for comparison. The calculated-to-test ratios (CTRs) of the sums are deemed to be more informative than the individual ratios because they weight the measure in proportion to the magnitude of the k factors. We consider CTR values between 0.5 and 2.0 as indicating reasonably good correlation. Values >2.0 or <0.5 clearly indicate poor correlation.

The CTR values shown in Tables 5 and 6 for models with $D/T < 100$ show that the Code equations are in reasonably good agreement with the test data for both out-of-plane moment (k_o, Table 5) and in-plane moment (k_i, Table 6); CTR = 1.04 and 0.71, respectively. In fact, all five

Table 5. Out-of-plane moment flexibility factors for unreinforced
branch connections ($d/D \leqslant 0.5$, $D/T < 100$) — comparisons
with test data

Ref. No.	Model parameters				k_o					
	D/T	d/D	t/T	L/D^a	Test	Code[b]	M&S[c]	LUGS[d]	WRC-297[e]	FAST2
30	76	0.18	0.76	9.1^2	31	25.0	34	59.0	57	37.6
34	78	0.13	0.45	2.1^2	11	17.0	15	18.9	24	14.6
33	93	0.12	0.42	1.4^2	10	20.5	15	19.6	26	19.6
33	93	0.18	0.75	1.4^2	27	33.5	41	54.2	79	38.1
15	99	0.50	0.50	3.9^1	60	50.0	52	83.0	160	74.4
15	49	0.13	0.32	3.9^1	6.4	7.2	5.4	6.2	7.6	7.0
36^f	19	0.33	0.43	7.0^2	2.3	3.4	4.6	6.2	7.4	5.1
35^f	31	0.41	0.56	5.3^2	11.8	8.7	14.0	15.8	27.0	13.1
35^f	15	0.42	0.28	5.3^2	1.7	2.2		3.0	4.4	3.4
Sums					161.2	167.5	181.0	265.9	392.4	212.9
CTR[g]						1.04	1.13	1.64	2.43	1.32

[a]Superscripts 1 or 2 indicate whether one or both ends of the run were restrained (fixed) during the test. See text for use of L/D in the analyses.

[b]Equation (8) of text.

[c]Equation (11) of text and M&S charts;[23] see Fig. 9.

[d]See Sect. 3.2.2 and Eq. (12).

[e]Equation (15) and Fig. 13 of text.

[f]These models were drawn outlets; see Fig. 23.

[g]CTR is the ratio of the sum of the calculated values to the sum of the test values.

Table 6. In-plane moment flexibility factors for unreinforced branch connections (d/D ≤ 0.5, D/T < 100) -- comparisons with test data

Ref. No.	Model parameters				k_i					
	D/T	d/D	t/T	L/D[a]	Test	Code[b]	M&S[c]	LUGS[d]	WRC-297[e]	FAST2
30	76	0.18	0.76	9.1^2	17.0	5.7	12.0	15.4	16.0	10.6
34	78	0.13	0.45	2.1^2	5.6	3.8	7.1	8.0	8.1	6.6
33	93	0.12	0.42	1.4^2	4.0	4.2	6.8	8.9	9.1	8.8
33	93	0.18	0.75	1.4^2	8.0	6.9	12.0	18.7	17.0	13.0
15	99	0.50	0.50	3.9^1	11.2	10.0	4.4	8.8	10.7	9.6
15	49	0.13	0.32	3.9^1	3.1	2.0	2.6	3.0	3.3	3.4
36[f]	19	0.33	0.43	7.0^2	1.1	1.5	1.5	2.2	2.2	1.9
35[f]	31	0.41	0.56	5.3^2	2.7	3.1	3.4	4.7		3.5
35[f]	15	0.42	0.28	5.3^2	1.1	1.0		1.2	1.1	1.2
Sums					53.8	38.2	49.8	70.9	67.5	58.6
CTR[g]						0.71	0.94	1.32	1.32	1.09

[a]Superscripts 1 or 2 indicate whether one or both ends of the run were restrained (fixed) during the test. See text for use of L/D in the analyses.

[b]Equation (9) of text.

[c]Equation (11) of text and M&S charts;[23] see Fig. 10.

[d]See Sect. 3.2.2 and Eq. (12).

[e]Equation (15) and Fig. 13 of text.

[f]These models were drawn outlets; see Fig. 23.

[g]CTR is the ratio of the sum of the calculated values to the sum of the test values.

Table 7. Flexibility factors for unreinforced branch connections
(d/D < 0.5, D/T > 900)

Model (Ref.)	Model parameters				k_o for out-of-plane moment					k_i for in-plane moment				
	D/T	d/D	t/T	L/D[a]	Test	Code	WRC-297	FAST2	Steele[b]	Test	Code	WRC-297	FAST2	Steele[b]
LPV2 (44)	960	0.0042	1.00	0.33^2	18	193	20	15.1		12	12.5	14	12.4	
CBI-1 (41)	1050	0.011	0.63	0.43^2	52	284	75	56.7	55.4	32	17.5	44	39.9	38
CBI-2 (41)	1050	0.028	1.09	0.43^2	310	595	580	278.3	296	140	36.7	200	142.8	150
CBI-3 (42)	2530	0.010	0.52	0.24^2	130	927	250	176.2	18	57	36.8	150	121.9	120
CBI-4 (43)	2530	0.050	0.53	0.24^2	810	2070	2200	712.3	740	240	82.4	330	269.8	280
Sums					1320	4069	3125	1238.6	1275.4	481	185.9	738	586.8	588
CTR						3.08	2.37	0.94	0.98		0.39	1.53	1.22	1.25

[a]Superscripts 1 or 2 indicate whether one or both ends of the run were restrained (fixed) during the test. See text for use of L/D in the analyses.

[b]Calculated from stiffness factors given in Steele and Steele.[13]

44
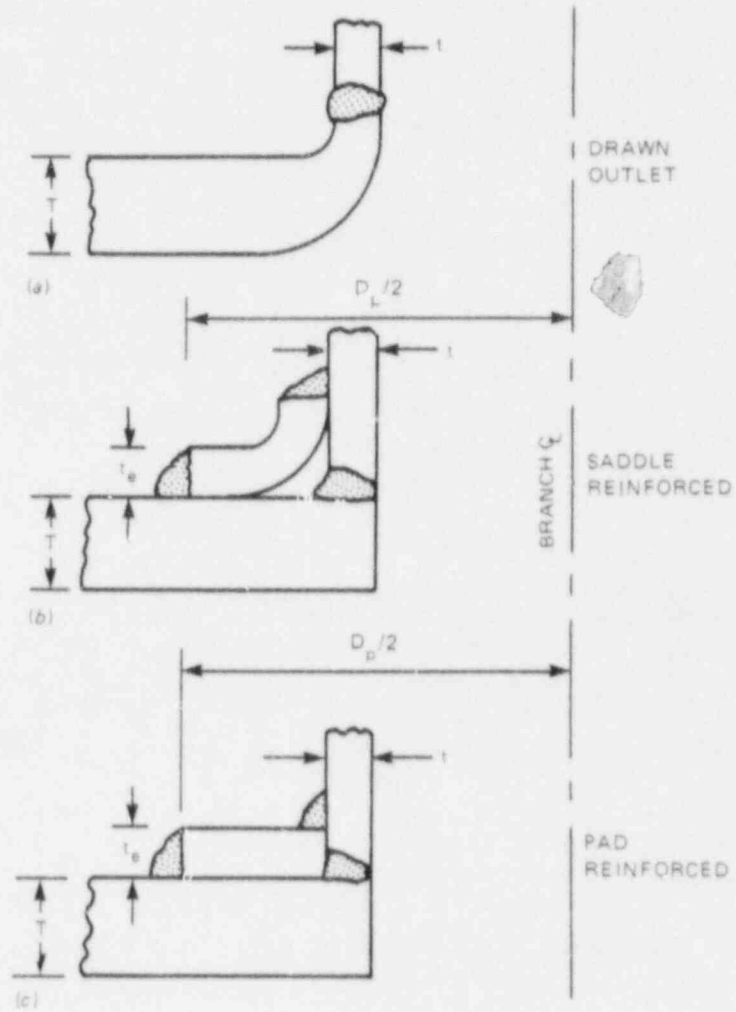
Fig. 23. Special types of branch connections.

methods appear to give reasonable agreement with the test data for in-plane moment k_i, and only the WRC-297 method appears not to correlate with the test data for out-of-plane moment k_o. The LUGS program consistently gave higher flexibility factors than the M&S design charts because of the influence of the length parameter L/R, discussed earlier in Sect. 3.2 The M&S charts were all developed for $L/R = 4$, whereas the LUGS results were calculated using L/R from the test specimens.

The data in Table 7 for models with $D/T > 900$ indicate that the Code equations do a rather poor job of representing the test results (CTR = 3.08 for k_o and 0.39 for k_i). This is not surprising, however, because the Code equations were developed empirically from $D/T < 100$ data; the $D/T > 900$ data did not exist at that time. Bijlaard's theory (LUGS program) also does a poor job because of convergence problems for large D/T models and because the M&S charts are limited to $D/T < 300$. Table 7 does not include results from Bijlaard's theory. The WRC-297 method fails to correlate with the test data for k_o (CTR = 2.37) although the values calculated directly from Steeles' theory (FAST2) appear to give excellent results (CTR = 0.94).

5.2 NOZZLE-REINFORCED BRANCH CONNECTIONS WITH $d/D < 0.52$

The available test data, along with flexibility factors calculated by the various design methods, are summarized in Table 8. The model parameters are summarized in Table 9. Note that all of the branch connections for which we have data are specialty product items sold commercially by either Bonney Forge or WFI International. The WFI data only became available recently. All of the models were fully reinforced by increased nozzle wall thickness to meet the ASME Code requirements (NB-3643), except for the three items 45-15, -23, and -24, which were experimental models with only 50% reinforcement. Table 8 includes three pairs of nominally identical test models: 45-5 and -6, 45-7 and -8, and 45-17 and -18. For each pair, the k_o values are reasonably close, indicating the reproducibility of the test results.

Because of the nozzle wall reinforcement, many of the test models had mean diameter ratios d/D and outside nozzle diameter ratios d_o/D that are greater than the stated applicability of the Code equations [Eqs. (8) and (9)]. Nevertheless, the Code equations gave reasonably good agreement with the test data (i.e., CTR = 0.94 for k_o and 1.07 for k_i).

The values of k_o and k_i given in Table 8 for Bijlaard's theory (M&S; LUGS) are based on using d_n/D rather than d_o/D to calculate the parameter B, although extrapolation of the M&S design curves was necessary for some of the models; M&S curves extend to $B = 0.55$. Using d_n/D reduced the calculated values for k significantly and brings them into better agreement with the test data, although for this limited set of data, the Code equations still seem to correlate somewhat better.

The values of k_o given in Table 8 under WRC-297 obviously do not correlate well with the test data (CTR = 5.58). This may be because the curves in the bulletin were not intended to apply to nozzle-wall-reinforced branch connections. The bulletin curves are based on uniform wall thickness branch connections that are effectively infinite in length.

Table 8. Flexibility factors for nozzle-reinforced branch connections
(d/D ≤ 0.52, D/T < 100)

Ref. No.	Branch type	k_o for out-of-plane moment						k_i for in-plane moment				
		Test	Code	M&S	LUGS	WRC-297	FAST2	Test	Code	M&S	LUGS	FAST2
39	12X6W[a]	7.9	5.9	-11	17.6	42	9.6	1.2	2.0	1.6	5.2	2.2
40	14X6IW[b]	10.2	8.1	15	12.2	44	14.4	2.5	2.6	2.8	3.9	3.0
45-5	8X3P[c]	5.6	4.3	13	4.2	21	7.5					
45-6	8X3P	4.3	4.3	13	7.5	21	7.5					
45-7	8X4P	5.9	5.3	10	4.2	32	8.2					
45-8	8X4P	6.5	5.3	10	8.8	32	8.2					
45-15	8X4P — 50%	6.1	6.0	11	4.4	34	8.9					
45-17	12X6V[d]	5.5	7.2	14	2.1	47	7.8					
45-18	12X6V	4.9	7.2	14	6.9	47	7.8					
45-23	12X6V — 50%							2.6	2.8	2.7	2.1	2.4
45-24	12X6V — 50%	6.2	8.1	16	8.1	50	9.2					
37	12X4W	5.6	3.5	6.2	12.1	16	8.3	2.4	1.3	1.3	2.1	2.0
Sums		69.2	65.2	133.2	88.1	386	97.4	8.1	8.7	8.4	13.3	9.6
CTR			0.94	1.92	1.27	5.58	1.41		1.07	1.04	1.64	1.19

[a]W indicates Bonney Forge Weldolet; see Fig. 3(c) for generic shape.

[b]IW indicates Bonney Forge welded insert; see Fig. 3(a) for generic shape.

[c]P indicates WFI Pipette, fillet welded in place; see Fig. 3(a) for generic shape.

[d]V indicates WFI Vesselot, insert welded in place; see Fig. 3(a) for generic shape.

Table 9. Dimensional parameters for nozzle-reinforced branch connections
(d/D ≤ 0.52, D/T < 100)

Ref. No.	Branch type[a]	D_o (in.)	d_o (in.)	T (in.)	t (in.)	t_n (in.)	L_n (in.)	L_1[b] (in.)	L_2[b] (in.)	D/T	d/D	t/T	t_n/T	d_n/D[c]
39	12X6W	12.75	6.625	0.375	0.280	1.19	2.375	48	96	33.0	0.513	0.747	3.173	0.683
40	14X6IW	14.00	7.625	0.375	0.280	0.78	1.73	44.5	48	36.3	0.466	0.747	2.080	0.560
45-5	8X3P	8.625	4.250	0.322	0.216	0.591	1.75	18.75	31.25	25.8	0.396	0.671	1.835	0.513
45-6	8X3P	8.625	4.250	0.322	0.216	0.591	1.75	18.75	31.25	25.8	0.396	0.671	1.835	0.513
45-7	8X4P	8.625	5.250	0.322	0.237	0.612	2.00	18.75	31.25	25.8	0.513	0.736	1.901	0.632
45-8	8X4P	8.625	5.250	0.322	0.237	0.612	2.00	18.75	31.25	25.8	0.513	0.736	1.901	0.632
45-15	8X4P - 50%	8.625	5.000	0.322	0.237	0.487	2.00	18.75	31.25	25.8	0.513	0.736	1.512	0.602
45-17	12X6V	12.75	7.750	0.375	0.280	0.825	2.69	18.75	32.1	33.0	0.513	0.747	2.200	0.624
45-18	12X6V	12.75	7.750	0.375	0.280	0.825	2.69	18.75	32.1	33.0	0.513	0.747	2.200	0.624
45-23	12X6V - 50%	12.75	7.375	0.375	0.280	0.638	2.69	18.75	32.1	33.0	0.513	0.747	1.701	0.593
45-24	12X6V - 50%	12.75	7.375	0.375	0.280	0.638	2.69	18.75	32.1	33.0	0.513	0.747	1.701	0.593
37	12X4W	12.75	6.514	0.375	0.207	0.862	2.125	58	58	28.7	0.346	0.552	2.301	0.487

[a] See Table 8 for nomenclature.

[b] L_1 and L_2 are the distances from the branch connection centerline to the ends of the run during the test. All these tests were conducted with end 1 restrained and end 2 unrestrained.

[c] $d_n/D = d/D + (2t_n/T - t/T)/(D/T)$.

48

The values given in the table are based on using d_n/D rather than d_o/D to calculate the parameter λ; that is, $\lambda_n = (d_n/D) \sqrt{D/T}$, and T/t_n rather than T/t to interpolate between the Bulletin curves (see Fig. 13). Using d_n/D rather than d_o/D reduces the calculated k_o's significantly and brings them into better agreement with the test data, but using an increased nozzle wall thickness t_n decreases the stiffness parameter $M/ET^3\theta$ and, thus, increases k_o. This is opposite to what one would expect.*

On the other hand, the flexibility factors k_o and k_i obtained directly from Steeles' theory (FAST2) agree remarkably well with the test data (CTR = 1.41 for k_o and 1.19 for k_i). These results were obtained by including the length of the nozzle wall reinforcement L_n, as well as the other model dimensions in the analyses. From this, we conclude that L_n may also be an important model parameter, and its influence should be studied further.

5.3 UNREINFORCED BRANCH CONNECTIONS WITH d/D > 0.5

Table 10 summarizes the available test data for unreinforced branch connections with large-diameter branches (d/D > 0.5). None of the analytical design methods for calculating flexibility factors is applicable for these models, including the Code equations. Nevertheless, we have used the Code equations and somewhat surprisingly found reasonably good agreements with the test data. The one exception is the full outlet (d/D = 1.0), 24- by 24-in. model (No. 30-2) where the test data gave a significantly smaller out-of-plane flexibility factor than the Code equations. If this one data point is neglected, CTR = 1.08 for k_o.

The experimental out-of-plane flexibility factor k_o for the two other full outlet models, 47-1 and 47-2, agreed very well with the Code equation. For in-plane bending, the Code equation agreed reasonably well with the experimental data over the full range of d/D; CRT = 1.00 for k_i.

Although there are only ten data points, the general trend is for k_o to increase with increasing d/D and then to decrease at or near d/D = 1.0. Although this may reflect a testing or test evaluation error, we think it may be a real phenomenon. If one considers a transverse section of a branch connection with d/D = 1.0, the branch pipe is tangent to the run pipe, giving a membrane-like transfer of branch load to the run pipe in the transverse plane. When d/D is <1.0, however, the branch is not tangent to the run pipe, and more shell bending is involved. It is possible that k_o increases up to some value of d/D around 0.8 and then decreases significantly between d/D = 0.8 and d/D = 1.0. An analogous phenomenon appears to exist for stresses caused by out-of-plane moments.

---

*See discussion in "Summary," Sect. 12.1.

Table 10. Flexibility factors for unreinforced branch connections
(d/D > 0.5, D/T < 100)

Ref. No.	Nominal size	Model parameters			k_o		k_i	
		D/T	d/D	t/T	Test	Code	Test	Code
30-1	24 × 12	76	0.53	0.80	44	44.0	8.4	10.0
30-2	24 × 24	76	1.00	1.00	16	67.6	17	15.4
45-1	8 × 6	26	0.76	0.87			3.5	4.4
45-2	8 × 6	26	0.76	0.87	11.2	11.4		
45-3	12 × 10	33	0.84	0.97	13.1	17.9		
45-4	12 × 10	33	0.84	0.97	12.8	17.9		
36-1	20 × 12	19	0.64	0.69			1.2	2.5
36-2	20 × 12[a]	19	0.64	0.69	3.5	5.9	1.8	2.5
47-1	10 × 10	41.4	1.00	1.00	28.0	26.6	8.25	8.28
47-2	10 × 10	24.7	1.00	1.00	13.1	12.3	7.67	4.94
Sums					141.7	203.6	47.8	48.0
CTR						1.44 $(1.08)^b$		1.00

[a]Model 36-2 was a drawn outlet; see Fig. 23.

[b]CTR if model 30-2 is neglected.

5.4 NOZZLE-REINFORCED BRANCH CONNECTIONS WITH d/D > 0.5

Table 11 summarizes the available test data for nozzle-reinforced
branch connections with large-diameter branches (d/D > 0.5). All of
these data are for specialty product items sold by WFI,[45] Pipettes indi-
cated by a "P" in the second column and Vesselets indicated by a "V."
Four of the items, 45-16, -22, -25, and -26, were experimental models
intended to test the influence of nozzle wall reinforcement; 50% indi-
cates that the nozzle wall provides only 50% of the Code-required rein-
forcement. Most of the flexibility data are for out-of-plane moments
with only two data points for in-plane moments.

None of the analytical design methods are applicable for these
models, including the Code equations, because of the large d/D ratios.
Nevertheless, the comparisons shown in Table 11 suggest that the Code
equations give reasonably good design guidance for d/D ratios up to about
0.75. The two data points, 45-13 and -14, for d/D = 1.00 from two nomi-
nally identical test models are so different that conclusions are not
possible for d/D > 0.75. The other three pairs of nominally identical
models (45-9, -10); (45-11, -12); and (45-20, -21) gave test results that
are in reasonably good agreement.

Table 11. Flexibility factors for nozzle-reinforced branch connections
(d/D > 0.5, D/T < 100)

Ref. No.	Branch type[a]	Model parameters				k_o		k_i	
		D/T	d/D	t/T	t_n/T	Test	Code[b]	Test	Code[c]
45-9	8X5P	26	0.64	0.80	2.45	7.2	5.1		
45-10	8X5P	26	0.64	0.80	2.45	6.3	5.1		
45-11	8X6P	26	0.76	0.87	2.42	8.2	6.8		
45-12	8X6P	26	0.76	0.87	2.42	7.4	6.8		
45-13	8X8P	26	1.00	1.00	2.75	14.3	8.5		
45-14	8X8P	26	1.00	1.00	2.75	5.3	8.5		
45-16	8X6P — 50%	26	0.76	0.87	1.94	6.1	7.6		
45-19	12X8V	33	0.67	0.86	2.86			2.2	2.8
45-20	12X8V	33	0.67	0.86	2.86	5.3	8.3		
45-21	12X8V	33	0.67	0.86	2.86	6.0	8.3		
45-22	12X8V — 100%	33	0.67	0.86	3.19	4.3	7.8		
45-25	12X8V — 50%	33	0.67	0.86	2.03			2.6	3.4
45-26	12X8V — 50%	33	0.67	0.86	2.03	6.0	9.8		
Sums						76.9	82.6	4.8	6.2
CFR							1.07		1.29

[a]P stands for WFI Pipette, V stands for WFI Vessolet, and percentage values refer to Code-required reinforcement.

[b]Equation (8) of text.

[c]Equation (9) of text.

5.5 SADDLE-, PAD-, AND SLEEVE-REINFORCED BRANCH CONNECTIONS

The available experimental data for saddle-, pad-, and sleeve-reinforced branch connections are summarized in Table 12; the dimensional parameters are given in Table 13. Figure 23 shows the major design features. Note that all the data are for branch connections with d/D < 100 that were obtained prior to 1962. Perhaps this reflects a lack of interest in these types of branch connections, and indeed our survey of design practice in the nuclear industry indicated that the specialty product reinforced branch connections were preferred. However, the potential exists for using pad-reinforced vessel nozzles at the vessel-pipe interface for the design of more-flexible nuclear piping.[48]

None of the analytical design methods considered in this report are applicable to nonintegral reinforced branch connections. The two that gave the best correlations are shown in Table 12. The FAST2 analyses were made on *integral* reinforced models as shown in Fig. 24. The results, shown in Table 12, tend to agree quite well with the test data.

Table 12. Flexibility factors for saddle-, pad-, and sleeve-reinforced branch connections[a] (d/D < 0.52, D/T < 100)

Ref. No.	Nominal size	k_o for out-of-plane			k_i for in-plane		
		Test	Code	FAST2	Test	Code	FAST2
Saddles							
31	12 × 4	18	31.8	6.0	4.5	7.66	2.13
32	24 × 4	15	25.0	12.5	1.5	5.70	2.68
32	24 × 8	22	35.8	11.5	2.1	8.15	3.29
32	24 × 12	12	44.0	16.5	2.8	10.00	3.50
35	16 × 6	3	8.7	2.4	1.3	3.07	0.99
Sums		70	145.3	48.9	12.2	34.58	12.59
CTR			2.08	0.70		2.83	1.03
Pads							
32	24 × 4	20	25.0	14.9	4.7	5.70	4.23
32	24 × 8	28	35.8	22.8	3.6	8.15	5.00
32	24 × 12	18	44.0	18.1	5.6	10.00	5.12
35	16 × 6	8.4	8.7	3.7	1.5	3.07	1.66
34	48 × 6	10	17.0	8.0	1.6	3.82	3.11
Sums		84.4	130.5	67.5	17.0	30.74	19.12
CTR			1.55	0.80		1.81	1.12
Sleeve							
32	24 × 12	22	44		5.6	10.00	
Overall sums		176.4	319.8	116.4	34.8	75.32	31.71
Overall CTR			1.81	0.75		2.16	1.09

[a]See Fig. 23 and Table 13 for dimensional parameters.

The Code equations tended to overestimate the flexibility by about a factor of 2.

A frequent concern is how to adjust design guidance for integral reinforced branch connections to apply to nonintegral reinforcements. Some speculation is therefore appropriate. We might, for example, attempt to find an equivalent pipe wall thickness, T_e, that could be used in the Code equations to give a better estimate of the flexibility factors.

First, note from Table 12 that the overall CTRs give the ratios $k_{oc}/k_{oe} = 1.81$ and $k_{ic}/k_{ie} = 2.16$ for out-of-plane and in-plane moments, where the added subscripts indicate "Code" and "experiment," respectively. Then note that the Code equations [herein, Eqs. (8) and (9)],

Table 13. Dimensional parameters for saddle-, pad-, and sleeve-reinforced branch connections[a]
(d/D < 0.52, D/T < 100)

Ref. No.	Nominal size	D_o (in.)	T (in.)	d_o (in.)	t (in.)	L_1[b] (in.)	L_2[b] (in.)	D_p (in.)	t_p (in.)	D/T	d/D	t/T	D_p/d_o	t_p/T
							Saddles							
31	12 × 4	12.75	0.1875	4.500	0.165	24	24	7.313	0.368	67.0	0.345	0.88	1.625	1.96
32	24 × 4	24.00	0.312	4.500	0.237	75	150	9.625	0.344	75.9	0.180	0.76	2.139	1.10
32	24 × 8	24.00	0.312	8.625	0.250	180	48	17.250	0.438	75.9	0.354	0.80	2.000	1.40
32	24 × 12	24.00	0.312	12.750	0.250	109.5	109.5	23.750	0.438	75.9	0.526	0.80	1.863	1.40
35	16 × 6	16.00	0.500	6.625	0.280	21	21	11.625	0.500	31.0	0.409	0.56	1.755	1.00
							Pads							
32	24 × 4	24.00	0.312	4.500	0.237	36	192	7.750	0.375	75.9	0.180	0.76	1.722	1.20
32	24 × 8	24.00	0.312	8.625	0.250	78	150	15.750	0.375	75.9	0.354	0.80	1.826	1.20
32	24 × 12	24.00	0.312	12.750	0.250	109.5	109.5	25.000	0.375	75.9	0.528	0.80	1.960	1.20
35	16 × 6	16.00	0.500	6.625	0.280	21	21	12.125	0.500	31.0	0.409	0.56	1.830	1.00
34	48 × 6	49.25	0.625	6.625	0.280	41	73	10.500	0.625	77.8	0.130	0.45	1.585	1.00
							Sleeve							
32	24 × 12	24.00	0.312	12.750	0.250	109.5	109.5	c	0.375	75.9	0.528	0.80	c	1.20

[a]See Fig. 23 for identification of dimensions.

[b]All of these tests were for nozzles in headers with both ends more or less restrained. L_1 and L_2 are the distances from the nozzle centerline to the ends of the header.

[c]The axial length of reinforcement for this model, L_n = 25.0 in.; L_n/d_o = 1.96.

ORNL-DWG 87-4639 ETD
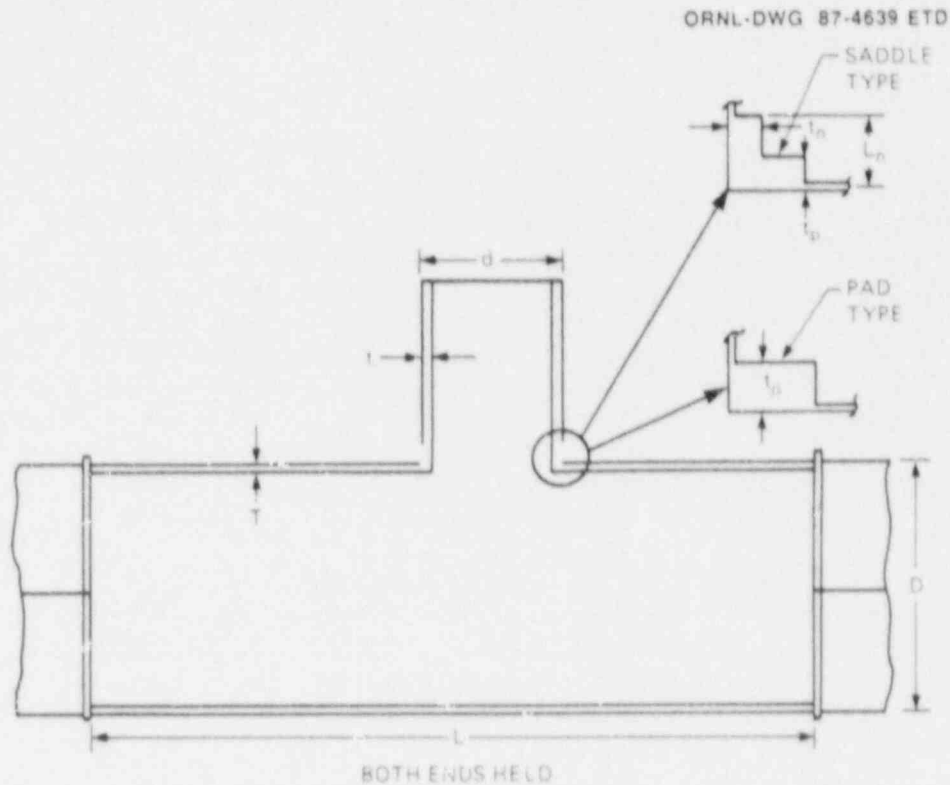
Fig. 24. Saddle- and pad-reinforced models used for FAST2 analysis.

can be written as

$$k_{oc} = T^{-2} G_o \quad ; \quad k_{ic} = T^{-3/2} G_i, \tag{22}$$

where G_o and G_i contain all the terms except T. Similar expressions can be written for k_{oe} and k_{ie} in terms of the equivalent pipe wall T_e:

$$k_{oe} = T_e^{-2} G_o \quad ; \quad k_{ie} = T^{-3/2} G_i, \tag{23}$$

so that the CTR ratios give

$$(k_{oc}/k_{oe}) = (T_e/T)^2 = 1.81 ,$$

and

$$(24)$$

$$(k_{ic}/k_{ie}) = (T_e/T)^{3/2} = 2.16 .$$

The equivalent wall thicknesses are then

$$T_e = (1.81)^{1/2} T = 1.35 T \qquad \text{for } k_o ,$$

and   (25)

$$T_e = (2.16)^{2/3} T = 1.67 T \qquad \text{for } k_i .$$

Note that T_e is considerably less than $(t_p + T)$, which ranges from 2T to 2.96T for the models in Table 13.

It is also informative to look at the saddle data and the pad data separately because they are quite different types of reinforcement.

Type of reinforcing	For k_o		For k_i	
	CTR	T_e/T	CTR	T_e/T
Saddles	2.08	1.44	2.83	2.00
Pads	1.55	1.24	1.81	1.49

As might be expected, these data indicate that saddles are more effective than pads in reducing flexibility. Conversely, if one were interested in retaining flexibility while increasing the bending strength of the branch connection, then pads would be more effective than saddles. The relative values of the parameters t_p/T and D_p/d_o shown in Table 13 probably both influence this saddle-vs-pad relationship as well.

If one were to seriously consider modifying the Code flexibility equations to also cover nonintegral reinforcements, a much larger data base would be needed. Because the FAST2 computer program appears to fit the existing data, an exploratory parameter study should be done to provide the needed additional data.

5.6 ANSI B16.9 TEES AND SWEEPOLETS

ANSI B16.9 tees are a class of commercially available, butt-welding tees fabricated in accordance with either the ANSI B16.9 or MSS-SP48 manufacturing standard.[49,50] These standards include overall dimensional and basic pressure strength requirements, as well as controls for certain manufacturing variables. In the design rules for nuclear piping, ANSI B16.9 tees are recognized as a class of piping products distinct from other types of branch connections. By common usage, the term includes only those tees that are characterized by a smooth transition region between the branch and run outlets and are forged from a segment of straight pipe using an external-surface die and some means for extruding

the branch outlet. Machined tees and welded tee joints, as well as
specialty products that are welded to the run pipe, are not included.
The manufacturing standards include dimensional controls for tees with
d/D ratios between about 1/3 and 1.0.

Figures 25 and 26 are photographs of two of the tees that were
tested under the ORNL Piping Program.[51] Figure 25 is a cut-away model of
a 12 × 6 sched. 40 stainless steel tee (ORNL T-8) showing the character-
istic contour and wall thickness variation that is typical of reducing
tees. Figure 26 is an external view of a 24 × 24 sched. 40 carbon steel
tee (ORNL T-10) that shows the smooth transition and tangent intersection
at the side that is characteristic of full outlet tees.

Sweepolets are forged, smooth transition, specialty product items,
trademarked and sold by the Pressure Fittings Division of Gulf and
Western Manufacturing Company, that are insert-welded to straight pipe to

ORNL PHOTO 78304
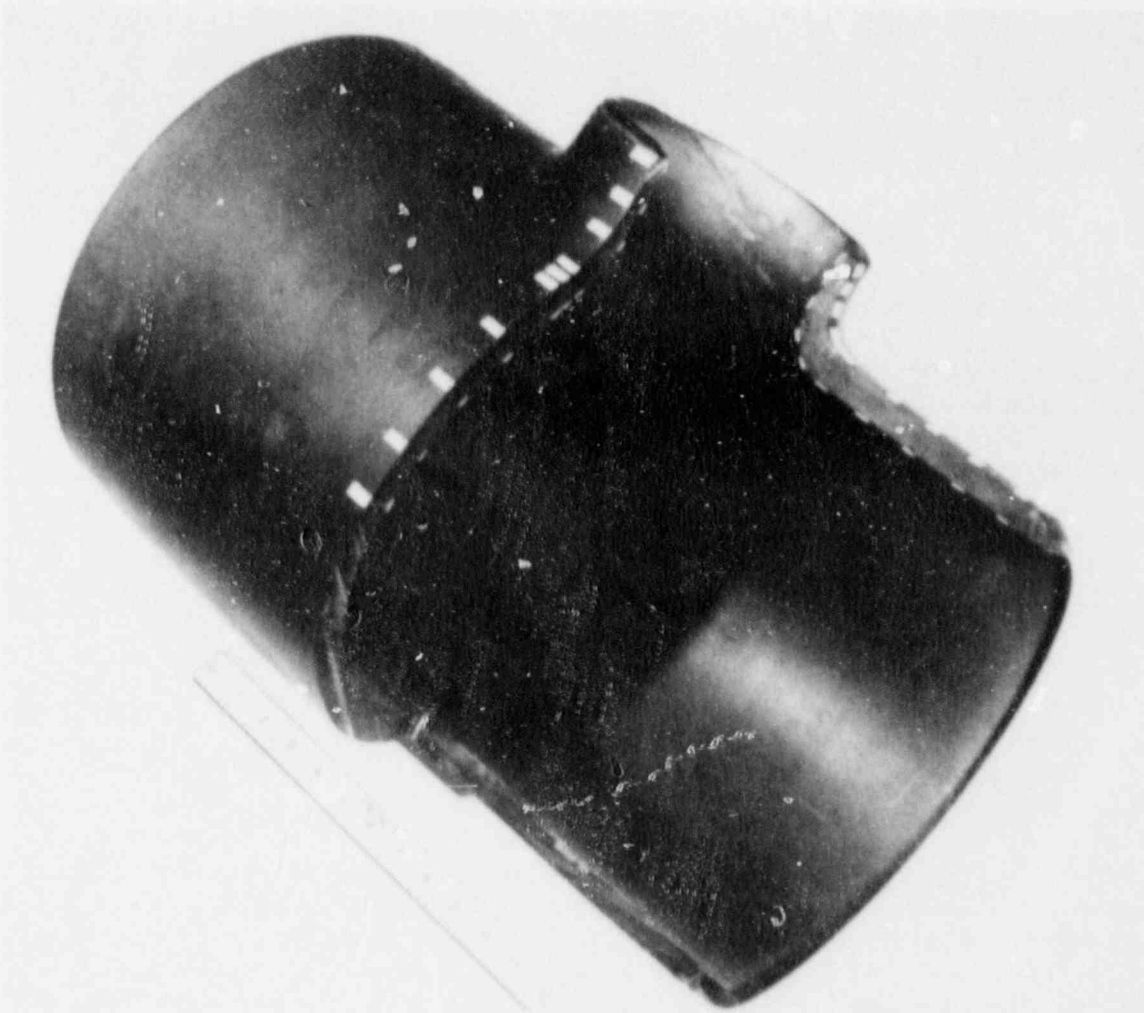
Fig. 25. Epoxy model of a 12- by 6-sched. 40 ANSI B16.9 tee,
ORNL T-8.
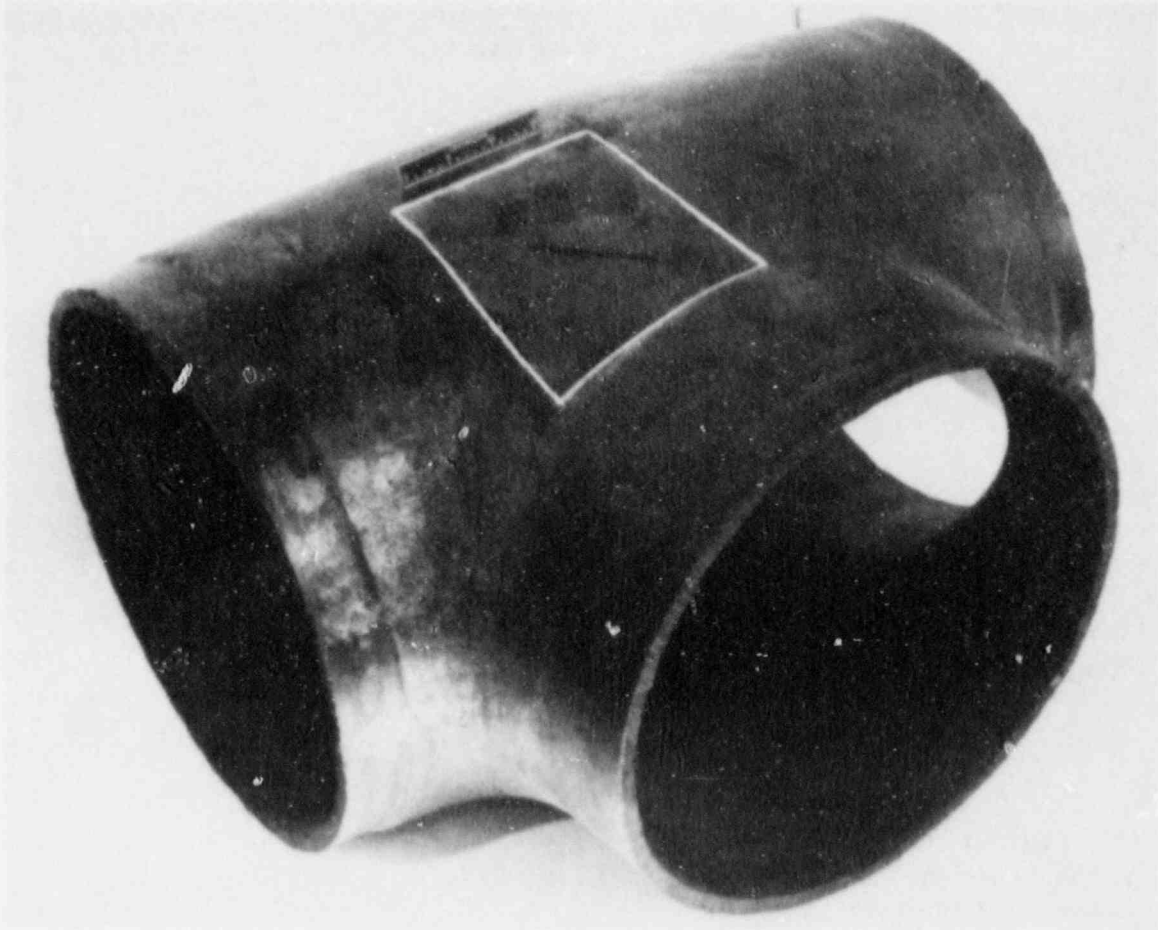
Fig. 26.   A 24- by 24-sched. 40 ANSI B16.9 tee, ORNL T-10, following the fatigue-to-failure test.

form a branch connection. The contour geometry is similar to that of ANSI B16.9 tees as shown in Fig. 27.

The available flexibility data are summarized in Table 14. All the tests were conducted with one end of the run pipe fixed; the flexibility factors discussed here were determined from the displacement data using the "point spring" branch connection model discussed in Sect. 4.1. These "k"s are different from the flexibility factors given in Ref. 46 because of the different strength-of-materials models used in analyzing the data. The negative test value for the sched. 160 tee T11 simply reflects the fact that the tee was heavier and consequently stiffer than the "point spring" model used in analyzing the data.

Table 14 contains two evaluations for ORNL T-16[46] that was ordered as sched. 10 with a nominal wall thickness of 0.250 in. Because of manufacturing practices (materials availability, scheduling, etc.), however, the tee was actually formed as sched. 20, with a nominal wall thickness
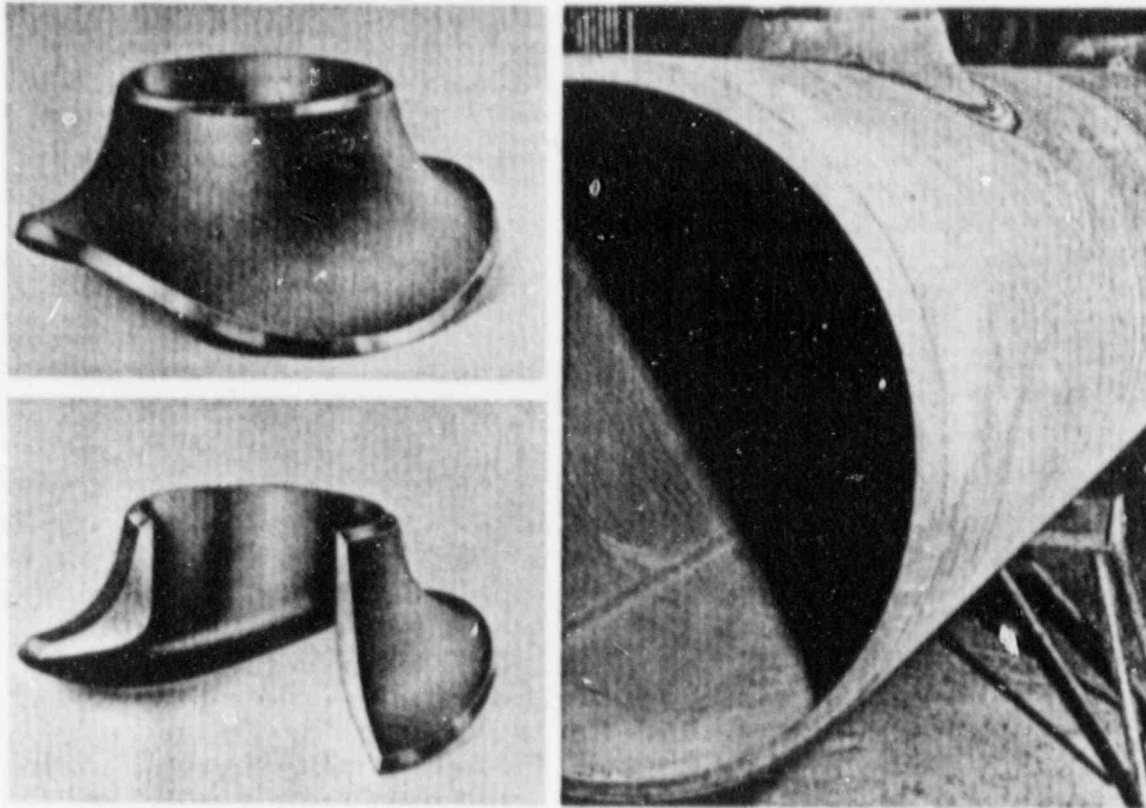
Fig. 27. Specialty product branch connection insert Sweepolet, made by the Pressure Fittings Div., Gulf and Western Manufacturing Co. (formerly Bonney Forge, Inc.).

of 0.375 in. This procedure is permitted under the ANSI B16.9 Standard as long as the welding ends are machined to match the smaller schedule pipe that will be welded to the tee. This was done for ORNL T-16, but in addition the wall thickness of the body of the tee was also reduced by through-boring the run to match the nominal inside diameter of sched. 10 pipe. This produced a variable wall thickness tee that is not typical of either sched. 10 or sched. 20 ANSI B16.9 tees. The test model was fabricated using sched. 10 pipe welded to the tee.

Comparisons of the experimental flexibility factors with the Code branch connection formulas given in Table 14 show that those formulas overpredict the flexibilities by wide margins (CTR = 6.94 for k_o and 2.14 for k_i). The test values are relatively low, however, and the main message is that the flexibility of B16.9 tees is not likely to be significant in the design of typical piping systems.

Table 14. Flexibility factors for ANSI B16.9 tees and Sweepolets

Ref. No.	Nominal size NPS	Nominal wall thickness		Model parameters			k_o		k_i	
		Run (in.)	Branch (in.)	D/T	d/D	t/T	Test[a]	Code[a]	Test[a]	Code[a]
37	12 × 10	0.500	0.500	24.5	0.837	1.000	4.4	11.8	4.8	4.66
37	12 × 10	0.500	0.500	24.5	0.837	1.000	7.6	11.8	4.5	4.66
37	12 × 10	0.429	0.450	23.7	0.836	1.049	7.3	15.2	4.2	5.56
46-T10	24 × 24 Sched. 40	0.687	0.687	33.9	1.000	1.000	1.3	20.6	3.5	6.98
46-T11	24 × 24 Sched. 160	2.343	2.343	3.24	1.000	1.000	-0.3[b]	5.9	0.8	2.05
46-T12	24 × 10 Sched. 40	0.687	0.365	33.9	0.445	0.531	2.3	10.0	0.9	3.39
46-T13	24 × 10 Sched. 160	2.343	1.125	9.24	0.444	0.480	0.4	1.51	0.2	0.95
46-16A[c]	24 × 24 Sched. 20	0.375	0.375	63.0	1.000	1.000	1.8	51.2	6.0	12.8
46-16B[c]	24 × 24 Sched. 10	0.250	0.250	95.0	1.000	1.000	0.8	94.1	3.8	19.2
38[d]	12 × 6 Sched. 40S	0.375	0.280	33.0	0.513	0.747	8.2	12.3	1.4	4.21
Sums							33.8	234.41	30.1	64.46
CTR								6.94		2.14

[a] Even though the ASME Code gives flexibility guidance for ANSI B16.9 tees, the data were analyzed for this report as if they were branch connections as discussed in Sect. 3.1.

[b] Negative numbers imply that the "point spring" in the model was stiffer than the branch pipe.

[c] ORNL T-16 was ordered as sched. 10, but was manufactured as sched. 20 and "through bored" to sched. 10 on the run. The displacement data were analyzed as if the entire model was sched. 20 for T-16A and as if the entire model was sched. 10 for T-16B.

[d] This is the only Sweepolet data that we have.

6. BRANCH MOMENT FLEXIBILITY FACTORS COMPARED
WITH ANALYTICAL DATA

6.1 FINITE-ELEMENT DATA

The available benchmark finite-element data and corresponding flexibility factors are summarized in Tables 15–19. The finite-element analysis (FEA) data listed in Tables 15–18 for nozzles with $D/T < 100$ and $d/D < 0.5$ were used earlier as the essential data base for the present ASME Code flexibility factors. As one might expect, the comparisons are very good between the Code equations and the FEA data shown in Tables 15 and 16 for the unreinforced branch connections and in Table 17 for the nozzle-reinforced branch connections. Table 18 gives the dimensional parameters for the models listed in Table 17. The overall CFR values for the out-of-plane flexibility factor k_o from Tables 15 and 17 are shown below.

	Overall CFR[a] values for k_o				
	Code	M&S	LUGS	WRC-297	FAST2
UBC models (Table 15)	0.98	1.08	1.67	2.96	0.99
S1 models (Table 17)	0.86	1.55	2.84	6.56	0.97
P30 models (Table 17)	1.28	2.88	4.36	7.81	1.82

[a]CFR is the ratio of the sum of the calculated values to the sum of the finite-element values.

M&S design charts and the LUGS computer program, representing Bijlaard's theory, both show good comparisons for the standard nozzle-reinforced S1 models. Neither method is strictly applicable for the P30 models, however, because of the shape of the reinforcement. This shows up as an extreme overestimate for the P30A model, as well as a general overestimate for the other P30 models.

Steeles' theory, FAST2, shows very good comparisons for both the UBC and S1 models, even though the dimensional parameters for a number of the models were outside the theoretical thin-shell theory range. The comparison for the P30 models is not so good, again because of the reinforcement shape. The Code equations do a better job for these models.

The WRC-297 method, based on Steele's theory, overestimated k_o by a considerable amount for all three sets of models. The values shown in Table 15 for the UBC models are based on the $A > 100$ pair of lines from

Table 15. Out-of-plane moment flexibility factors for unreinforced branch connections ($d/D \leq 0.5$, $D/T < 100$) — comparisons with finite-element data[a]

Model No.	Model parameters[b]			k_o					
	D_o/T	d_o/D_o	t/T	FEA	Code	M&S	LUGS	WRC-297	FAST2
UA	102	0.50	0.50	47.0	51.5	51	84.1	170	44.7
UB	82	0.50	0.50	37.2	37.1	36	65.3	120	36.3
UC	42	0.50	0.50	16.2	13.6	17	28.3	46	18.3
UD	22	0.50	0.50	6.92	5.16	8	12.04	17	8.57
UE	12	0.50	0.50	2.84	2.08		4.89	16	3.99
UF	12	0.08	0.08	1.96	0.33		0.36	0.06	0.07
Sums				112.12	109.77		194.99	369.1	111.93
CFR[c]					0.98	1.04	1.74	3.29	1.00
J11	59.5	0.115	0.238	6.92	7.59	5.1	5.37	6.4	5.96
J22	20.0	0.020	0.020	0.00	0.18	0.0	0	0	0
J33	20.0	0.080	0.474	0.96	1.74	0.94	0.98	1.0	0.02
J44	20.0	0.320	1.000	7.75	5.06	12.0	14.54	16.0	7.84
J3	49.0	0.114	0.840	10.10	10.60	13.0	13.72	15.0	10.08
Sums				25.73	25.17	31.04	34.61	38.40	23.90
CFR[c]					0.98	1.21	1.35	1.49	0.93
Overall sums				137.85	134.94	143.04	229.6	407.46	135.83
Overall CFR[c]					0.98	1.08	1.67	2.96	0.99

[a]All the finite-element data in this table are from Refs. 15 and 21. The models were analyzed with one end of the run fixed and the other end free.

[b]$L/D = 4.0$ and 2.0 for the U models and the J models, respectively.

[c]CFR is the ratio of the sum of the calculated values to the sum of the finite-element values.

Table 16. In-plane moment flexibility factors for unreinforced branch connections ($d/D \leq 0.5$, $D/T < 100$) — comparisons with finite-element data[a]

Model No.	Model parameters[b]			k_i					
	D_o/T	d_o/D_o	t/T	FEA	Code	M&S	LUGS	WRC-297	FAST2
UA	102	0.50	0.50	8.89	10.2	4.3	8.73		8.79
UB	82	0.50	0.50	7.68	8.2	4.2	7.82		7.38
UC	42	0.50	0.50	4.58	4.2	3.2	5.08		4.28
UD	22	0.50	0.50	2.65	2.2	1.9	2.96		2.51
UE	12	0.50	0.50	1.50	1.2		1.54	1.5	1.53
UF	12	0.08	0.08	1.91	0.2		0.24	0.05	0.06
Sums				27.21	25.0		26.37		24.49
CFR[c]					0.92	0.57	0.97		0.90
J11	59.5	0.115	0.238	3.99	1.97	2.4	2.64	2.8	3.22
J22	20.0	0.020	0.020	0	0.08	0	0	0	0
J33	20.0	0.080	0.474	0.75	0.78	0.6	0.63	0.61	0.60
J44	20.0	0.320	1.000	2.81	2.26	4.2	5.24	4.8	3.21
J3	49.0	0.114	0.840	5.26	3.03	6.7	7.05	6.6	5.35
Sums				12.81	8.12	13.9	15.56	14.81	12.48
CFR[c]					0.63	1.09	1.21	1.16	0.97
Overall sums				40.02	33.12		41.93		36.97
Overall CFR[c]					0.83	0.75	1.05	1.01	0.92

[a]All the finite-element data in this table are from Refs. 15 and 21. The models were analyzed with one end of the run fixed and the other end free.

[b]$L/D = 4.0$ and 2.0 for the U models and the J models, respectively.

[c]CFR is the ratio of the sum of the calculated values to the sum of the finite-element values.

Table 17. Flexibility factors for nozzle-reinforced, finite-element models
(d/D ≤ 0.5, D/T ≤ 100)

Model No.	k_o for out-of-plane moments						k_i for in-plane moments					
	FEA	Code	M&S	LUGS	WRC 297	FAST2	FEA	Code	M&S	LUGS	WRC 297	FAST2
S1A	17.8	17.5	34	62.1	160	18.04	2.70	3.46	2.3	5.36		3.2
S1B	14.5	13.1	24	47.3	115	14.84	2.42	2.90	2.1	4.63		2.62
S1C	6.32	5.43	10	19.3	41	6.56	1.46	1.68	1.3	2.62		1.43
S1D	2.33	2.33		8.0	14	3.10	0.72	0.99		1.31		0.82
S1E	0.69	1.06		2.5	4.6	1.68^{α}	0.24	0.61		0.46		0.57α
S1F	4.07	3.08	5.8	9.11	15.0	4.38	1.09	0.95	1.2	1.86		0.99
S1G	1.41	1.32	2.1	3.31	5.2	1.75^{α}	0.49	0.57	0.5	0.80		0.50^{α}
S1H	0.33	0.61		1.21	1.6	0.74^{α}	0.07	0.35		0.32	0.28	0.27^{α}
S1I	2.11	1.27	1.6	2.11	3.2	1.42^{α}	1.14	0.39	0.6	0.72	0.58	0.45^{α}
S1J	0.95	0.55	0.5	0.69	0.89	0.50^{α}	0.71	0.24	0.2	0.26	0.28	0.20^{α}
S1K	0.35	0.26		0.23	0.26	0.19^{α}	0.28	0.15		0.09	0.08	0.09^{α}
S1L	2.02	0.52	0.33	0.43	0.55	0.33^{α}	1.85	0.16	0.2	0.20	0.19	0.15^{α}
S1M	1.43	0.23	0.09	0.12	0.15	0.11^{α}	1.39	0.10	0.05	0.06	0.06	0.06^{α}
S1N	0.81	0.11		0.04	0.04	0.04^{α}	0.80	0.06		0.02	0.02	0.02^{α}
Sums	55.12	47.37		156.41	361.49	53.68	15.36	12.61		18.71		11.37
CFR		0.86	1.55	2.84	6.56	0.97		0.82	0.64	1.22		0.74
P30A	6.91	10.44	24	35.84	73.0	15.46	1.89	2.07	3.1	5.05		2.68
P30B	3.20	3.38	6.3	14.29	18.0	4.73	1.07	1.04	1.4	3.06		1.11
P30C	1.20	1.48	2.3	3.61	5.7	1.93	0.54	0.49	0.6	0.94	0.81	0.58
P30D	0.33	0.68		1.31	1.9	0.86^{α}	0.17	0.39		0.38	0.35	0.33^{α}
P30E	0.99	0.13		0.04	0.05	0.04^{α}	0.98	0.07		0.02	0.02	0.03^{α}
Sums	12.63	16.11		55.09	98.65	23.02	4.65	4.06		9.45		4.73
CFR		1.28	2.88	4.36	7.81	1.82		0.87	1.46	2.03		1.02
Sums	67.75	63.48		211.50	460.14	76.70	20.01	16.67		28.16		16.10
CFR		0.94	1.79	3.12	6.79	1.13		0.83	0.81	1.41		0.80

$^{\alpha}$Model parameters are outside Steele's theoretical limits.

63

Table 18. Dimensional parameters for nozzle-reinforced, finite-element models[a]

Model No.[a]	D_o (in.)	d_o (in.)	T (in.)	t (in.)	t_n (in.)	L_n (in.)	D/T	d/D	t/T	t_n/T	d_n/D
S1A	10.0	5.0	0.098	0.049	0.3763	0.651	101	0.50	0.50	4.34	0.581
S1B	10.0	5.0	0.122	0.061	0.4282	0.7123	81	0.50	0.50	4.01	0.593
S1C	10.0	5.0	0.2381	0.1191	0.6285	0.9487	41	0.50	0.50	3.14	0.641
S1D	10.0	5.0	0.4545	0.2273	0.8862	1.2834	21	0.50	0.50	2.45	0.710
S1E	10.0	5.0	0.8333	0.4167	1.1832	1.7658	11	0.50	0.50	1.92	0.804
S1F	10.0	3.2	0.2381	0.0762	0.5333	0.7143	41	0.32	0.32	2.56	0.437
S1G	10.0	3.2	0.4545	0.1454	0.7545	0.9662	21	0.32	0.32	1.98	0.493
S1H	10.0	3.2	0.8333	0.2667	1.0000	1.9324	11	0.32	0.32	1.52	0.567
S1I	10.0	1.6	0.2381	0.0381	0.4095	0.4658	41	0.16	0.16	1.88	0.248
S1J	10.0	1.6	0.4545	0.0727	0.5772	0.6321	21	0.16	0.16	1.43	0.289
S1K	10.0	1.6	0.8333	0.1333	0.7667	0.8707	11	0.16	0.16	1.08	0.342
S1L	10.0	0.8	0.2381	0.1091	0.3096	0.3081	41	0.08	0.08	1.38	0.142
S1M	10.0	0.8	0.4545	0.0364	0.4317	0.4203	21	0.08	0.08	1.03	0.174
S1N	10.0	0.8	0.8333	0.0667	0.5333	0.6213	11	0.08	0.08	0.72	0.204
P30A	10.0	3.2	0.098	0.0314	0.2812	0.7444	101	0.32	0.32	3.19	0.380
P30B	10.0	3.2	0.2381	0.0762	0.4310	1.1771	41	0.32	0.32	2.13	0.416
P30C	10.0	3.2	0.4545	0.1454	0.5818	1.6646	21	0.32	0.32	1.60	0.457
P30D	10.0	3.2	0.8333	0.2667	0.7583	2.3543	11	0.32	0.32	1.23	0.515
P30E	10.0	0.8	0.8333	0.0667	0.3749	1.1771	11	0.08	0.08	0.53	0.169

[a]The S1 models look like Fig. 3(a); the P30 models look like Fig. 3(c). See Ref. 15. $L/D = 4$ for all these models. One end was fixed, and the other end was free for the finite-element analyses.

Table 19. Flexibility factors for nozzles in very large
diameter tanks[a] — FEA models

Model No.	Model parameters				k_o for out-of-plane moment				k_i for in-plane moment			
	D/T	d_o/D	t/T	L/D[b]	FEA	Code	WRC-297	FAST2	FEA	Code	WRC-297	FAST2
B1	400	0.0255	0.2	7.26	18	57	21	18	12	6	9	11
B2	2,500	0.0102	0.5	2.91	210	893	260	200	122	36	130	119
B3	10,000	0.0051	1.0	1.46	1,400	7,140	2,000	1,250	746	101	1,000	782
B4	40,000	0.00255	2.0	0.73	11,000	57,100	16,000	9,168	5,600	571	8,200	5,981
Sums					12,628	65,190	18,281	10,636	6,480	714	9,339	6,893
CFR						5.16	1.45	0.84		0.11	1.45	1.06

[a]Taken from Appendix B, *WRC Bulletin 297*.[27]

[b]Both ends of the vessel were restrained.

WRC-297 Fig. 60 (Fig. 13 herein). If we had used the $\lambda = 14$ line, even though it is not applicable because $T/t > 1.0$, the estimated k_o values would have been about 30% lower and would have agreed a little better with the FEA results. The reduction would need to be on the order of 300%, however, to agree as well as the Code equations.

The values shown in Table 17 for the locally reinforced S1 and P30 models were based on redefining the nozzle-diameter-to-shell diameter ratio (d/D) and the wall thickness ratio (T/t) to account for the reinforcement; that is, we used T/t_n and $\lambda = (d_n/D) \sqrt{D/T}$, where

$$d_n = (d/D) + (2 t_n/T - t/T)/(D/T) . \qquad (26)$$

As noted previously, however, using t_n instead of t appears to be going in the wrong direction.* Both d_n and t_n were also used in the M&S and LUGS calculations.

Comparisons between the finite-element data and the various design methods for the in-plane moment flexibility factor k_i are shown in Table 16 for the unreinforced UBC models and in Table 17 for the nozzle-reinforced S1 and P30 models. The overall CFR values are shown below.

	Overall CFR values for k_i				
	Code	M&S	LUGS	WRC-297	FAST2
UBC models (Table 16)	0.83	0.75	1.05		0.92
S1 models (Table 17)	0.82	0.64	1.22		0.74
P30 models (Table 17)	0.87	1.46	2.03		1.02

No CFR values are given for the WRC-297 method because the parameter $\lambda = (d_o/D) \sqrt{D/T}$ is outside the range of the WRC figure for most of the models. The few models that fell within the range of the figure do not give enough data for the CFR to be meaningful. Those WRC-297 k_i values that are included in Tables 16 and 17, however, agree rather well with the values calculated with FAST2. The design methods, in general, appear to give reasonably good estimates for k_i for the parameter range $D/T < 100$, $d/D < 0.5$.

Table 19 summarizes the finite-element data and comparisons for nozzles in very large thin-walled vessels (tanks) from Appendix B of WRC

*See discussion in the "Summary" section.

Bulletin 297. The two smaller D/T models, B1 with D/T = 400 and B2 with D/T = 2500 are within the range of interest discussed in Sect. 2 of this report. The other two, B3 and B4, with D/T values of 10,000 and 40,000 are not realistic structures but perhaps do provide some indication of how the theories compare for those extreme D/T ratios. In making these comparisons, however, remember that the FEA method is also subject to error. Bijlaard's theory is not applicable because of series convergence problems for very large D/T.

The CFR values given in Table 19 show that the Code equations are poor estimators for these very large D/T ratios, overpredicting k_o and underpredicting k_i just like the earlier comparisons with test data. Both FAST2 and WRC-297 are in reasonably good agreement with the FEA data. This is a definite encouragement for Steeles' theory and the FAST2 computer program. We feel that it is fortuitous, however, for the WRC-297 method because of the better correspondence between the model parameter $\Lambda = 145$ and the Bulletin curves for $\Lambda = 100$.

6.2 HANSBERRY AND JONES THEORY FOR k_i

In 1969 Hansberry and Jones[52] (H&J) presented a theoretical solution, based on thin-shell theory, for a small unreinforced branch connection, d/D = 0.10, t/T = 1.0, with an in-plane moment acting on the branch and equilibrium reaction moments on both ends of the run (vessel). They did not indicate the length of the run, but more than likely considered it as effectively infinite. For the FAST2 calculations, we used a value of L = 100 in.; that is, L/D = 10. Several trial calculations using L from 50 to 500 in. indicated that the effect of L/D had essentially stabilized at L/D = 10.

In-plane flexibility factors k_i, converted from their paper for D/T values ranging from 200 to 1000, are listed in Table 20, along with values from the Code equation and FAST2. If we assume that the FAST2 values are more nearly correct, it is apparent that the H&J solution underestimates k_i by 20 to 50%. As before, the Code equation does a poor job for this range of D/T, being even lower than H&J by about 50%.

Table 20. In-plane moment flexibility
factors from Hansberry and Jones[a]
theory for unreinforced
branch connections
($d/D = 0.10$; $t/t = 1.0$; $L/D = 10$[b])

| D/T | k_1 for in-plane moment | | | H/F ratio[c] |
	H&J[a]	Code	FAST2	
200	16	13	32	0.50
300	35	19	49	0.71
400	52	25	66	0.79
600	82	38	99	0.83
800	103	51	130	0.79
1000	117	63	161	0.73
Sums	405	209	537	
CHJR		0.52	1.33	Av 0.75

[a]See Ref. 52.

[b]The length of the run L was not
given in Ref. 52. For the FAST2 calcula-
tions, $L/D = 10$ was used.

[c]H/F ratio is k_1(H&J)/k_1 (FAST2).

7. FLEXIBILITY FACTORS FOR TORSIONAL BRANCH MOMENTS

Experimental data on the angular rotation of a branch connection or nozzle due to a torsional moment on the branch are very sparse. Mills, Rodabaugh, and Atterbury[37] and Moore, Hayes, and Weed[46] provided test data for eight ANSI B16.9 tees. In most cases, the measured torsional rotation θ_m was of the same order of magnitude as the nominal rotation θ_n, so that $(\theta_m - \theta_n) \ll \theta_m$. Thus, an accurate determination of the "point spring" model flexibility factor could not be made for the B16.9 tees.

Moffat and Kirkwood,[47] however, obtained experimental torsional flexibility factors k_{tb} for four full outlet unreinforced branch connection models ($d/D = t/T = 1.0$) that were of the same order of magnitude as the in-plane and out-of-plane flexibility factors noted below:

Model	1	2	3	4
D/T	42.4	25.7	16.2	12.4
k_{tb}	15.23	8.06	3.90	3.81
k_{ob}	28.04	13.12		
k_{ib}	8.25	7.67		

They also analyzed Model 2 by the finite-element method with essentially the same results. These data indicate that torsional flexibility may be significant in design for the larger d/D branch connections.

Although Steeles' theory and the FAST2 computer code have the capability for calculating torsional flexibility factors k_θ, the numerical parameter studies have not been done. For nozzles with very small d/D, however, an upper-bound solution might be appropriately developed by modeling the cylindrical shell as an infinite flat plate with a round hole of diameter $d = 2r_i$ at the origin and a torsion moment load M_t uniformly distributed around the inside edge of the hole. Equilibrium conditions would then require that

$$M_t = S_s(2\pi r^2 T) \quad \text{for } r = r_i \text{ to } \infty , \tag{27}$$

where S_s is the shear stress and T is the thickness of the flat plate (cylindrical shell). For a differential element in cylindrical coordinates, the shear stress is related to shear strain by

$$S_s = (d\theta)rG/(dr) , \tag{28}$$

where G is the shear modulus. Combining Eqs. (27) and (28) leads to the simple differential equation

$$\frac{d\theta}{dr} = \frac{M_t}{2\pi GTr^3} ,$$

(2?)

which may be solved by integration over the range $r_i < r < $; that is,

$$\theta = \frac{M_t}{2\pi GT} \int_{r_i}^{\infty} \frac{dr}{r^3} = \frac{M_t}{4\pi GT} \frac{1}{r_i^2} .$$

(30)

Additional test data and more-refined analyses are needed to adequately answer the question of the design significance of torsional flexibility, especially for $d/D > 0.5$.

8. FLEXIBILITY FACTORS FOR RADIAL LOADS

Axial stresses are not routinely evaluated in a piping system design, primarily because they are generally <3000 psi in a properly supported piping system. This value is not significant with respect to either the allowable stresses or to the stresses caused by internal pressure or moment loads. Axial loads, however, are routinely calculated in the piping system analysis (flexibility analysis) and used in the design of the supports. In addition, pressure vessels and tanks usually have design allowable radial loads for the nozzles that impose limits on the axial loads from the attached piping. Recent reports on damage to piping systems during earthquakes also suggest that the axial forces within the piping may be important for dynamic loadings.

One important consideration in calculating radial loads on vessel nozzles is the tendency of the attached pipe to shed additional load by displacing laterally when the axial load on the pipe exceeds a critical value. This critical load will depend on several factors, including the straightness and length of the pipe between supports, the rotational rigidity of the supports, and lateral loads on the pipe from dead-weight, etc. A first approximation can be obtained from Euler's buckling equation for a hinged-end column:

$$W/A = \pi^2 E/(L_c/r_g)^2 , \tag{31}$$

where W/A is the axial compressive stress in the pipe, L_c is the critical buckling length, and

$$r_g = (1/4) \sqrt{d_o^2 + d_i^2} \tag{32}$$

is the radius of gyration of the pipe. For the particular case of W/A = 3000 psi, the associated critical pipe length, in feet, is given by

$$L_c = (\pi^2 E/3000)^{1/2} r_g/12 . \tag{33}$$

For sched. 40 pipe, Eq. (33) gives

Size (NPS)	2	4	8	16	24
L_c, ft	21	40	77	143	216

Considering that "straight" pipe is not very straight and that a lateral deadweight load exists for horizontal pipe runs, L_c from Euler's equation will probably be larger than the actual critical buckling length of the attached pipe. This potential nonlinearity should be remembered in the following discussion.

Table 21 summarizes the available experimental data for thrust loads W in terms of the flexibility factor k_w defined as [see Eq. (13) Sect. 3.3.2]

$$k_w = \delta/(Wd/EA_n) ,\qquad(34)$$

where δ is the inward radial displacement of the shell, d is the midwall diameter of the attached pipe, and A_n is the cross-sectional area of the attached pipe:

$$A_n = \pi/4\ (d_o^2 - d_i^2) .\qquad(35)$$

Table 21 contains three sets of data. The first set is the four data points obtained by Cranch[34] in 1960 from tests on the 48-in.-diam by

Table 21. Thrust-load flexibility factors — experimental data[a] and analytical comparisons

Model (type)	Model parameters				k_w				
	D/T	d_o/D	t/T	L/D	Test	Theory[b]	LUGS	WRC-297	FAST2
Attachment 1 (Trunion)	77.8	0.136	0.448	2.143	77	84	92	40	81
Attachment 2 (UBC)	77.8	0.136	0.448	2.143	110	86	92	40	84
Attachment 3 (Pad)	77.6	0.136	0.448	2.143	120[c]	70	92	40	63
Attachment 5 (Bar)	77.8	0.072	Solid bar	2.143	450	310	316	210	295
Sums					757	550	592	330	523
CTR						0.727	0.782	0.436	0.691
CBI-1 (1 1/8 in.)	1050	0.0113	0.632	0.432	1200	1400		1200	1223
CBI-2 (UBC)	1050	0.0278	1.088	0.432	1800	2100		1300	1475
CBI-3 (5/8 in.)	2530	0.0100	0.527	0.239	2100[d]	1700		2100	2327
CBI-4 (1 in.)	2530	0.0500	0.527	0.239	1300[d]	2800		<300	882
LPV2 (UBC)	960	0.00417	1.000	0.332	1400			1500	1696
Sums					7800			6400	7603
CTR						1.25		0.82	0.98

[a]Data for the first four models are from Cranch,[34] data for the CBI models are from Whipple et al.,[41-43] and data for model LPV2 are from Schroeder.[44]

[b]Theory is Bijlaard's cited by Cranch[34] for the first four models, and Steeles'[13] for the CBI models.

[c]Questionable data.

[d]Nonlinear data; see Figs. 19 and 20.

0.624-in.-wall vessel with five attachments, shown in Fig. 28. Attachments 1—3 were made by welding 6-in. NPS sched. 40ST pipe (d_o = 6.625, t = 0.280) to the vessel as shown. There was no opening in the vessel wall for attachment 1 (Trunion), whereas for both attachments 2 and 3 there was an opening in the vessel wall equal in diameter to the outside diameter of the pipe. Attachment 2 (UBC) was unreinforced, whereas attachment 3 (Pad) was reinforced with a 10.5-in.-OD by 0.625-in.-thick ring welded to the vessel and to the pipe. Attachment 4 had a rectangular cross section and is not of direct interest here. Attachment 5 (Bar) was a 3.5-in.-diam solid round bar. Cranch's tests were conducted both with and without internal pressure in the vessel (p = 193 and 0 psi). These are the only test data we are aware of that considered the effects of internal pressure (see Sect. 9). Details of how the displacements were measured or how the dial gages were supported were not reported. The CBI models, tested by Whipple et al.[41-43] and the LPV2 model tested by Schroeder[44] were discussed earlier.

Table 21 gives the nondimensional model parameters, the experimental flexibility factors k_w, and corresponding analytical k factors for zero pressure. The experimental values for the four Cranch models appear to be consistent except for the pad-reinforced attachment 3 that was reported to be more flexible than the unreinforced attachment 2. Test data for the pressurized case are in the proper order. The experimental values given in Table 21 for CBI-3 and CBI-4 are Steele's interpretation[13] of the displacement data reported in Ref. 43 (see Figs. 19 and 20).

ORNL-DWG 87-4640 ETD
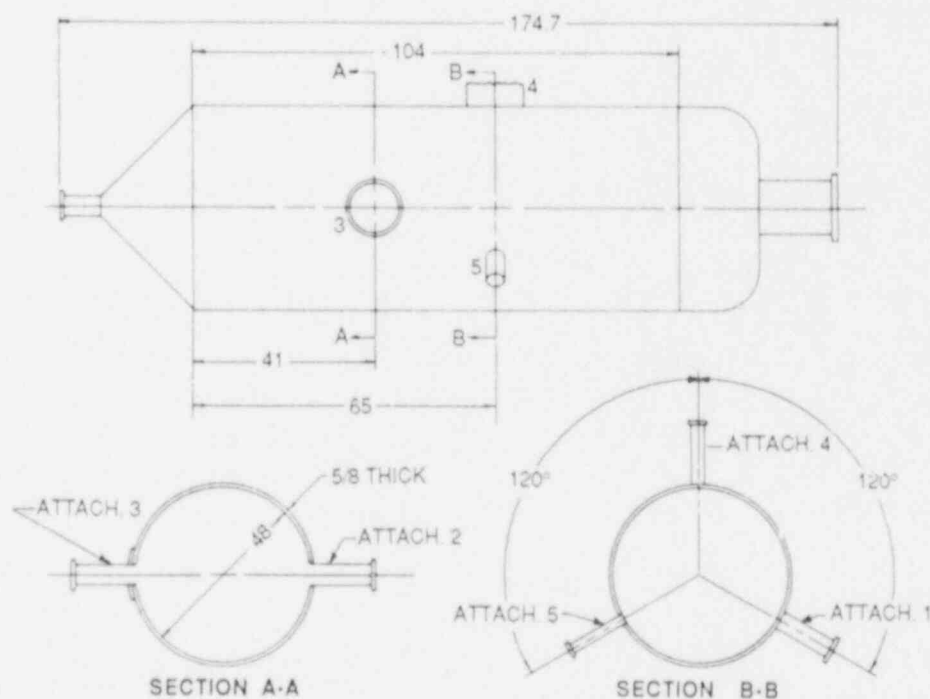
Fig. 28. Cranch's pressure vessel nozzle test model from Fig. 6 of Ref. 34.

The analytical values of k_w given under the theory column of Table 21 are from Bijlaard's theory as cited by Cranch for the first four models and from Steeles' theory as reported in the 1981 Shelltech progress report to PVRC.[13] Reasonable correlation seems to exist between the "theory" values and the experimental values in view of the three questionable data points. Both Bijlaard's theory, as expressed in the LUGS computer program, and Steele's theory, as expressed in the FAST2 program, appear to give reasonable correlations with Cranch's data; the WRC-297 results appear to be low. We would expect the WRC-297 results for attachment 5 to agree much better because the design curves in the Bulletin were derived specifically for a solid bar attachment. All three columns based on Steeles' theory give good correlations for the large D/T models. Bijlaard's theory is not applicable.

9. INFLUENCE OF INTERNAL PRESSURE

Bijlaard's original paper[12] includes an internal pressure term in the general solution for the radial shell displacement w [Eq. (15), Ref. 12]. Moreover, the influence of internal pressure is shown to be nonlinear; for example, doubling the internal pressure P does not double the influence of P on w. Both M&S[23] and Dodge[26] have included the pressure term in their computer programs. M&S also provided design graphs for P = 500 and 1000 psi, which illustrate the nonlinear influence of pressure. Their choice of P as a general design parameter, however, is not good because it does not normalize the design graphs with respect to dimensions of engineering interest. For example, if D/T were 300, then the only values that can be read directly from the graphs are for cases with a nominal hoop stress of 75,000 or 150,000 psi, respectively. Because the effect of pressure is nonlinear, interpolation between the graphs is subject to considerable error. A better choice would have been to plot curves normalized to PR/T.

Table 22 shows the influence of internal pressure on the thrust load flexibility factor k_w for four of the five attachments tested by Cranch.[34]

Table 22. Influence of internal pressure
on thrust-load flexibility factors

(D/T = 77.8)

Model[a]	Pressure (psi)	k_w		
		Test[a]	Theory[b]	LUGS[c]
Attachment 1	0	77	84	92
(Trunion)	193	73	68	81
Reduction		5.2%		
Attachment 2	0	110	86	92
(UBC)	193	77	70	81
Reduction		30.0%		
Attachment 3	0	120	70	92
(Pad)	193	41	53	81
Reduction		65.8%		
Attachment 5	0	450	310	316
(Bar)	193	200	260	280
Reduction		55.6%		
Sums		1148	1001	1115
CTR			0.87	0.97

[a]Tests conducted by Cranch[34]; see text and Fig. 28 for model dimensions.

[b]Theory is Bijlaard's cited by Cranch.[34]

[c]LUGS is Bijlaard's theory programmed by Dodge.[26]

The pressure load of 193 psi that was used gives a nominal hoop stress of $PR/T = 7500$ psi, which is well within the range of allowable design stress. As may be seen, the internal pressure reduced k_N by 5 to 60%. Bijlaard's theory, as expressed under the "theory" and LUGS columns, correlates quite well with Cranch's data and appears to do as well with internal pressure as without it.

Table 23 shows the influence of internal pressure on the in-plane (M_i) and out-of-plane (M_o) flexibility, as well as on the thrust load (W) flexibility. Because Cranch did not test his model with moment loadings on the attachment, all that we can show is the influence predicted by Bijlaard's theory as expressed in his original paper and as programmed in the LUGS computer program. The two sets of numbers tend to agree, with LUGS giving slightly higher values because more terms were used in evaluating the series. Both indicate that the internal pressure effect on the flexibilities could be significant in design.

Table 23. Effect of internal pressure on flexibility

Attachment No.[a]	R/T	d_o/D	Type load	Pressure (psi)	$(\theta/M \text{ or } \delta/w) \times 10^6$	
					Bijlaard	LUGS
2	38.9	0.136	M_o	0	0.113	0.124
				193	0.103	0.112
			Reduction		8.8%	9.7%
			M_i	0	0.043	0.046
				193	0.041	0.045
			Reduction		4.7%	2.2%
			W	0	3.40	3.42
				193	2.76	3.05
			Reduction		18.8%	10.8%
5	38.9	0.072	M_o	0	0.176	0.193
				193	0.167	0.180
			Reduction		5.1%	6.7%
			M_i	0	0.090	0.102
				193	0.087	0.101
			Reduction		3.3%	1.0%
			W	0	3.80	3.83
				193	3.11	3.39
			Reduction		18.2%	11.5%

[a]Tests conducted by Cranch.[34] See text and Fig. 28 for model dimensions.

How significant the influence of internal pressure might be for large D/T tanks and vessels is, at this time, simply a matter of conjecture because we have neither experimental data nor valid theory. We do know that it could be significant for vessels with D/T ≤ 100, and we know that the influence is nonlinear, both with respect to D/T and P. From the little data that we do have, however, we can guess that reasonable design pressures might reduce the flexibility by about a factor of 3 for out-of-plane moment and thrust loads and by about half that much (1.2 to 1.5) for in-plane moments. Obviously, if nozzle flexibility is to be used in design to reduce the vessel-nozzle piping-support interaction problem, the influence of internal pressure cannot be ignored. Additional study is needed to provide appropriate design guidance.

10. FLEXIBILITY FACTORS FOR RUN MOMENTS

So far we have been discussing flexibility factors associated with applied branch moments that are reacted by moments at either one or both ends of the run. There are also conditions in real piping systems where the branch moments are so low that the moments at one end of the run are reacted almost entirely by moments at the other end of the run. Under those conditions, the existence of the branch might influence the flexibility of the run pipe. To accommodate such a possibility in the piping system flexibility analysis, we could put a "point-spring" in the strength-of-materials flexibility model at the intersection of the branch and run centerlines, that is, at point P in Fig. 1(e). Test data and analyses could then be used to develop the run moment flexibility factors associated with that point-spring.

For small d/D branch connections, it seems apparent that the only run moment flexibility factor that might be different from zero would be k_{zv} associated with in-plane bending, M_{zv} in Fig. 1(e). Even k_{zv}, however, would be close to zero. For larger d/D branch connections, all three flexibility factors might be different from zero as evidenced by the experimental data of Moffat and Kirkwood[47] for full outlet (d/D = 1.0) unreinforced models:

Model	1	2	3	4
D/T	42.4	25.7	16.2	12.4
k_{xv}	7.03	2.54	1.57	1.05
k_{yv}	0.39	0.41		1.88
k_{zv}	3.20	3.23	1.38	1.38

References 35 and 46 contain run-moment rotation data for ANSI B16.9 tees and for a WFI Weldolet. Both types of branch connections are fully reinforced; consequently, the derived experimental flexibility factors are quite small and subject to large experimental errors.

If significant-for-design run moment flexibility factors do exist, they are probably associated with unreinforced branch connections with large D/T and d/D ratios, for example, a 24 × 16 std. wt. fabricated branch connection. Our survey of industrial design practice discussed in Sect. 2.3 indicated that these types of branch connections are not used in nuclear power plant construction. We, therefore, conclude that development of run-moment flexibility factors for vessel nozzles and piping branch connections would have very low priority. [The development of run-moment stress intensification factors (SIFs), however, is of interest.]

11. NOZZLES IN VESSEL HEADS

For pressure vessels it is quite common to have nozzles in the heads. The attached piping system then imposes moment and thrust loads on the nozzles and there is potential for the same type of piping system-vessel nozzle interface problem that exists for cylindrical vessels. Pressure vessel heads may be spherical, but more often they are ellipsoidal or torospherical, consisting of a toridal knuckle at the outer edge and a spherical control portion in the center. These are the so-called flanged and dished heads.

In 1966, Rodabaugh and Atterbury[53] used Bijlaard's theory[54] for radial and moment loadings on a spherical shell to develop nozzle-to-sphere flexibility design guidance. The published result is a series of ten design graphs for the parameter ranges $0 < D/T < 250$, $0.01 < d/D < 0.5$, and $0.01 < t/T < 3.0$. Because Bijlaard's solution was based on a shallow-shell theory that is only generally valid for $d/D < 1/3$, Rodabaugh and Atterbury checked their design graphs, up to $d/D = 0.5$, by comparison with results from a general-purpose axisymmetric shell theory computer program written by Kalnins[55] that is not limited to shallow shells. The difference between the two sets of results was consistently

$$\delta_b \cos \theta = \delta_k , \qquad (36)$$

where δ_b is the displacement given by Bijlaard's theory, δ_k is the corresponding displacement given by Kalnins program, and $\theta = \sin^{-1} (d/D)$ is related to the nozzle-to-sphere diameter ratio. For $d/D < 0.5$, the R&A design curves overpredict the flexibility relative to the more accurate Kalnins theory by $<13.5\%$. Accordingly, the simpler R&A flexibility curves were considered to be sufficiently accurate for design guidance.

In 1984, Batra and Sun[56] (B&S) developed similar design guidance but only for radial loading over the parameter ranges $d/D < 0.1$, $75 > D/T < 225$, and $2.5 < d/t < 7.5$. Their results were published as a series of four design graphs that can be converted to flexibility factors compatible with the R&A curves by:

$$k = \pi E (t/T)/(K_R/t) , \qquad (37)$$

where K_R is the B&S parameter

$$K_R = (W/\delta)(t/T) , \qquad (38)$$

in terms of the radial load W and the shell displacement δ.

Apparently, B&S used a shallow shell theory that was similar but not identical to the shallow shell theory used by Bijlaard. Comparisons between the R&A and B&S flexibility factors, given in Table 24, show that

Table 24. Comparison between flexibility
factors for radial loads on a nozzle
in a spherical shell

D/T	d/D	t/T	k	
			R&A[a]	B&S[b]
250	0.06	0.5	45	31
	0.04	0.5	53	45
	0.02	0.5	70	66
250	0.03	0.25	38	30
	0.02	0.25	42	36
	0.01	0.25	.4	41
100	0.03	0.10	6.9	6.02
	0.02	0.10	6.9	6.52
	0.01	0.10	6.9	6.69
250	0.012	0.10	18.	17.
	0.008	0.10	18.	17.
	0.004	0.10	18.	17.

[a]R&A refers to Rodabaugh and
Atterbury[53] flexibility factors.

[b]B&S refers to Batra and Sun flex-
ibility factors as defined by Eqs. (37) and
(38) of the text and the curves of Ref. 56.

the B&S curves generally give lower flexibilities. The differences, how-
ever, are not large enough to be significant in design (see Sect. 2.2).

The solutions of R&A[53] and B&S[56] are only applicable to isolated
radial nozzles in spherical shells and not to a cluster of closely spaced
nozzles or to a nozzle near to or in the knuckle region of a torospherical
head. Accordingly, an "isolation" condition should be kept in mind when
dealing with the flexibility of nozzles in vessel heads.

Because the geometry of isolated radial nozzles in spherical shells
is axisymmetric, the theory is relatively simple. Further, results from
Bijlaard's theory can be easily checked against results from general-
purpose thin-shell theory computer programs. Our study of nozzle flex-
ibility for cylindrical shells, however, suggests that internal pressure
may have a significant and nonlinear influence on the flexibility fac-
tors, especially for large D/T vessels. There is no reason to indicate
that the same type of influence will not exist for nozzles in spherical
shells. Unfortunately, Bijlaard's theory for spherical shells[54] does not
include the internal pressure term, and most thin-shell theory computer
programs assume that linear superposition is valid for combined loads.
Thus, if the influence of internal pressure on the flexibility of nozzles
in heads is to be studied further, some basic modifications need to be
made in the analytical tools. Nozzles in vessel heads are also just as
likely to be reinforced as the nozzles in the cylindrical body. Accord-
ingly, a general study should also include the effects of reinforcement.

Test data on flexibility of nozzles in spherical shells are relatively sparse. Although we did not conduct an exhaustive search, we have identified only one set of data, reported by Dally[57] in 1963. In *WRC Bulletin 84*, Dally reported the results of tests on six models, shown in Fig. 29, one of which had an isolated radial nozzle in a spherical head.
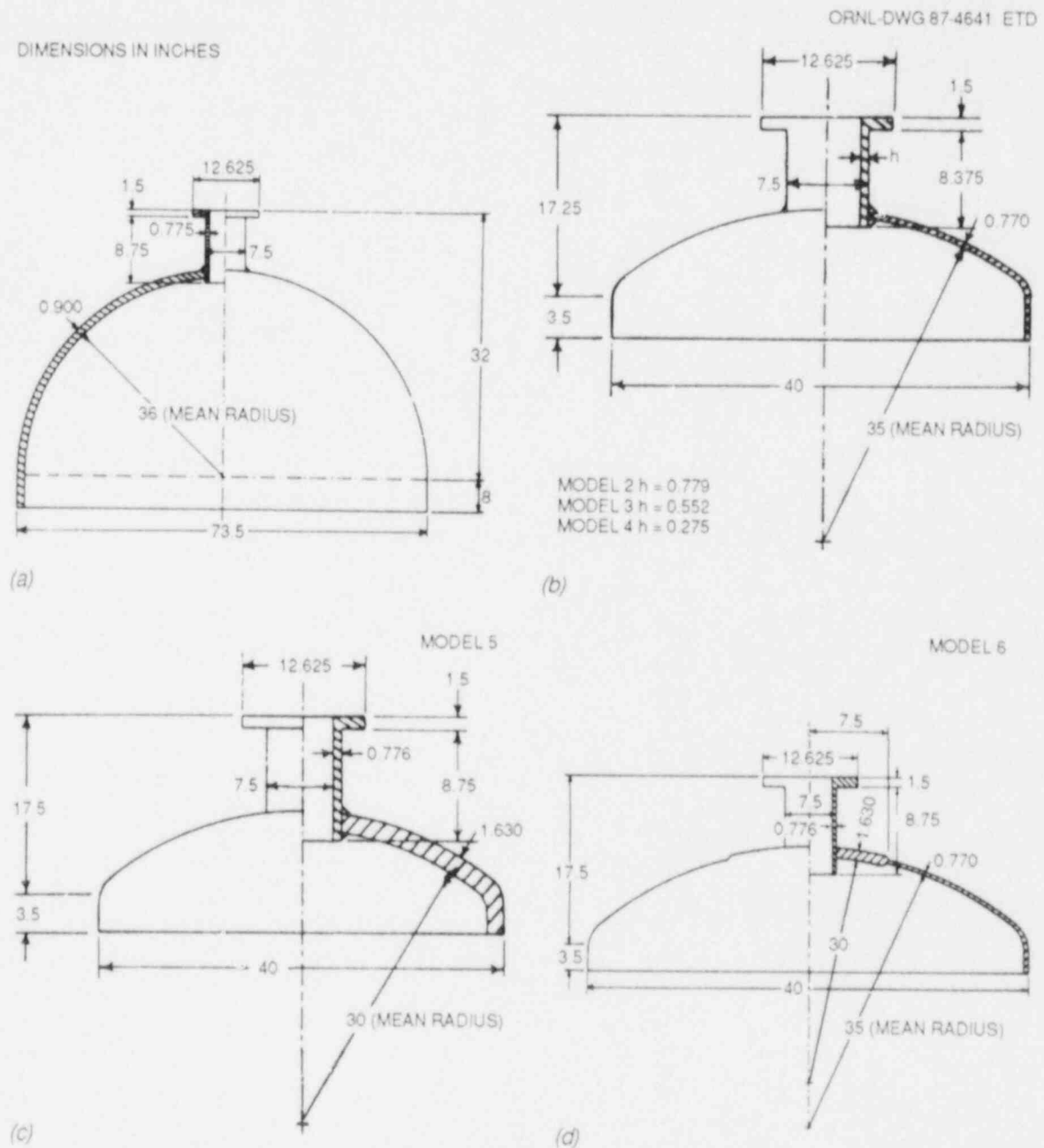
Fig. 29. Dally's[56] test models for nozzles in vessel heads. (*a*) Dimensions of Model No. 1, (*b*) dimensions of Model Nos. 2–4, (*c*) dimensions of Model No. 5, (*d*) dimensions of Model No. 6.

The other five models had torospherical heads. All the models were rein-
forced in the sense that the nozzle-head intersection region contained
more material than needed to satisfy internal pressure membrane stress
design criteria. Dally's test data, therefore, gave some clues on the
effects of such reinforcing. Dally also compared his measured displace-
ments with those calculated by Bijlaard's theory with reasonable agree-
ment.

12. SUMMARY, CONCLUSIONS, AND RECOMMENDATIONS

12.1 SUMMARY

The study reported here was conducted primarily to (1) summarize available flexibility data for nozzles in cylindrical shell structures (pressure vessels and tanks) and branch connections and tees in piping systems and (2) compare those data with available analytical methods for calculating flexibility factors for use in nuclear power plant design. This interest in flexibility factors comes directly from recent efforts to develop design criteria for nuclear piping that will permit the construction of more flexible, less costly, and perhaps safer piping systems.

Flexibility factors under consideration are for nozzles and branch connections within the piping system itself and for nozzles in cylindrical vessels that interact with connected piping. An adequate characterization of the flexibility factors for both types of nozzles is important to the development of improved design criteria.

The analytical and experimental flexibility data summarized in this report span a period of about 30 years of research, with the first papers published in the early 1950s. Flexibility data reported in those early papers, and most of the data reported since, were obtained as auxiliary information in studies of stresses at the intersection of nozzles in cylindrical shells. The first serious attempt to study nozzle *flexibility* as a unique discipline was done by Rodabaugh and Atterbury[20] in 1967 as one in a series of studies on the structural behavior of reinforced openings in pressure vessels sponsored by the U.S. Atomic Energy Commission through the PVRC. In that study, R&A collected and evaluated available shell deformation data and compared those data with analytical predictions based on theoretical deformation (and stress) studies of spherical and cylindrical shells under local loadings conducted by Bijlaard[12, 16-19, 54] of Cornell University between 1955 and 1960. Although the agreement between the experimental data and the theoretical predictions was far from exact, they were able to use the results as reference material in the development of flexibility factors for in-plane and out-of-plane moment loads on nozzles for use in the ASME Code. That early design guidance was updated by Rodabaugh and Moore in 1977,[21] and again in 1979,[15] to the present ASME Class 1 piping flexibility factor equations. The ASME Code does not include guidance for calculating nozzle flexibility for thrust loads on the nozzle.

In addition to the ASME Code equations for in-plane and out-of-plane moment flexibility factors, direct evaluation of Bijlaard's theory is available to the designer via design charts published by Murad and Sun (M&S)[23] in 1984 and the computer program LUGS by Dodge[26] in 1974. Both of these also permit consideration of thrust loads with and without internal pressure.

Since 1979, some additional flexibility data as well as major new theoretical work that permit consideration of nozzles in cylindrical shells with much larger diameter-to-thickness ratios (D/T) have become available. Steeles' thin-shell theory solution has the potential of

providing the basis for the development of flexibility design guidance
for vessel and tank nozzles and piping branch connections with dimen-
sional parameters in the range $d/D < 0.5$, $D/T < 2500$. This range of
dimensional parameters will cover the range of greatest interest for
nuclear power plant construction (see Sect. 2.3). Steeles' theory is
available to the designer in the form of a computer program, FAST2,
through Shelltech Associates, Stanford, Calif., and in the form of
design curves in *WRC Bulletin 297*,[27] published in 1984.

An analysis of design data from a survey of seven different nuclear
power plant architect engineers or NSSS vendors indicate that essentially
two distinct dimensional regimes are of interest: one for branch connec-
tions in LWR piping and nozzles in reactor pressure vessels and steam
generators, and a somewhat different regime for lower-pressure vessels
and auxiliary tanks. For high-pressure vessels and pipe, the vessel (run
pipe) diameter-to-thickness ratio D_o/T ranges from <10 to about 115; the
branch-to-run (vessel) diameter ratio d_o/D_o ranges from almost zero, for
drains and instrument connections, to about 0.5 for "standard" reinforced
nozzles or up to 1.0 for specialty product connections or ANSI B16.9
tees; and the branch pipe diameter-to-thickness ratio d_o/t ranges from <5
(a solid bar has $d_o/t = 2.0$) to about 100. The pipe (vessel) length-to-
diameter ratio L/D is generally >4.0.

For low-pressure vessels and auxiliary tanks, the diameter-to-
thickness ratios D_o/T are fairly evenly distributed between about 75 and
2000; the range of d_o/t is the same as for high-pressure vessels and
piping, that is, <5 to about 100. For low-pressure vessels and auxiliary
tanks, the diameter ratio d_o/D is not a constant, but decreases steadily
as D/T increases. The wall-thickness ratio t/T, however, is fairly con-
sistent with D/T and ranges between about 0.2 and 2.0. The length-to-
diameter ratio of the vessels L/D ranges from about 0.25 to slightly
<2.0. Note that this parameter range is less than essentially all the
available design data developed from Bijlaard's theory.

Also note that the parameter space of specific design interest for
both regimes is considerably smaller than indicated by the range of
variables plotted in WRC-297 Figs. 59 and 60. This point is especially
important, both for minimizing the cost of additional numerical studies
and for developing reasonably accurate design guidance.

The major portion of this report is a detailed evaluation of five
analytical methods for calculating nozzle flexibility factors for use in
design by comparison with experimental and analytical benchmark data.
The present study is considerably more extensive than previous studies
because we were able to include more types of nozzle reinforcement; more
loadings, that is, radial loads and torsional moments on the branch and
moments on the run; and the influence of internal pressure as well as a
wider range of dimensional parameters.

Tables 25 and 26 summarize the goodness-of-fit CTR values for the
out-of-plane and in-plane moment flexibility factors, k_o and k_i, respec-
tively, for the five different design methods evaluated in this report.
A CTR value of 1.00 for a given data set indicates that the design method
gave flexibility factors that agreed, in an overall sense, with the
benchmark data. Values >2.0 or <0.5 indicate that the goodness-of-fit is
quite poor. The tabulated data given in the text for each data set must
be examined separately for evaluation of the data scatter. The CTR

Table 25. Goodness-of-fit relative to benchmark data for
out-of-plane moment design flexibility methods

Table in text	Nozzle data set[b]	Dimensional parameters		Goodness-of-fit values[a]				
		d/D	D/T	Code (NB-3686)	Bijlaard's theory		Steeles' theory	
					M&S	LUGS	WRC-297	FAST2
T5	UBC-EXP	<0.5	<100	1.04	1.13	1.64	2.43	1.32
T15	UBC-FEA	<0.5	<100	0.98	1.08	1.67	2.96	0.99
T8	RBC-EXP	<0.52	<100	0.94	1.92	1.27	5.58	1.41
T17	RBC-FEA	<0.5	<100	0.86	1.55	2.84	6.56	0.97
T17	RP30-FEA	<0.5	<100	1.28	2.88	4.36	7.81	1.82
T12	RSPS-EXP	<0.52	<100	1.81				0.75
T7	LDT-EXP	<0.05	>900	3.08			2.37	0.94
T19	LDT-FEA	<0.03	>400	5.16			1.45	0.82
T10	UBC-EXP	>0.5	<100	1.08				
T11	RBC-EXP	>0.5	<100	1.07				
T14	B16.9T	>0.4	<100	6.94				

[a]See text for explanation of goodness-of-fit determination.

[b]The first set of letters stands for nozzle type: UBC = unreinforced branch connection; RBC = reinforced branch connection; RP30 = reinforced P30 models; RSPS = reinforced, saddle, pad, or sleeve; LDT = large diameter thin walled. The second set stands for type of data: EXP = experimental; FEA = finite-element analysis.

Table 26. Goodness-of-fit relative to benchmark data for
in-plane moment design flexibility methods

Table in text	Nozzle data set[b]	Dimensional parameters		Goodness-of-fit values[a]				
		d/D	D/T	Code (NB-3686)	Bijlaard's theory		Steeles' theory	
					M&S	LUGS	WRC-297	FAST2
T6	UBC-EXP	<0.5	<100	0.71	0.94	1.32	1.32	1.09
T16	UBC-FEA	<0.5	<100	0.83	0.75	1.05	1.01[c]	0.92
T8	RBC-EXP	<0.52	<100	1.07	1.04	1.64		1.19
T17	RBC-FEA	<0.5	<100	0.82	0.64	1.22		0.74
T17	RP30-FEA	<0.5	<100	0.87	1.46	2.03		1.02
T12	RSPS-EXP	<0.52	<100	2.16				1.09
T7	LDT-EXP	<0.05	>900	2.36			2.03	1.01
T19	LDT-FEA	<0.03	>400	0.11			1.45	1.06
T20	LDT-HJ[b]	0.10	200-1000	0.52				1.33
T10	UBC-EXP	>0.5	<100	1.00				
T11	RBC-EXP	>0.5	<100	1.29				
T14	B16.9T			2.14				

[a]See text for goodness-of-fit determination.

[b]See Table 25 for nomenclature; HJ stands for Hansberry and Jones[52] theory.

[c]This value is for a reduced set of data since the WRC-297 curves do not cover the models with D/T > 60. See Table 16 for more information.

method for evaluating goodness-of-fit is explained in more detail in Sect. 5.1.

The numbers in Tables 25 and 26 indicate that the Code equations do a good job of estimating k_o and k_i for both unreinforced (UBC) and integrally reinforced (RBC and RP30) nozzles with dimensional parameters in the range $d/D < 0.5$, $D/T < 100$. This is no surprise because the data base in this report is essentially the same as was used to develop the Code equations. The Code equations also do a surprisingly good job for nozzles with $d/D > 0.5$ and $D/T < 100$ (data sets T10 and T11). Those nozzles are outside the dimensional parameter range previously validated. The Code equations do a poor job for nonintegral reinforced nozzles (RSPS), for nozzles in large-diameter thin-walled vessels (LDT), and for ANSI B16.9 tees (T14).

The two design methods based on Bijlaard's theory (M&S and LUGS) both gave good results for in-plane moments (Table 26) for all the data sets with $d/D < 0.5$ and $D/T < 100$ except for the T17 RP30-FEA reinforced models. Bijlaard's theory is not applicable for nonintegral reinforced nozzles (T12 RSPS-EXP) or for nozzles with $d/D > 0.5$ or $D/T > \sim 300$. For out-of-plane moments (Table 25) both methods gave good results for unreinforced nozzles (T5 and T15) but poor results for the reinforced nozzles (T8, T17 RBC, and T17 RP30). We thus conclude that Bijlaard's theory is not *directly* applicable for reinforced nozzles.

Steeles' theory (FAST2) gave good results for both out-of-plane moment (Table 25) and in-plane moment (Table 26) flexibility factors for all of the models with $d/D < 0.5$, except perhaps for k_o, T17 RP30-FEA, where the CTR value shown in Table 25 is 1.82. These particular models had a very compact reinforcement that thin-shell theory is not capable of accurately representing. The Code equations do a better job for these particular models because an additional variable r_p was included to account for the reinforcement. Additional studies using FAST2 need to be conducted to determine the most appropriate way to represent the effects of reinforcement.

The WRC-297 method, based on Steeles' theory and design curves published in Ref. 27, is completely inadequate for calculating out-of-plane moment flexibility factors as shown by the large CTR values in Table 25. None of the experimental data and only one set of analytical data (T19) gave CTR values <2.00. That data set, however, was not benchmarked against experimental data (it consists of four somewhat unrealistic models with D/T values that range from 400 to 40,000) and was included in our evaluations only because it gives some indication of the theoretical limits of Steele's theory. For in-plane moment loads, Table 26 indicates that WRC-297 does a reasonably good job for in-plane moment loads for unreinforced nozzles with $d/D < 0.5$ and $D/T < 100$ but is not applicable for reinforced nozzles.

Recent correspondence from Dr. Steele[58] and additional calculations[59] using FAST2 confirmed our suspicions concerning WRC-297 Fig. 60 (Fig. 13 herein). The curves given for out-of-plane moment loading were inadvertently mislabeled. It was concluded, however, that even though correcting the labels would result in more logical trends in the curves, the designer would not have much better guidance than presently available. In view of this we did not repeat our comparison calculations even

though they are, admittedly, incorrect. Our overall conclusions and recommendations for further work are unaltered.

Flexibility factors for radial loads on the nozzle are discussed in Sect. 8. Although the ASME Code does not include radial-load flexibility guidance for either piping or vessel design, radial-load flexibility (or stiffness) is expected to be as important as in-plane or out-of-plane moment flexibility for the design of less rigid nuclear piping systems. Both Bijlaard's theory and Steele's theory are applicable. However, we were able to find only three sets of experimental data and no analytical benchmark data for use in evaluating the theories. One set, obtained by Cranch[34] in 1960 for comparison with Bijlaard's theory, includes radial displacement data for five attachments on a single cylindrical pressure vessel with $D/T = 77.8$. The other two sets include radial displacement data for five unreinforced nozzles obtained by Whipple et al.[41-43] and Shroeder[44] from tests on large-diameter thin-walled tank models with dimensional parameter values in the range $d/D \leqslant 0.05$ and $960 \leqslant D/T \leqslant 2530$.

The CTR values from Table 21 in the text and summarized below indicate that both Bijlaard's theory (LUGS) and Steele's theory (FAST2)

Nozzle data	Bijlaard	Steeles'	
	LUGS	WRC-297	FAST2
Cranch	0.78	0.44	0.69
LDT		0.82	0.92

do a reasonably good job of estimating the radial load flexibility factor k_w for Cranch's data ($D/T = 77.8$). Steeles' theory (WRC-297, FAST2) also does a good job for the large-diameter thin-walled tank (LDT) data. Bijlaard's theory is not applicable. FAST2 did a better job than WRC-297 for Cranch's data because the computer program was better able to model the test specimens. Even though the CTR values are all <1.0, the extremely small amount of test data and its relatively poor quality (see Sect. 8 and Table 21) make it impossible to draw more definitive conclusions.

The influence of internal pressure on the nozzle flexibility is discussed in Sect. 9. The available data (Cranch's model) are summarized and compared with Bijlaard's theory in Tables 22 and 23 in the text. Steeles' theory is not applicable. Indications are that internal pressure might reduce the flexibility factors significantly for large D/T vessels. If nozzle flexibility is to be used in design to reduce the vessel-nozzle piping-support interaction problem inherent with stiff piping systems, the influence of internal pressure cannot be ignored. Additional theoretical development is needed, however, before appropriate design guidance can be developed.

Flexibility factors for torsional moments on the nozzle and for moments on piping runs are discussed in Sects. 7 and 10, respectively. Neither of these would appear to be significant for design, except perhaps for large d/D.

Flexibility factors for nozzles in spherical and torospherical heads are discussed in Sect. 11. The design guidance given by Bijlaard's theory[54] appears to be adequate for isolated, unreinforced nozzles for both thrust and moment loads. The theory does not include the internal pressure term, however, and there is reason to believe that its influence could be significant in design.

12.2 CONCLUSIONS

In brief, our evaluations of the available design analysis methods for calculating flexibility factors for branch connections in piping and nozzles in vessels with attached piping show the following:

1. The ASME Code Class 1 piping flexibility factors for in-plane and out-of-plane moment loadings on the branch are the best available design guidance for both reinforced and unreinforced branch connections and vessel nozzles within the parameter range $d/D < 0.5$, $D/T < 100$. The ASME Code equations are not adequate for nozzles with $D/T > 100$. The Code does not include flexibility guidance for thrust loads on the nozzle.

2. Bijlaard's basic theory and the derived design methods for calculating flexibility factors for in-plane moment, out-of-plane moment, and thrust loads on the nozzle appears to be adequate for unreinforced nozzles but not for reinforced nozzles. Bijlaard's theory is not applicable for nozzles with $d/D > 0.5$ or $D/T > \sim 600$.

3. Steeles' basic theory appears to be adequate for calculating flexibility factors for in-plane moment, out-of-plane moment, and thrust loads for unreinforced and for some types of integrally reinforced nozzles within the parameter range $d/D < 0.5$ and $D/T < \sim 2500$. Non-integral reinforcement and some integral reinforcement designs are problem areas. The flexibility guidance, based on Steele's theory given in *WRC Bulletin 297*, is totally inadequate.

4. Flexibility factors for torsional moment on the branch may be small and not significant for design, except possibly for large d/D. Additional experimental data and/or theoretical studies are needed to explore the significance of torsional flexibility over a wider range of parameters.

5. Flexibility factors for moment loading on the run are probably not significant for design purposes, except possibly for large d/D. Some additional study is needed to confirm this conclusion, however. Moments on the vessel ends are not a design consideration.

6. Internal pressure equal to the design pressure will affect nozzle flexibility for the thinner walled vessels and auxiliary tanks that are used in a nuclear power plant. Bijlaard's theory includes the nonlinear internal pressure effect, but Steele's theory does not.

7. Flexibility factors for isolated radial nozzles in spherical and torospherical heads developed from Bijlaard's theory appear to be adequate for thrust and moment loads. Additional theoretical work is needed, however, to include the effects of internal pressure that we believe could be significant.

12.3 RECOMMENDATIONS

To develop improved flexibility guidance for the design of more flexible nuclear piping systems, it is apparent that a considerable amount of additional work is needed. To reach that goal we recommend the following:

1. Use Steeles' theory, FAST2, to conduct two separate parameter studies designed to cover the ranges of interest for nuclear power plant construction (see Sect. 2.3):

   (a) One study designed specifically for branch connections in straight pipe and nozzles in pressure vessels. The dimensionless parameter ranges are:

   $$5 < D_o/T < 120,$$
   $$0.01 < d_o/D < 0.5,$$
   $$2 < d_o/t < 100,$$
   $$L/D > 4 ,$$

   where L/D is the length-to-diameter ratio of the analyzed model.

   (b) A second study designed specifically for nozzles in thinner-walled vessels and auxiliary tanks. The dimensionless parameters and ranges are:

   $$75 < D/T < 2500,$$
   $$2 < d_o/t < 100,$$
   $$0.2 < t/T < 2.0,$$
   $$0.2 < L/D > d_o/D < 2.0.$$

   Both parameter studies should be run for three loadings on the nozzle: thrust and in-plane and out-of-plane moments.

2. Using the results from item 1, develop simple design guidance equations similar in format to the ASME Code Class 1 piping flexibility factor equations. Because four independent dimensionless parameters are involved, there does not appear to be any simple way to present the results in accurate graphical form without the need for extensive interpolations. Moreover such interpolations are time-consuming and subject to error. Even at the expense of some loss in accuracy, simple design formulas are preferred to design graphs.

3. Develop corollary parameter studies to investigate the influence of reinforcement design. Two such studies would be (a) to characterize the influence of nozzle reinforcement length and (b) to characterize the influence of vessel pad reinforcement. Using the results from those studies attempt to modify the formulas developed under item 2 in as simple a fashion as possible to characterize reinforcement effects. Some suggestions are given in the text.

4. Conduct corollary parameter studies to identify the influence of torsional moments on the branch.

5. Modify Steele's basic theory to include the nonlinear effects of internal pressure and incorporate the modifications into the FAST computer programs. Because pressure effects are nonlinear, super-position is not permissible. The basic differential equations need to be modified, and a particular solution needs to be developed. Exploratory numerical studies would then need to be conducted to determine how best to include the effect of internal pressure in the design guidance.

6. Modify Bijlaard's theory for spherical shells to include the in-fluence of internal pressure and proceed as discussed under item (5).

7. Develop criteria for defining an "isolated" nozzle in a spherical or torospherical vessel head.

REFERENCES

1. A. R. C. Markl, "Piping Flexibility Analysis," *Trans. ASME*, pp. 127–49 (February 1955).

2. *ASME Boiler and Pressure Vessel Code*, Nuclear Power Plant Components, Section III — Div. 1, 1983 Ed., Winter 1985 addenda, ASME, New York.

3. S. E. Moore, "Flexibility Factors for Elbows and Curved Pipe with End Effects," submitted for publication in *J. Press. Vessel Tech., Trans. ASME*.

4. E. C. Rodabaugh, *Sources of Uncertainty in the Calculation of Loads on Supports of Piping Systems*, NUREG/CR-3599 (ORNL/Sub/82-22252/2), Oak Ridge Natl. Lab., June 1984.

5. D. L. Rehn, Duke Power Company, letter to S. E. Moore, Oak Ridge National Laboratory, April 2, 1985.

6. C. Germain, FRAMATOME, letter to S. E. Moore, Oak Ridge National Laboratory, June 18, 1985.

7. H. L. Hwang, General Electric Company, letter to S. E. Moore, Oak Ridge National Laboratory, July 5, 1985.

8. G. Kitz, Sargent and Lundy Engineers, Inc., private communication to S. E. Moore, Oak Ridge National Laboratory, 1986.

9. F. Sestak, Jr., Stone and Webster Engineering Corp., letter to S. E. Moore, Oak Ridge National Laboratory, March 28, 1985.

10. R. O. Barnett, Tennessee Valley Authority, letter to S. E. Moore, Oak Ridge National Laboratory, March 20, 1985.

11. D. H. Roarty, Westinghouse Electric Corporation, letter to S. E. Moore, Oak Ridge National Laboratory, April 23, 1985.

12. P. P. Bijlaard, "Stresses from Local Loadings in Cylindrical Pressure Vessels," *Trans. ASME* 77, 805–16 (1955).

13. C. R. Steele and M. L. Steele, *Reinforced Openings in Large Steel Pressure Vessels: Effect of Nozzle Wall Thickness*, Shelltech Report 81-5 to PVRC Subcommittee on Reinforced Openings and External Loadings, Unpublished, December 1981.

14. C. R. Steele and M. L. Steele, "Stress Analysis of Nozzles in Cylindrical Vessels with External Load," *J. Press. Vessel Tech. Trans. ASME* 105, 191–200 (August 1983).

15. E. C. Rodabaugh and S. E. Moore, *Stress Indices and Flexibility Factors for Nozzles in Pressure Vessels and Piping*, NUREG/CR-0778 (ORNL/Sub-2913/10), Oak Ridge Natl. Lab., June 1979.

16. P. P. Bijlaard, "Stresses from Radial Loads in Cylindrical Pressure Vessels," *Welding J. Res. Suppl.* 33(12), 615–23 (1954).

17. P. P. Bijlaard, "Stresses from Radial Loads and External Moments in Cylindrical Pressure Vessels," *Welding J. Res. Suppl.* 34(12), 608–17 (1955).

18. P. P. Bijlaard, "Additional Data on Stresses in Cylindrical Shells Under Local Loading," *WRC Bulletin 50*, pp. 10–55, New York, 1959.

19. P. P. Bijlaard and E. T. Cranch, "Interpretive Commentary on the Application of Theory to Experimental Results for Stresses and Deflections Due to Local Loads on Cylindrical Shells," *WRC Bulletin 60*, pp. 1–2, New York, 1960.

20. E. C. Rodabaugh and T. J. Atterbury, "Flexibility of Nozzles in Cylindrical Shells," in *Evaluation of Experimental and Theoretical Data on Radial Nozzles in Pressure Vessels*, USAEC Report TID-24342, December 1967.

21. E. C. Rodabaugh and S. E. Moore, *Flexibility Factors for Small (d/D < 1/3) Branch Connections with External Loadings*, ORNL/Sub/2913-6, Oak Ridge Natl. Lab., March 1977.

22. K. R. Wickman, A. G. Hopper, and J. L. Mershon, "Local Stresses in Spherical and Cylindrical Shells due to External Loadings," *WRC Bulletin 107*, New York, August 1965, revised March 1979.

23. F. P. Murad and B. C. Sun, "On Radial and Rotational Spring Constants of Piping-Nozzles," in *Proc. Fifth Int'l Conf. on Press. Vessel Tech.*, *Vol. 1*, *Design and Analysis*, ASME, New York, 1984.

24. W. G. Dodge, "Secondary Stress Indices for Integral Structural Attachments to Straight Pipe," *WRC Bulletin 198*, pp. 1–13, New York, 1974.

25. E. C. Rodabaugh, W. G. Dodge, and S. E. Moore, "Stress Indices at Lug Supports on Piping Systems," *WRC Bulletin 198*, pp. 14–45, New York, 1974.

26. ORNL LUGS, NESC Program 648, National Energy Software Center, 9700 S. Cass Ave., Argonne, Ill. 60439.

27. J. L. Mershon et al., "Local Stresses in Cylindrical Shells Due to External Loadings on Nozzles — Supplement to WRC Bulletin No. 107," *WRC Bulletin 297*, New York, August 1984.

28. C. R. Steele, *Evaluation of Reinforced Openings in Large Steel Pressure Vessels*, Shelltech Report 80-2 to PVRC Subcommittee on Reinforced Openings and External Loadings, Unpublished, Dec. 20, 1980.

29. A. J. Durelli, E. A. Phillips, and C. H. Tsao, "Dimensional Analysis," Chap. 12 in *Introduction to the Theoretical and Experimental Analysis of Stress and Strain*, McGraw-Hill, New York, 1958.

30. L. R. Jackson et al., *Stresses in Unreinforced Branch Connections*, Battelle-Columbus Lab., Columbus, Ohio, Sept. 30, 1953.

31. E. C. Rodabaugh, *Cyclic Bending Tests of a Half-Scale Model of an 8" x 24" Saddle Reinforced Branch Connection*, Tube Turns Report 8.011, Tube Turns, Louisville, Ky., 1953.

32. G. M. McClure, J. A. Sweeney, and H. J. Gross, *Investigation of Stresses in Pipeline Branch Connections*, Battelle-Columbus Lab., Columbus, Ohio, March 30, 1956.

33. F. J. Mehringer and W. E. Cooper, "Experimental Determination of Stresses in the Vicinity of Pipe Appendages to a Cylindrical Shell," *Proc. Soc. Exp. Stress Analysis* 14(2), 1957.

34. E. T. Cranch, "An Experimental Investigation of Stresses in the Neighborhood of Attachments to a Cylindrical Shell," *WRC Bulletin 60*, New York, May 1960.

35. E. J. Mills, T. J. Atterbury, and G. H. McClure, *Study of Effects of Cyclic Bending Loads on Performance of Branch Connections*, Battelle-Columbus Lab., Columbus, Ohio, May 1962.

36. A. G. Pickett, *Low Cycle Fatigue Testing of One-Half Scale Model Pressure Vessels*, Progress Reports 9-12 to PVRC Subcommittee on Reinforced Openings and External Loadings, AEC Contract No. AT(11-1)-1228, Southwest Research Institute, San Antonio, Tex., July 1964-January 1965.

37. E. J. Mills, E. C. Rodabaugh, and T. J. Atterbury, *Determination of Stress Indices and Flexibility Factors for Submarine Piping Components*, Report to Naval Ship and Research Development Center, Battelle-Columbus Lab., Ohio, July 13, 1968.

38. C. E. Jaske and H. Mindlin, *Fatigue Evaluation of Sweepolet Branch Connections in Carbon Steel Pipe*, Report to Bonney Force and Foundary Inc., Battelle-Columbus Lab., Cleveland, Ohio, May 15, 1970.

39. K. B. Davis and C. E. Jaske, *Fatigue Evaluation of 12 x 6 Weldolet Branch Connections in Carbon Steel Pipe*, Report to Bonney Forge Div., Gulf and Western, Battelle-Columbus Lab., Cleveland, Ohio, June 25, 1975.

40. T. P. Forte and C. E. Jaske, *Fatigue Evaluation of 14 x 16 Insert Weldolet Branch Connections in Carbon Steel Pipe*, Report to Gulf and Western (Bonney Forge), Battelle-Columbus Lab., Cleveland, Ohio, April 30, 1981.

41. *Experimental Testing Program for Nozzle Connections in Cylindrical Shells (CBI 1-2)*, CBI Report 74-9453, Chicago Bridge and Iron Co., Oak Brook, Ill., 1979.

42. R. A. Whipple, J. Hagstron, and H. Dykstra, "Experimental Investigation of Cylindrical Shell Stresses due to Penetration Loads Where R/T = 1264," *J. Press. Vessel Tech.*, *Trans. ASME* 105, pp. 201—6 (August 1983).

43. R. A. Whipple, "Experimental Investigation of Nozzle Induced Cylindrical Shell Stresses Where R/T = 1264," *J. Pressure Vessel Tech.*, *Trans. ASME* 108, pp. 98—107, February 1986.

44. J. Schroeder, *Experimental Validation of the Evaluation of Reinforced Openings in Large Steel Pressure Vessels*, Progress Report to PVRC Subcommittee on Reinforced Openings and External Loadings, Unpublished, October 1983.

45. A. S. Khan, *A Study of Fatigue Crack Initiation and Failure in Reinforced Shell-to-Shell Intersections*, University of Oklahoma Report OU-AMNE-84-1 to WFI International, Inc., Unpublished, April 1984.

46. S. E. Moore, J. K. Hayes, and R. A. Weed, *Experimental Stress Analysis and Fatigue Tests of Five 24-in. NPS ANSI Standard B16.9 Tees*, ORNL/TM-9409, March 1985.

47. D. G. Moffat and M. G. Kirkwood, "Flexibility Factors for Fabricated Equal Diameter Branch Pipe Intersections," *Proc. Conf. on Pipework Design and Operation*, pp. 49—58, I. Mech. E., London, 1985.

48. E. B. Branch et al., "Technical Position on Industry Practice," prepared by the Task Group on Industry Practice of the PVRC Technical Committee on Piping, *WRC Bulletin 300*, New York, December 1984.

49. ANSI Standard B16.9-1971, *Factory-Made Buttwelding Fittings*, ASME, New York, 1971.

50. MSS Standard SP87-1977, *Factory-Made Buttwelding Fittings for Class 1 Nuclear Piping Applications*, Manufacturers Standardization Society of the Valves and Fittings Industry, Arlington, Va., 1977.

51. S. E. Moore and W. L. Greenstreet, *Program Plan for the ORNL Piping Program — Design Criteria for Piping, Pumps, and Valves (Rev. 1973)*, Oak Ridge Natl. Lab., Unpublished, 1973.

52. J. W. Hansberry and N. Jones, "A Theoretical Investigation of the Elastic Behavior of Two Normally Intersecting Cylindrical Shells," *J. Engr. Industry, Trans. ASME*, August 1969.

53. E. C. Rodabaugh and T. J. Atterbury, "Flexibility of Nozzles in Spherical Shells," in *Evaluation of Experimental and Theoretical Data on Radial Nozzles in Pressure Vessels*, USAEC Report TID-24342, 1967.

54. P. P. Bijlaard, "Stresses in a Spherical Vessel from Radial Loads Acting on a Pipe" and "Stresses in a Spherical Vessel from External Moments Acting on a Pipe," *WRC Bulletin 49*, New York, April 1959.

55. A. Kalnins, "Analysis of Shells of Revolution Subjected to Symmetrical and Nonsymmetrical Loads," *J. Applied Mech. Trans. ASME*, September 1964.

56. B. Batra and B. C. Sun, "On Radial Spring Constants at the Juncture of a Radial Nozzle and a Spherical Shell," in *Proc. Fifth Int'l Conf. on Press. Vessel Tech., Vol. 1, Design and Analysis*, ASME, New York, 1984.

57. J. W. Dally, "An Experimental Investigation of the Stresses Produced in Spherical Vessels by External Loads Transferred by a Nozzle," *WRC Bulletin 84*, New York, January 1963.

58. C. R. Steele, Shelltech Associates, letter to W. C. Kroenke, Babcock and Wilcox, July 27, 1986.

59. K. Mokhtarian, CBI-Na Con, letter to W. C. Kroenke, Babcock and Wilcox, August 15, 1986.

Internal Distribution

1.	J. J. Blass	18-27.	S. E. Moore
2.	C. J. Chang	28.	H. L. Mosley
3.	R. D. Cheverton	29.	D. G. O'Conner
4.	C. J. Claffey	30.	C. B. Oland
5.	J. A. Clinard	31.	C. E. Pugh
6.	W. L. Cooper	32.	J. J. Robinson
7.	J. M. Corum	33.	W. K. Sartory
8.	J. A. Getsi	34.	H. E. Trammell
9.	W. L. Greenstreet	35.	G. T. Yahr
10.	R. C. Gwaltney	36.	F. C. Zapp
11.	W. R. Hendrich	37-38.	Mechanics Applications,
12.	R. L. Huddleston		Bldg. 9204-1, MS 11
13.	R. C. Hudson	39.	ORNL Patent Office
14.	Y. L. Lin	40.	Central Research Library
15.	C. S. Luttrell	41.	Document Reference Section
16.	M. F. Marchbanks	42-43.	Laboratory Records Department
17.	J. G. Merkle	44.	Laboratory Records (RC)

External Distribution

45-46. K. Mokhtarian, CBI-NaCon, Inc., 800 Jorie Blvd., Oak Brook, IL 60522-7001

47-48. E. C. Rodabaugh, 4625 Cemetery Rd., Hilliard, OH 43026

49-68. D. J. Guzy, Structural and Seismic Engineering Branch, Nuclear Regulatory Commission, Washington, DC 20555

69. Office of Assistant Manager for Energy Research and Development, Department of Energy, ORO, Oak Ridge, TN 37831

70-71. Technical Information Center, DOE, Oak Ridge, TN 37831

72-231. Given distribution as shown under category RM

232-326. Special PVRC and ASME Code distribution.

4. TITLE AND SUBTITLE (Add Volume No., if appropriate)

Review and Evaluation of Design Analysis Methods for Calculating Flexibility of Nozzles and Branch Connections

2. (Leave blank)

3. RECIPIENT'S ACCESSION NO.

7. AUTHOR(S)

S. E. Moore, E. C. Rodabaugh, K. Mokhtarian, and
R. C. Gwaltney

5. DATE REPORT COMPLETED

MONTH	YEAR
December	1987

9. PERFORMING ORGANIZATION NAME AND MAILING ADDRESS (Include Zip Code)

Oak Ridge National Laboratory
P. O. Box Y
Oak Ridge, TN 37831

DATE REPORT ISSUED

MONTH	YEAR
December	1987

6. (Leave blank)

8. (Leave blank)

12. SPONSORING ORGANIZATION NAME AND MAILING ADDRESS (Include Zip Code)

Division of Engineering
Office of Nuclear Regulatory Research
U.S. Nuclear Regulatory Commission
Washington, DC 20555

10. PROJECT/TASK/WORK UNIT NO.

11. FIN NO.

B0474

13. TYPE OF REPORT

Topical

PERIOD COVERED (Inclusive dates)

15. SUPPLEMENTARY NOTES

14. (Leave blank)

16. ABSTRACT (200 words or less)

Modern piping system design generally includes an analytical determination of displacements, rotations, moments, and reaction forces at various positions along the piping system by means of a so-called flexibility analysis. The analytical model is normally based on a strength-of-materials description of the piping system as an interconnected set of straight and curved beams along with "flexibility factors" that are used to compensate for inaccuracies in the model behavior. This report gives an in-depth evaluation of the various analytical descriptions of the flexibility factors associated with piping system branch connections and nozzles. Recommendations are given for developing needed improvements.

17. KEY WORDS AND DOCUMENT ANALYSIS

17a. DESCRIPTORS

ASME Code, Piping, Flexibility Analysis,
Design Nozzles, Branch Connections

17b. IDENTIFIERS/OPEN-ENDED TERMS

18. AVAILABILITY STATEMENT	19. SECURITY CLASS (This report)	21. NO. OF PAGES
Unlimited	Unclassified	
	20. SECURITY CLASS (This page)	22. PRICE
	Unclassified	